การค้นหาสารออกฤทธิ์ทางชีวภาพจากพืชบางชนิดของกาลิมันตันตะวันออกเพื่อการรักษา
โรคเบาหวาน

นายริโก รามาดาน

วิทยานิพนธ์นี้เป็นส่วนหนึ่งของการศึกษาตามหลักสูตรปริญญาวิทยาศาสตรดุษฎีบัณฑิต
สาขาวิชาเทคโนโลยีชีวภาพ
คณะวิทยาศาสตร์ จุฬาลงกรณ์มหาวิทยาลัย
ปีการศึกษา 2558
ลิขสิทธิ์ของจุฬาลงกรณ์มหาวิทยาลัย

EXPLORATION OF BIOACTIVE COMPOUNDS FOR DIABETES THERAPY FROM SELECTED

EAST KALIMANTAN FLORA

Mr. Rico Ramadhan

A Dissertation Submitted in Partial Fulfillment of the Requirements

for the Degree of Doctor of Philosophy Program in Biotechnology

Faculty of Science

Chulalongkorn University

Academic Year 2015

Thesis Title	EXPLORATION OF BIOACTIVE COMPOUNDS FOR DIABETES THERAPY FROM SELECTED EAST KALIMANTAN FLORA
By	Mr. Rico Ramadhan
Field of Study	Biotechnology
Thesis Advisor	Associate Professor Preecha Phuwapraisirisan, Ph.D.

Accepted by the Faculty of Science, Chulalongkorn University in Partial Fulfillment of the Requirements for the Doctoral Degree

　　　　　　　　　　　　　　　　　　　　　　　Dean of the Faculty of Science

(Associate Professor Polkit Sangvanich, Ph.D.)

THESIS COMMITTEE

　　　　　　　　　　　　　　　　　　　　　　　Chairman

(Associate Professor Vudhichai Parasuk, Ph.D.)

　　　　　　　　　　　　　　　　　　　　　　　Thesis Advisor

(Associate Professor Preecha Phuwapraisirisan, Ph.D.)

　　　　　　　　　　　　　　　　　　　　　　　Examiner

(Assistant Professor Warinthorn Chavasiri, Ph.D.)

　　　　　　　　　　　　　　　　　　　　　　　Examiner

(Assistant Professor Kanoktip Packdibamrung, Ph.D.)

　　　　　　　　　　　　　　　　　　　　　　　External Examiner

(Associate Professor Surat Laphookhieo, Ph.D.)

ริโก รามาดาน : การค้นหาสารออกฤทธิ์ทางชีวภาพจากพืชบางชนิดของกาลิมันตันตะวันออกเพื่อการ
รักษาโรคเบาหวาน (EXPLORATION OF BIOACTIVE COMPOUNDS FOR DIABETES THERAPY
FROM SELECTED EAST KALIMANTAN FLORA) อ.ที่ปรึกษาวิทยานิพนธ์หลัก: รศ. ดร.ปรีชา ภูวไพรศิริ
ศาล, 107 หน้า.

ในการค้นหาสารยับยั้งอัลฟากลูโคซิเดสเพื่อใช้รักษาโรคเบาหวานชนิดที่ 2 และโรคเรื้อรัง ได้ทำการ
ทดสอบฤทธิ์การยับยั้งกับพืชบางชนิดที่เก็บมาจากกาลิมันตันตะวันออก ประเทศอินโดนีเซีย ซึ่งได้แก่ *Leucaena
leucocephala, Swietenia macrcophylla, Pycnarrhena tumefacta, Luvunga eleutherandra,
Crescentia cujete, Ceriops tagal* and *Horsfieldia macrobotrys* จากข้อมูลภูมิปัญญาท้องถิ่นประกอบกับ
การคัดกรองด้วยการทดสอบฤทธิ์ชีวภาพและการทดสอบทางเคมี จึงได้คัดเลือกพืชบางชนิดเพื่อมาศึกษาต่อไป
เพื่อให้ได้สารออกฤทธิ์ สารสกัดเมทานอลจากใบ *Ceriops tagal* ให้สารสกัดกลุ่มเพนตาเทอร์พีนอยด์ 3 ชนิด คือ
lupeol (1), betulone (2) และ betulin (3) ในบรรดาสารที่แยกได้ สาร 3 ออกฤทธิ์สูงสุดในการยับยั้งอัลฟากลูโค
ซิเดสจากยีสต์ด้วยค่า IC_{50} 18.87 mM รองลงมาได้แก่ สาร1 และสาร 2 ตามลำดับ สาร1-3 ยับยั้งอัลฟากลูโคซิเดส
ในแบบ non competitive นอกจากนี้ยังได้ศึกษาสารสกัดเมทานอลจากเปลือกหุ้มเมล็ดของ *Horsfieldia
macrobotrys* ในการยับยั้งอัลฟากลูโคซิเดส และต้านทานการเกิดออกซิเดชัน สามารถแยกสารกลุ่มเอริลอัลคาโนน
ได้ 2 ชนิด คือ1-(2,4,6-trihydroxyphenyl)-9-phenylnonan-1-one (4) และ malabaricone A (5) รวมทั้ง ฟลา
วาโนนที่มีชื่อว่า 7-hydroxyflavanone (6) เอริลอัลคาโนน 4 เป็นสารยับยั้งอนุมูลอิสระและอัลฟากลูโคซิเดสได้ดี
ที่สุด โดยมีค่า IC_{50} เท่ากับ 2.6 mM และ 10.8 mM ตามลำดับ ที่น่าสนใจคืออนุพันธ์เมทิลอีเทอร์ 4a และ 5a ที่
สังเคราะห์จากเอริลอัลคาโนน 4 และ 5 โดยทำปฏิกิริยากับ MeI/K_2CO_3 แสดงฤทธิ์ยับยั้งที่ลดลงอย่างมาก ผลสังเกต
นี้แสดงให้เห็นว่าหมู่ไฮดรอกซี (-OH) มีบทบาทสำคัญในการยับยั้งอนุมูลอิสระและอัลฟากลูโคซิเดส การศึกษาสาร
4 ยังพบอีกว่าสามารถยับยั้งอัลฟากลูโคซิเดสผ่านกลไกแบบ mixed เนื่องจากเอริลอัลคาโนนที่แยกจากเปลือกหุ้ม
เมล็ดของ *H. macrobotrys* มีฤทธิ์การยับยั้งที่น่าสนใจ ผู้วิจัยจึงได้ทำการศึกษาส่วนอื่นของพืชชนิดนี้ การแยกสาร
สกัดจากเปลือกต้นทำให้ได้เอริลอัลคาโนนชนิดใหม่ 2 ชนิด คือ horsfieldone A (7) และ maingayone D (8)
รวมทั้งฟลาวาโนนกลัยโคไซด์ชชิดใหม่คือ8-C-β-D-glucopyranosylpinocembrin (9) สาร maingayone D (8) มี
ฤทธิ์ยับยั้งอัลฟากลูโคซิเดสและอนุมูลอิสระที่ดีกว่าสาร 7 อย่างมีนัยสำคัญ จากการศึกษายังพบว่าสาร 7 และ 8
ยับยั้งอัลฟากลูโคซิเดสแบบผสม ผลของการศึกษานี้ยังแสดงให้เห็นว่าการใช้ภูมิปัญญาท้องถิ่นของชาวดายัคในกาลิ
มันตันตะวันออกผนวกกับการคัดกรองด้วยการทดสอบฤทธิ์ทางชีวภาพและการทดสอบทางเคมีเป็นหลักการที่
ประสบความสำเร็จในการค้นหาสารต้านเบาหวานที่มีประสิทธิภาพ

สาขาวิชา   เทคโนโลยีชีวภาพ   ลายมือชื่อนิสิต   ....

ปีการศึกษา 2558   ลายมือชื่อ อ.ที่ปรึกษาหลัก   ....

5672883623 : MAJOR BIOTECHNOLOGY

KEYWORDS: ALPHA-GLUCOSIDASE INHIBITOR / ETHNOPHARMACOLOGICAL INFORMATION / CERIOPS TAGAL / HORSFIELDIA MACROBOTRYS / DIABETES MELLITUS / FREE RADICALS

RICO RAMADHAN: EXPLORATION OF BIOACTIVE COMPOUNDS FOR DIABETES THERAPY FROM SELECTED EAST KALIMANTAN FLORA. ADVISOR: ASSOC. PROF. PREECHA PHUWAPRAISIRISAN, Ph.D., 107 pp.

In search of α-glucosidase inhibitors for the treatment of type 2 diabetes mellitus and its complications, we examined the inhibitory effect of selected plants collected from East Kalimantan, Indonesia which included *Leucaena leucocephala*, *Swietenia macrcophylla*, *Pycnarrhena tumefacta*, *Luvunga eleutherandra*, *Crescentia cujete*, *Ceriops tagal* and *Horsfieldia macrobotrys*. On the basis of ethnopharmacological knowledge together with biological and chemical screenings, selected plants were further investigated to afford active compounds. The methanol extract from leaves of *Ceriops tagal* yielded three compounds classified as pentacyclic triterpenoids named lupeol (1), betulone (2) and betulin (3). Of isolated compounds, 3 showed highest inhibition against yeast α-glucosidase with IC_{50} value of 18.87 μM followed by 1 and 2, respectively. The kinetic study of 1-3 showed noncompetitive inhibition against baker's yeast α-glucosidase. In addition, the methanol extract from *Horsfieldia macrobotrys* seed coats was investigated using an α-glucosidase and antioxidant-guided isolation. Two arylalkanones named 1-(2,4,6-trihydroxyphenyl)-9-phenylnonan-1-one (4) and malabaricone A (5) together with a flavanone named 7-hydroxyflavanone (6) were isolated. Arylalkanone 4 was the most potent inhibitor against free radical and baker's yeast α-glucosidase with IC_{50} value of 2.6 mM and 10.8 μM, respectively. Interestingly, the methyl ether analogues 4a and 5a, prepared by methylation of 4 and 5 with MeI/K_2CO_3, showed dramatic drop in inhibition. This observation indicated the critical role of hydroxy groups (-OH) in exerting radical scavenging and α-glucosidase inhibition. The kinetic study of 4 indicated that baker's yeast α-glucosidase was mixed manner.

Since promising bioactivity of isolated arylalkanones from seed coats of *H. macrobotrys*, we further investigated other parts of this plant. Bioassay-guided isolation of stem bark extract resulted in two new arylalkanones named horsfieldone A (7) and maingayone D (8) together with a new flavanone-C-glycoside named 8-C-β-D-glucopyranosylpinocembrin (9). Maingayone D (8) displayed significantly more potent inhibition than 7 against α-glucosidase and free radical. Kinetic study of 7 and 8 indicated their mixed inhibition against α-glucosidase. The results of this study showed that ethnopharmacological knowledge from Dayak people in East Kalimantan together with biological and chemical screenings provided a successful strategy to discover potent antidiabetic agents.

Field of Study: Biotechnology	Student's Signature
Academic Year: 2015	Advisor's Signature

ACKNOWLEDGEMENTS

CONTENTS

LIST OF TABLES

LIST OF FIGURES

LIST OF SCHEMES

LIST OF ABBREVIATIONS

APS	Autoimmune polyglandular syndrome
brs	Broad singlet (NMR)
Calcd	Calculated
CC	Column chromatography
$CDCl_3$	Deuterated chloroform
CD_3OD	Deuterated methanol
CE	Catechin equivalent
CH_3CN	Acetonitrile
COSY	Correlated spectroscopy
d	Doublet (NMR)
dd	Doublet of doublet (NMR)
DPPH	2,2-Diphenyl-1-picrylhydrazyl
DM	Diabetes mellitus
GAE	Gallic acid equivalent
HMBC	Heteronuclear multiple bond correlation experiment
HRESIMS	High resolution electrospray ionization mass spectrum
HSQC	Heteronuclear single bond correlation experiment
Hz	Hertz
IC_{50}	Concentration that required for 50% inhibition in vitro
IDDM	Insulin dependent diabetes mellitus
J	Coupling constant
K_m	Michaelis constant
K_2CO_3	Potasium carbonate
MeI	Methyl iodide
mg	Milligram
mL	Milliliter
MPA	α-methoxyphenylacetic acid
m/z	Mass per charge

NADH	Nicotinamide adenine dinucleotide
NIDDM	Non-Insulin dependent diabetes mellitus
NMR	Nuclear magnetic resonance
pNPG	*p*-nitrophenyl **α**-D-glucopyranoside
QCC	Quick column chromatography
ROS	Reactive oxygen spesies
TLC	Thin layer chromatography
U	Unit
^{13}C NMR	Carbon-13 nuclear magnetic resonance
^{1}H NMR	Proton nuclear magnetic resonance
2D NMR	Two dimensional nuclear magnetic resonance
δ_H	Chemical shift of proton
δ_C	Chemical shift of carbon
λ_{max}	Maximum wavelenght
μM	Micromolar
μL	Microliter
UV	Ultraviolet
ε	Molar extinction coefficient
$[\alpha]_D$	Spesific optical rotation

CHAPTER I

INTRODUCTION

Diabetes mellitus (DM) is a metabolic disorder of multiple aetiololgy characterized by chronic hyperglycaemia with disturbance of carbohydrate, fat and protein metabolism resulting from defects in insulin secretion, insulin action or both [1]. In another information, diabetes mellitus is a common metabolic disease characterized by elevated blood glucose levels, resulting from absent or inadequate pancreatic insulin secretion, with or without the impairment of insulin action. Insulin is a hormone produced in the pancreas that helps transport glucose (blood sugar) from the bloodstream into the cells so they can break it down and use it for fuel [2, 3].

This illness affects approximately 150 millions of people worldwide (Figure 1.1) and its incidences rate is expected to double during the next 20 years. The number is projected to increase to at least 366 million by 2030 [4]. A worldwide survey reported that diabetes mellitus is affecting nearly 10% of the population annually [5].
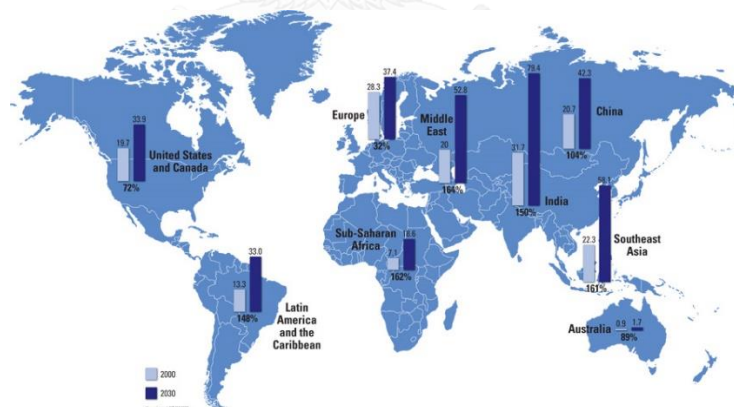
Figure 1.1 Global prevalence of diabetes [6]

Diabetes management can be done by using different strategis. Proper management requires control in preprandial and postprandial hyperglycemia. α-Glucosidase is an enzyme (EC.3.2.1.20) located in the brush-border surface membrane on intestinal cells. It catalyzes the hydrolysis of the α-glycosidic bond of oligosaccharides to liberate the monosaccharide units from dietary sources [7].

Diabetes was first identified as a disease associated with "sweet urine". Elevated levels of blood glucose (hyperglycemia) lead to spillage of glucose into the urine. Normally, the last process of carbohydrate hydrolyzing takes place at small intestine in which carbohydrate is broken down into monosaccharide (glucose). Glucose is absorbed through the cells of the intestine into bloodstream. High level of glucose in blood stream will promote the β-cell of pancreas to release more insulin into bloodstream for transporting glucose into the cells, leading to the decline in the glucose levels (Figure 1.2). However, if pancreas cannot produce insulin or if do not have enough insulin, this will result in diabetes.
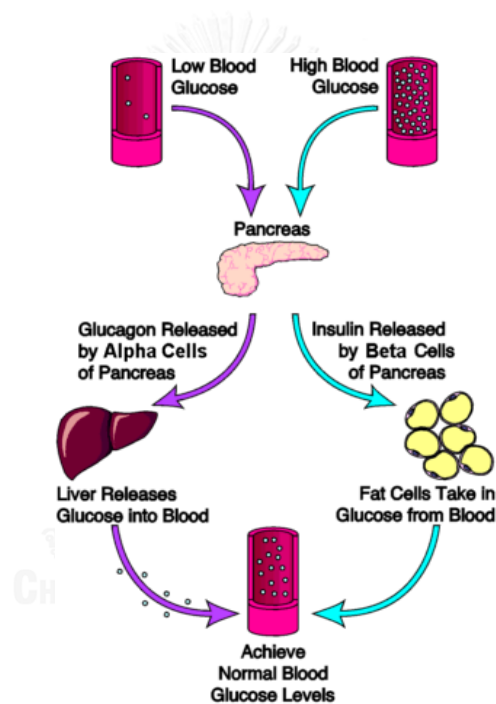
Figure 1.2 Blood sugar regulation (www.endocrineweb.com)

1.1 Diabetes mellitus: Types and differences

Diabetes mellitus can be classified into 3 major classes [8] including to insulin-dependent (type I diabetes), non-insulin-dependent (type II diabetes) and other specific types (such as gestational diabetes, secondary diabetes, wolfram diabetes and autoimmune polyglandular syndrome (APS)). Herein, only type 1 diabetes (IDDM) and type 2 diabetes (NIDDM) are described.
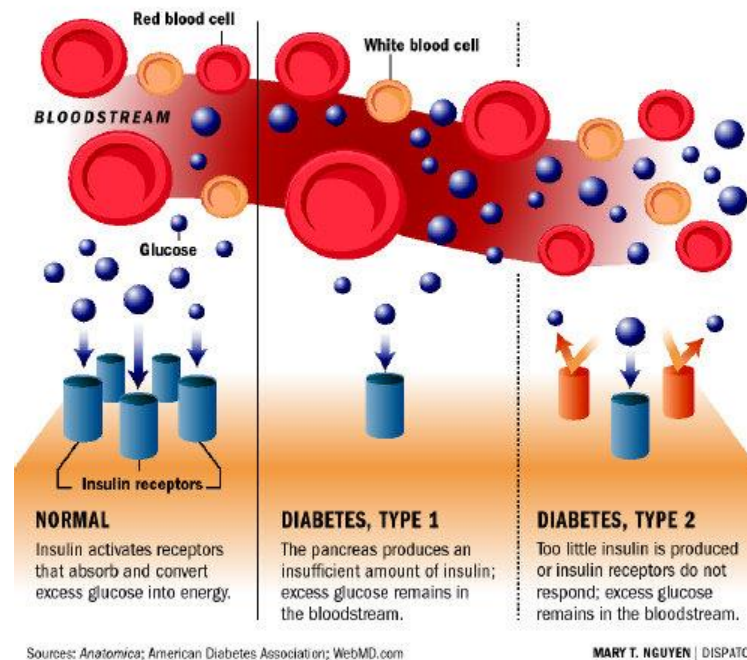
Figure 1.3 Classification of diabetes (www.diabetes.org)

1.1.1 Type I Diabetes mellitus

This form of diabetes, which accounts for only 5 – 10 % of those with diabetes, previously encompassed by terms insulin-dependent diabetes (juvenile-onset diabetes) [8]. It typically develops more quickly than other forms of diabetes. It is usually diagnosed in children and adolescents, and sometimes in young adults. To survive, patients must administer insulin medication regularly. Type 1 diabetes is a condition in which pancreatic-cell destruction usually leads to absolute insulin deficiency [9]. It most often occurs in children and young adults [10]. Since pancreas cannot produce insulin, therefore the patients necessarily to receive insulin injection for therapy (Figure 1.3)

1.1.2 Type II Diabetes mellitus

This form of diabetes, previously referred to as non-insulin-dependent diabetes (Type 2 Diabetes), accounts for 90-95 % of those with diabetes in which the

body cannot produce insufficient insulin. Type 2 diabetes is nearing epidemic proportions due to an increased number of elderly people [10, 11].

The decreased secretion of insulin by the pancreas and resistance to the action of insulin in various tissues (muscle, liver and adipose) results in impaired glucose uptake. An alternative therapheutic appoarch for treating non-insulin diabetes mellitus involves inhibiting α-glucosidase [12]. Insulin resistance is said to be present when the biological effects of insulin are less than expected for both glucose disposal in skeletal muscle and suppression of endogenous glucose production primarily in the liver [13].

The various factors showed that the pathogenesis of type 2 diabetes affect both insulin secretion and insulin action. Eventually, the pancreas cannot produce enough insulin to respond to the body's need for it. Many patients are predescribed antidiabetic agents. People with type 2 diabetes require regular monitoring and ongoing treatment to administer diabetes oral drug. Oral diabetes medications include: α-glucosidase inhibitor, biguanides, meglitinides, sulfonylureas, thiazolidinediones and a new group called DPP-4 inhibitors [14].

1.2 α-Glucosidase inhibitors

Blood sugar levels are mainly determined by absorption of glucose from gut, uptake of glucose by peripheral tissues (muscle, adipose tissue) and the insulin secretion from the pancreas. To enable glucose uptake and absorption by the body and availability as an energy source, intestinal cleavage of starch and oligosaccharides is required. Oligosaccharides are commonly cleaved into monosaccharides by enzyme complexes called α-glucosidases, which are present in the brush border membrane of the small intestine (Figure 1.4) [15, 16].
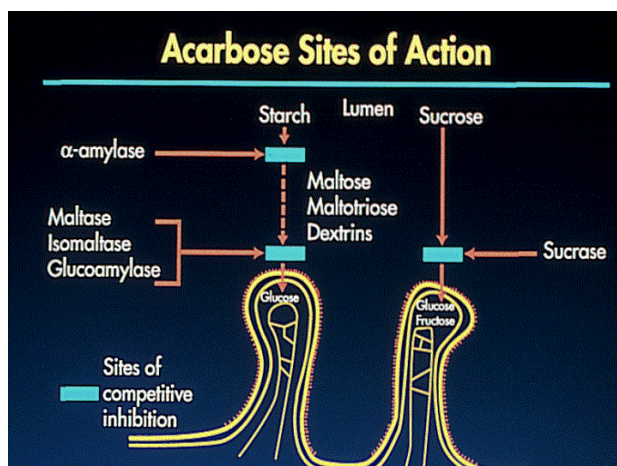
Figure 1.4. In normal digestion, oligosaccharides are hydrolyzed by α-glucosidase located in the intestinal brush border to monosaccharides, which are then absorbed.

Various oral anti-diabetic agents act by modifying the factors aiding in the control of hypoglycemia. These anti-diabetic agents include sulfonylureas (increase insulin secretion), biguannides (increase in glucose uptake) and alpha-glucosidase inhibitors [17].

To date, one potential theraphy for diabetes is inhibiting α-glucosidase, thereby providing an alternative to reduce postprandial hyperglycaemia. Oral antihyperglycemic drugs (Figure 1.5) currently used for alpha-glucosidase inhibitors include acarbose (Precose[®] or Glucobay[®]), miglitol (Glyset[®]) and voglibose (Basen[®]) [15, 17].

Acarbose   Voglibose   Miglitol
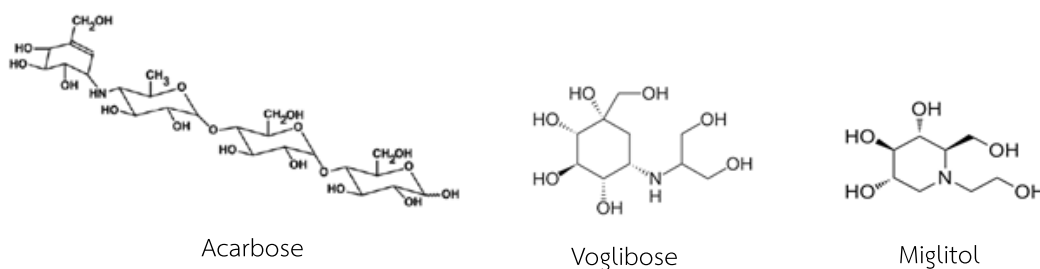
Figure 1.5 Structures of α-glucosidases inhibitors currently used to reduce hyperglycemic.

Acarbose (Figure 1.5) is a pseudomaltotetraose produced by strains of genus *Actinoplanes* sp. It is an inhibitor of **α**-glucosidases and is used in type II diabetes therapy [18]. Acarbose competitively inhibits the function of **α**-glucosidase in the brush border of enterocytes lining the intestinal villi (Figure 1.6). However, continuous use of those acarbose should be limited because long-term administration may cause side effects such as flatulence, abdominal cramp, vomiting and diarrhea.
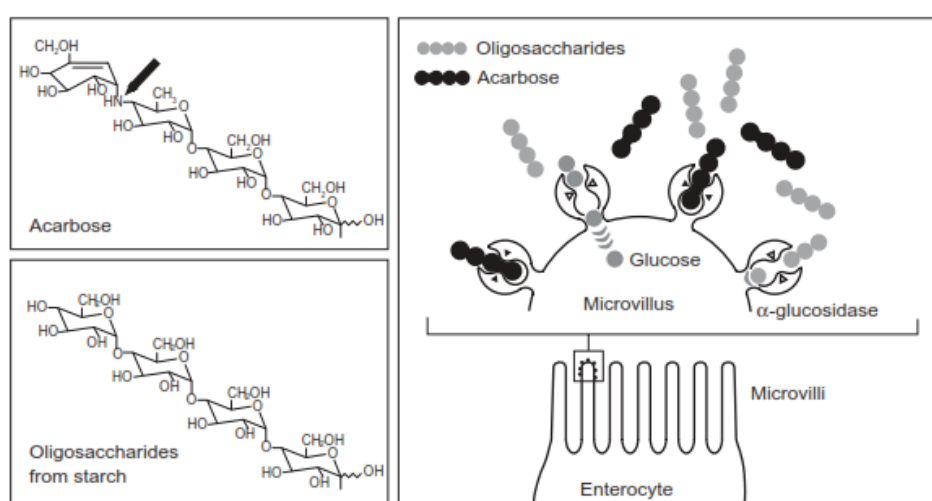
Figure 1.6 Competitive inhibition of acarbose toward intestinal enzymatic hydrolysis of oligosaccharides [15]

1.3 Oxidative stress – Free radicals

Free radical is defined as a species that can exist independently with one or more unpaired electrons (Figure 1.7) [19, 20]. In the living systems, free radicals are predominantly represented as oxidative stress with highly reactive molecules such as reactive oxygen species (ROS). Reactive oxygen species (ROS) include free radicals such as superoxide ($^{•}O_2^{-}$), hydroxyl ($^{•}OH$), peroxyl ($^{•}RO_2$) (Figure 1.8) [21]. In the biological systems, reactive oxygen species (ROS) are unstable and oxidized to other nearby molecules to release the extra energy and return to stable states.
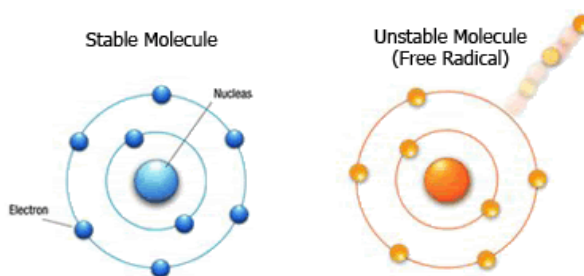
Figure 1.7 Comparison between stable molecule and unstable molecule (free radicals)
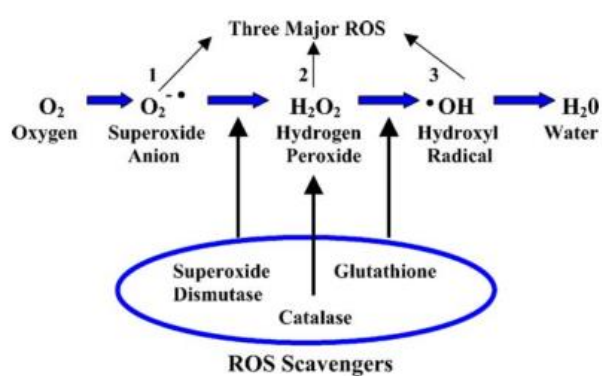
Figure 1.8 Mechanism of formation of reactive oxygen species (ROS)

1.4   Antioxidant

Antioxidants are molecules capable of reducing the causes or effects of oxidative stress. It is help by donating an electrons and stabilizing the free radical (Figure 1.9) [22].
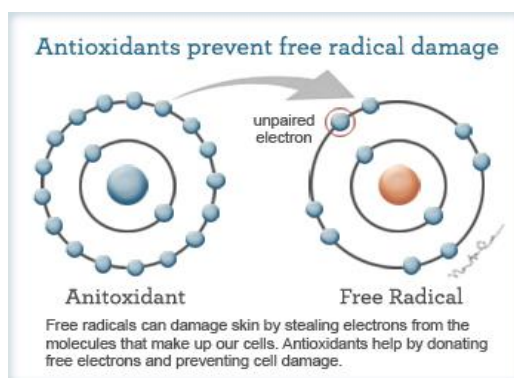
Figure 1.9 Preventive mechanism of antioxidant against free radicals

Antioxidants can inhibit the activity of free radical by several mechanism, which include:

1. Chelating metals that stimulate the production of free radicals
2. Donating electron to free radicals to free radicals to form stable species

Vitamin E (α-tocoferol) is an essensial nutrient which functions as a chain-breaking antioxidant by preventing the propagation of free radical reactions in all cell membranes in human body. Vitamin C (ascorbic acid) is also a part of the normal protecting mechanism [23].

1.5 Relationship of diabetes, oxidative stress and antioxidant

Chronic hyperglycemia in diabetes enhances production the production of free radicals in form of ROS through the non-enzymatic glycosylation and the unbalance of $NADH/NAD^+$ induced by the glucose in cell also from cytochrome P450 monooxygenases, protein glycation and glucose autoxidation, which lead to oxidative cellular damage. Thus far, glucose also reacts with proteins in non-enzymatic way leading to the improvement of advanced glycation end products which alters protein function (Figure 1.10) [24].
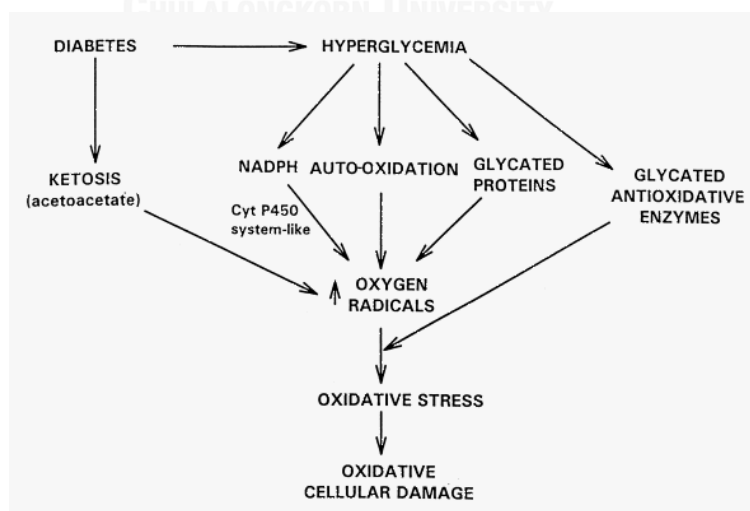
Figure 1.10 Generation of reactive species in diabetes

In diabetes, oxidative stress is likely to be caused by both increased production of free radical and sharp reduction in antioxidant defenses. On the other hand, increasing antioxidant potential may be valuable for the prevention of diabetes complications. Therefore, it is propective strategy to prevent diabetes complications using combination of agents that are capable of reducing hyperglycemia and oxidative stress.

1.6   Ethnopharmacology and biodiversity of Kalimantan island

Kalimantan, the Indonesian part of Borneo Island, is one of the biggest and most important tropical forests in the world. It comprises five main areas including West Kalimantan, Central Kalimantan, South Kalimantan, East Kalimantan as well as North Kalimantan, which is recently established as a new province.

East Kalimantan covers an area of 197.485 km^2 with the geographical position at 02° 27' 20" South Latitude – 04° 24' 55" North Latitude and 113° 49' - 119° 57' East Longitude along the equator of the Borneo Island (Figure 1.11). The topography of this area greatly varies from lowland to mountainous terrain that results in the high level of biological diversity [25, 26]. The influence factors that support the heterogeneity of biodiversity in Kalimantan Island are the rainfall throughout each year and soil types. The rainy season occurs between November and April, with average of annual rainfall around 1500-4500 mm and temperature range from 16.4-35.4°C. The large amount of rainfall and high temperature enhance the rate of decomposition, or the breakdown and decay of living matter that makes it possible for plants to absorb nutrients more quickly and promotes the rapid growth of plants in this area [27]. Therefore, tropical rainforests should have high diversity since they contain so many of these specialized conditions.

Although there have been annual botanical surveys in East Kalimantan flora, it is estimated that by 10 % of collected plants have been further investigated for potential applications in natural medicines. In addition, biological and chemical screenings of all collected plants are tedious, time-consumed and perharps low-hit-target. These problems could be addressed by taking ethnopharmacology into

account. Ethnopharmacology is considered as scientific evidence observed by local people who actually utilized medicinal plants for particular theraphy. On the basis of biological and chemical screenings together with ethnopharmacology, this is a good opportunity to discover potential bioactive compounds from plants collected from East Kalimantan.
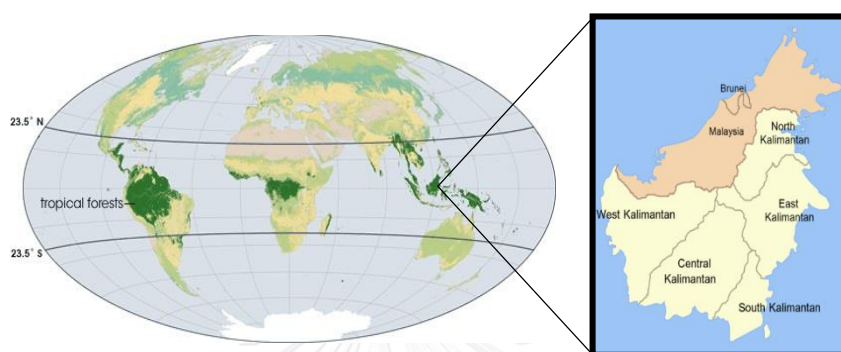
Figure 1.11 The map of Kalimantan Island and tropical rainforest ranges in the world.

Ethnopharmacology is defined as a study by ethic group or local people on their use of traditional drugs, which are mainly derived from plants. Moreover, ethnopharmacology recently includes scientific processes such as observation, description and experimental investigation of indigenous plants and their biological activities [28]. Ethnopharmacological information from local people is considered as important hints for natural product chemists who are searching for bioactive compounds from particular plants used for the therapy of certain diseases. Without this, discovery of bioactive compounds is generally tedious, time consumed and perhaps low-hit-target. Indigenous value and knowledge about medicinal plants species and their functional use and ecology are key aspects of Dayak people from East Kalimantan [26]. Dayak, meaning 'people of the upstream', are the indigenous non-Malay people in Borneo (Figure 1.12A).

Dayak communities are aware of their dependence on their natural resources and vital need to conserve. It is well recognized that degradation of resources can lead to serious negative consequences, mostly upon succeeding generations. Dayak

communities share important information including potential plants in the forest for religion, medicine and economy based on heredity or generation to generation [26]. Using traditional knowledge as a selection strategy has proven more rapidly and easily to indentify bioactive compounds, therefore giving priority to certain plants for depth examination (Figure 1.12B) [29]. Several ethnopharmacological surveys have been published during recent years on traditional medicine in several cultures with the aim of preserving their herbal remedies usage as well as finding an evidence-based approach to their corresponding use. Several medicinal plants in East Kalimantan forests have also been reported about their biological activities based on the ethnopharmacological information.

(A)   (B)

Figure 1.12 (A) Dayak people, (B) The Dayak women collecting medicinal plants.

1.7   Investigation of bioactive compounds from plants collected in East Kalimantan based on ethnopharmacology

Investigations on plants of East Kalimantan flora are quite limited because they are prohibited by the local government to be exported outside. However, this restriction is also allowed for the project that is jointly investigated by local researchers. Arung and colleagues at Mulawarman University are the pioneers in searching for bioactive compounds from plants collected from East Kalimantan forests. They applied ethnopharmacological information of Dayak to search for bioactive

compounds that could be developed for cosmetic products. Particular examples included buds of *Syzygium aromaticum* [30], leaves of *Eupatorium triplinerve* Vahl [31] and bulbs of *Eleutherine americana* L. Merr (bawang tiwai) [32]. The methanolic extracts of these plants, mostly containing coumarins, showed melanin inhibition approximately 40 – 60 % against human melanoma cell lines without significant toxicity. These results suggested potential use as whitening agents in cosmetic products. Phytochemical surveys of plants collected in Borneo by other teams were also carried out, which included *Macaranga triloba* [33], *Durio affinis* Becc [34], *Durio ibethinus* and *Durio kutejensis* [35] and *Durio carinatus* and *Durio oxleyanus* [36].

Even though many studies have reported the use of medicinal plants to cure various type of illness, there are only a few studies reported on treatment of diabetes mellitus by herbal remedies in East Kalimantan. Ethnobotanical studies of traditional herbal remedies used for diabetes around the world have identified more than 1,200 species of plants with hypoglycaemic activity [37] while less than 10 species have been reported in East Kalimantan [38].

The use of plant derived products containing high concentration of dietary fiber and complex polysaccharide for management of diabetes have been proposed. Natural products especially of plant origin have been found to be potential sources of novel molecules for the treatment of diabetes [39]. Major phytochemicals from plants e.g phenolic acid, flavonoid, coumarin etc., are known to protect against an oxidative stress in human body by maintaining a balance between oxidants and antioxidants. In addition, many efforts have been made to search for more effective and inexpensive inhibitors against α-glucosidase, from natural materials to treat diabetes. Moreover, the combination of α-glucosidase inhibitors and antioxidants will become more effective for the prophylaxis of type 2 diabetes [40].

The chronic exposure to hyperglycemia in diabetes patients is a major causative factor to induce the oxidative stress through over production of reactive oxygen species (ROS) that may be a contributory factor to several diabetic complications from cell injury and tissue damage [41]. The negative effects of oxidative stress may be mitigated by the consumption of antioxidants. Antioxidants are the compounds that

protect cells against the injury by delay or inhibit the oxidative chain reactions. They act by one or more of the following mechanisms: reducing activity, free radical scavenging, potential complexation of pro-oxidant metals and quenching of singlet oxygen [42]. Many epidemiological studies have shown that numerous phytonutrients found in plant are able to protect the human body against damage caused by ROS. Further evidence that antioxidants, in term of polyphenolic compounds from plant materials, are linked to prevention of diabetic complications was found from *in vivo* studies of diabetic rats [43]. The extracts are capable of reducing oxidative stress by scavenging reactive oxygen species and preventing cell damage. In fact, it is well established that the consumption of natural antioxidant phytochemicals was reported to have many potential health benefits. Therefore, the purposes of this research are to report the scientific information of the medicinal plants species used to relieve diabetes disorders by the population in the East Kalimantan area including their antioxidant properties, inhibitory effect of α-glucosidase and the mechanism of enzyme inhibition from isolated bioactive compounds.
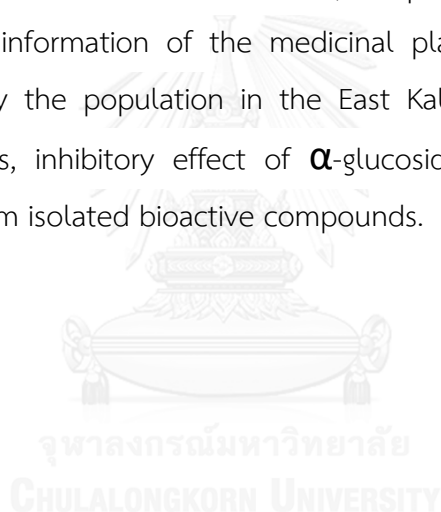
CHAPTER II

BIOPROSPECTING POTENTIAL OF SELECTED EAST KALIMANTAN PLANTS

AS α-GLUCOSIDASE INHIBITORS AND RADICAL SCAVENGERS

2.1   Introduction

East Kalimantan province in Borneo is one of the richest provinces in Indonesia with natural resources such as rainforests. These resources provided a lot of potential such as woods, mushrooms, medicinal plants and another resources. Many information about plants has potential for medicinal plants such as ethnopharmacology knowledge from local people.

Ethnopharmacology is scientific evidence observed by local people who actually utilized medicinal plants for particular therapy. This approach is usefull in natural products discovery to investigation indigenous medicinal plants [26].

Leucaena leucocephala   *Swietenia macrcophylla*   *Pycnarrhena tumefacta*

Luvunga eleutherandra   *Crescentia cujete*   *Ceriops tagal*

Figure 2.1 Selected plants from East Kalimantan flora

Traditionally, Dayak communities share important information including potential plants in the forest for religion, medicine and economy based on heredity or generation to generation [26]. Using traditional knowledge as a selection strategy has proven more rapidly and easily to indentify bioactive compounds, therefore giving priority to certain plants for depth examination [29]. It is of great interest to find out

whether the traditional plants used for diabetes theraphy, have activities that might be useful to prevent diabetes and its complications.

In this study, six plants were selected based on the ethnopharmacological knowledge of Dayak people for diabetes theraphy. The selected plants were *Leucaena leucocephala*, *Swietenia macrophylla*, *Pycnarrhena tumefacta*, *Luvunga eleutherandra*, *Crescentia cujete* and *Ceriops tagal* (Figure 2.1). The information in detail of selected plants is summarized in Table 2.1

Table 2.1 Six selected plants from East Kalimantan and their ethnopharmacological information

Scientific name	Local name	Plant part	Ethnopharmacological information	References
Leucaena leucocephala	Lamtoro	Seeds	1. A decoction of the seeds is administered in cases reduced of high blood sugar level. 2. Seeds used for lipid lowering effect and increased regeneration of β-cells of pancreas in STZ-induced diabetic rats.	[44], [45] together with personal communication
Swietenia macrophylla	Mahoni	Seeds	1. Raw seeds are crewed to treat blood sugar level. 2. Antihyperglycaemic activity by treatment of STZ-induced diabetic rats. 3. Antidiabetes acticivity by treatment of nicotinamide induced type 2 diabetic rats.	[46], [47] [48]
Pycnarrhena tumefacta (Syn. *Pycnarrhena cauliforia)*	Apa' Sengkubak	Leaves	1. A decoction of the leaves is used for natural tasty and local people used for reduced blood sugar level. 2. Antioxidant activity by scavenging free radicals DPPH.	[49], [50], [51] together with personal communication

Table 2.2 Six selected plants from East Kalimantan and their ethnopharmacological information (Cont.)

Scientific name	Local name	Plant part	Ethnopharmacological information	References
Luvunga eleutherandra (Syn. *L. augustifolia, Triphasia sarmentosa*)	Seluang belum	Roots	1. Crushed roots are soaked in hot water and administered used for reduced blood sugar level. 2. Bark and leaves are used to care pain in limbs and rheumatism. 3. Others part such as stems are used orally administered to treat malaria and fatigue.	[52], [53], [54], [55] together with personal communication
Crescentia cujete	Berenuk	leaves	1. Leave decoction is taken as a remedy for treat blood sugar level. 2. Other functions of leaves are used as diuretic, treat tumors and cough. 3. Cyanhidric acid from leaves is stimulatives of the insulin release. 4. Bioactivity has been documented is antibacterial and cytotoxicity.	[56], [57] [58] together with personal communication
Ceriops tagal	Tingi	leaves	1. A decoction of leave is taken orally to treat blood sugar level. 2. Antihyperglycaemic activity in normoglycaemic and STZ-induced diabetic rats. 3. Other parts such as bark also used for treat antihyperglycemic and hemorrhage.	[7], [59] [60] together with personal communication

Based on information above, the objective of this study was therefore to provide scientific basis for the use of selected plants in East Kalimantan through the verification of their ethnopharmacological use for diabetes theraphy.

2.2   Results and discussion

2.2.1   Total phenolic, total flavonoid and total antioxidant capacity

The total of phenolic, flavonoid and antioxidant capacity of selected plants from East Kalimantan flora are shown in Table 2.3. Total phenolic content of selected plants was evaluated using Folin-Ciocalteu method and expressed as mg gallic acid equivalent (GAE)/ g dry extract of selected plants. The content of total flavonoid was

measured by aluminium chloride method and expressed as mg catechin equivalent (CE)/g dry extract of selected plants. Whereas, the antioxidant capacity of selected plants was determined using colorimetric method by reduction of molybdenum formation and expressed as mg gallic acid equivalent (GAE)/ g dry extract of selected plants.

Table 2.2 Total phenolic, total flavonoid and antioxidant capacity of selected plants

Plants	Total phenolics mgGAE/g dry extract	Total flavonoid mgCE/g dry extract	Total antioxidant capacity mgGAE/g dry extract
Leucaena leucocephala	137.40±0.08	16.70±0.02	77.58±0.02
Swietenia macrcophylla	13.92±0.01	1.32±0.004	62.88±0.07
Pycnarrhena tumefacta	26.40±0.01	50.36±0.03	77.71±0.01
Luvunga eleutherandra	105.92±0.01	31.80±0.05	152.21±0.01
Crescentia cujete	53.92±0.01	139.85±0.04	168.63±0.01
Ceriops tagal	42.30±0.01	137.53±0.03	215.16±0.02

* Data shown as mean of triplicate experiments

Total phenolic content of selected plants ranged from 13.92 to 137.40 mgGAE/g dry extract. The highest concentrations of total phenolic (137.40 mgGAE/g dry extract) were found in *Leucaena leucocephala*. On the other hand, the highest total flavonoid (139.85 mgCE/g dry extract) was detected in *Crescentia cujete* followed by *Ceriops tagal* (137.53 mgCE/g dry extract). In the result of total antioxidant capacity found *Ceriops tagal* showed highest concentrations (215.16 mgGAE/g dry extract). However, *Swietenia macrcophylla* were relatively low in total phenolics, total flavonoid and antioxidant capacity. From this point of view, the selected plant can be concluded that extract of *Leucaena leucocephala*, *Crescentia cujete* and *Ceriops tagal* can become a valuable source of antioxidant.

2.2.2   Antioxidant activity

The antioxidant activity of selected plants was evaluated using DPPH assay as a stable radical. In table 2.4, *Ceriops tagal* showed the highest DPPH scavenging activities value of 26.24 ± 2.89 µg/mL followed by *Crescentia cujete* and *Luvunga*

eleutherandra with values of 37.87 ± 8.58 and 39.33 ± 3.88 µg/ml, respectively. This result suggested that *Ceriops tagal* provide potential as natural sources of antioxidant.

Table 2.3 DPPH scavenging activity of selected plants

Plants	DPPH Scavenging activity (IC_{50}) µg/mL*
Leucaena leucocephala	88.92±3.19
Swietenia macrcophylla	31.76±10.39
Pycnarrhena tumefacta	98.54±6.20
Luvunga eleutherandra	39.33±3.88
Crescentia cujete	37.87±8.58
Ceriops tagal	26.24±2.89
Ascorbic acid (Vit C)	11.09±2.58

* Data shown as mean of triplicate experiments

2.2.3 α-Glucosidase inhibition of selected plants

Selected plants were investigated for α-glucosidase inhibitory activity by using baker's yeast and rat intestine as a source of enzymes.

Table 2.4 α-Glucosidase inhibitory effect of selected plants

Plants	Plant parts	IC_{50} values (mg/mL)[a]		
		Yeast	Maltase	Sucrase
Leucaena leucocephala	Seeds	6.11±0.03	1.88±0.95	16.58±12.4
Swietenia macrcophylla	Seeds	8.09±0.48	4.56±2.20	5.88±4.47
Pycnarrhena tumefacta	Leaves	5.33±0.57	5.33±3.83	8.72±4.16
Luvunga eleutherandra	Roots	5.87±0.73	3.79±0.67	21.80±10.4
Crescentia cujete	Leaves	4.08±0.25	2.95±0.71	5.78±0.82
Ceriops tagal	Leaves	0.07±1.92	1.70±0.55	3.02±2.82
Acarbose		2.99±0.75	0.49±0.05	0.49±0.12

[a]Data shown as mean of triplicate experiments

In Table 2.5, *Ceriops tagal* showed strongest inhibitory effect among plants examined. It revealed highly potent inhibition against yeast α-glucosidase over other selected plants with IC_{50} value of 0.07 mg/mL while its inhibitions against rat intestinal α-glucosidase were in range of 1.70-3.02 mg/mL. The enhanced inhibition of *Ceriop tagal* was likely to be contribute by its highest antioxidant activity (Table 2.3). Based on the above results, *C.tagal* was selected for further investigation to isolate compounds responsible for such bioactivities.

2.2.4 Extraction and isolation

The air-dried leaves (57.81 g) of *C. tagal* were crushed and extracted with MeOH at room temperature for 48 h. After removing the solvent by evaporation under reduced pressure, the crude extract (24.5 g) was partitioned with *n*-hexane to obtain methanol (2.76 g) and *n*-hexane (0.2817 g) fractions. The methanol extract (2.76 g) was subjected to quick column chromatography (QCC) by silica gel and eluted with dicloromethane:*n*-hexane as a gradient to afford seven fractions; fraction A (17 mg); fraction B (30 mg); fraction C (87 mg); fraction D (93 mg); fraction E (141 mg); fraction F (278 mg) and fraction G (387 mg). All the fractions were checked for TLC profile to know character from compounds. Fractions C, D and E showed a good TLC profile with several interesting spots. Fraction C (87 mg) was chromatographed on silica gel and eluted with a mixture of 50 % dichloromethane: *n*-hexane to yield lupeol (**1**, 60 mg). Fraction D (93 mg) was chromatographed on Sephadex LH-20 column and eluted with 100 % MeOH. Further purification was also carried out using Sephadex LH-20 and eluted with a mixture of 10:10:80 EtOAc-MeOH-*n*-hexane to give betulone (**2**, 7 mg). Fraction E (141 mg) was first chromatographed on Sephadex LH-20 column (100 % MeOH) followed by silica gel chromatography eluted with a mixture of 10:90 EtOAc-*n*-hexane to give betulin (**3,** 19 mg). The isolation procedure is summarized in (Scheme 3.1).
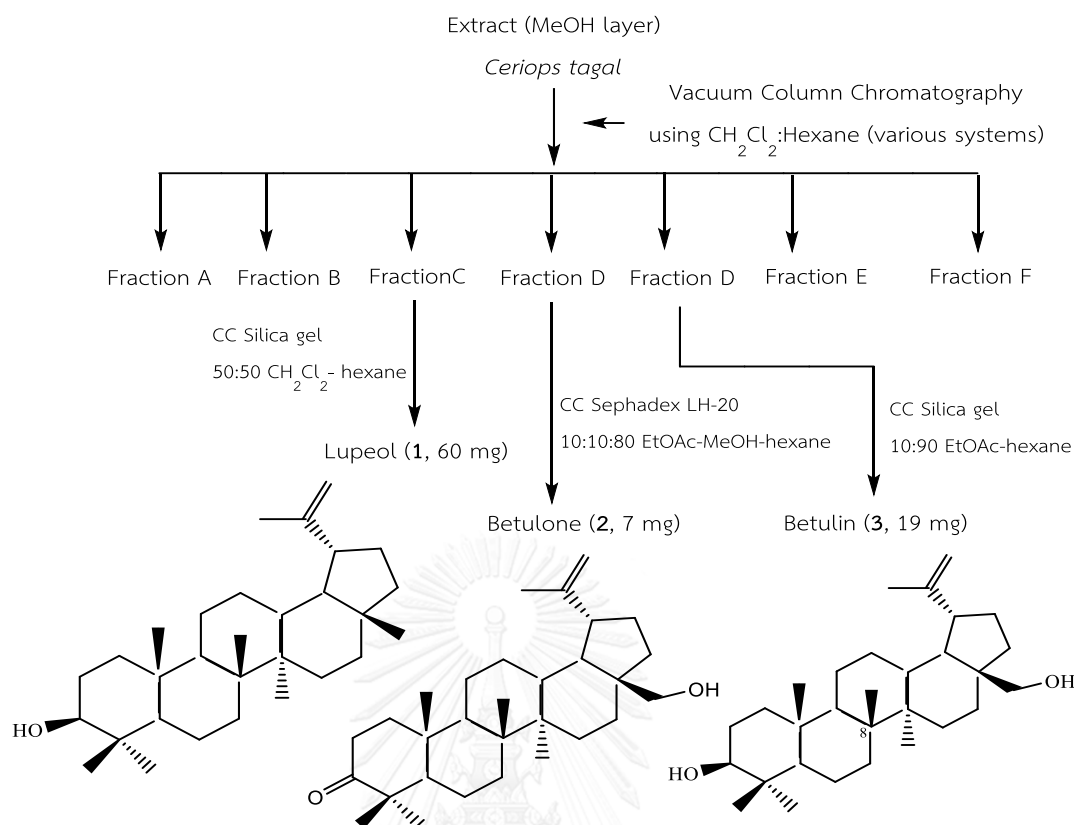
Scheme 2.1 Isolation procedure of isolated compounds from leaves of *Ceriops tagal*

2.2.5 Structure elucidation of 1

Lupeol (**1**) was obtained as a white powder. The structure was deduced by the results from ^{1}H, ^{13}C spectroscopic methods. The ^{1}H NMR spectral revealed the presence of seven tertiary methyl protons at δ_H 0.75, 0.78, 0.82, 0.94, 0.97, 1.02 and 1.67 (H-30). Two protons appeared at δ_H 4.56 and 4.68 as singlets, representing the olefinic protons at H-29a and H-29b. One proton at δ_H 2.37 were assigned as H-19. The H-3 proton showed a double of doublet at δ_H 3.18 (*J*= 5.08, 11.16 Hz). The ^{13}C NMR spectral showed 30 signals for the terpenoid of lupine skeleton which was represented by seven methyl groups. The carbon bonded to the hydroxyl group C-3 appeared at δ_C 79.0, while the olefinic carbon appeared at δ_C 150.9 and 109.3 were assigned as C-20 and C-19, repectively. In addition, the structure of lupeol as the same previously studies (Figure 2.2) [61].
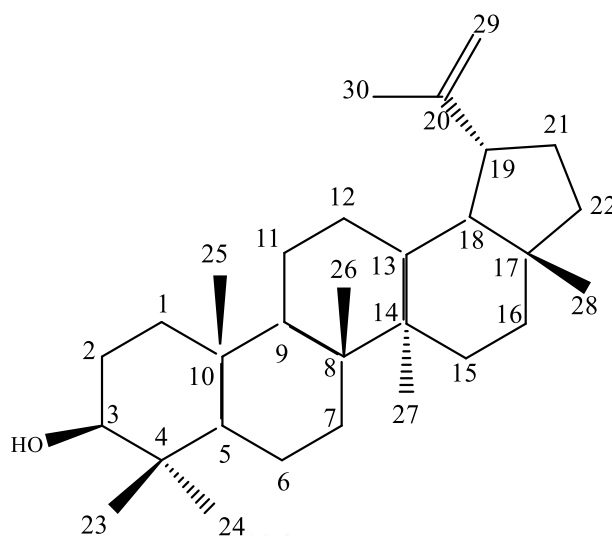
Figure 2.2 Lupeol **(1)**

2.2.6   Structure elucidation of 2

Betulone (**2**) was obtained as a white powder. The structure was deduced by the results from ^{1}H, ^{13}C spectroscopic methods. The ^{1}H NMR spectral revealed the presence of five tertiary methyl protons at δ_H 0.75, 0.78, 0.82, 0.94, 0.97, 1.02 (each 3H). Two pair of isopropylene proton signals at δ_H 4.68 (1H, s) and 4.58 (1H, s) were assigned as H-29a and H-29b, respectively. In addition, two germinal proton signals at δ_H 3.79 (1H, d, *J*= 10.8 Hz) and 3.34 (1H, d, *J*= 10.8 Hz) were assigned as H-28a and H-28b, repectively. The ^{13}C NMR spectral exhibited one carbonyl signal at δ_C 217.9 were assigned as C-3, while two olefinic proton signals at δ_C 150.4 and 109.7 were assigned as C-20 and C-19, respectively. In addition, one oxygenated proton signals at δ_C 60.6 were assigned as C-28. Therefore, the structure of betulone as the same previously studies (Figure 2.3) [62].
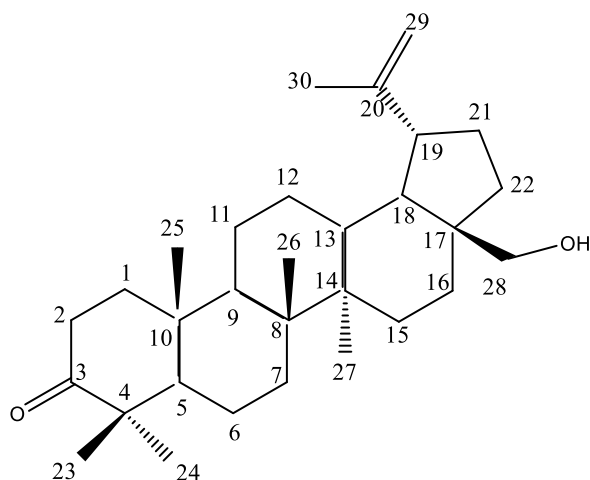
Figure 2.3 Betulone **(2)**

2.2.7 Structure elucidation of 3

Betulin (**3**) was obtained as a white powder. The structure was deduced by the results from ^{1}H, ^{13}C spectroscopic methods. The ^{1}H NMR spectral showed proton signals of isopropylene at δ_H 4.68 (1H, s) and 4.58 (1H, s) were assigned as H-29a and H-29b, respectively. Two germinal proton signals at δ_H 3.79 (1H, d, J=10.4 Hz), 3.33 (1H, d, J=10.8 Hz) were assigned as H-28b and H-28a, respectively. In addition, one proton signal at δ_H 3.18 (1H, dd, J=11.0, 4.84) were assigned as H-3 (3β-hydroxyl). The ^{13}C NMR spectral showed the double bond of lupeol was observed as shifts at δ_C 151.2 and 109.8 were assigned as C-20 and C-29, repectively. The oxygenated carbon of C-3 was observed at δ_C 79.2. Therefore, the structure of betulin as the same previously studies (Figure 2.4) [63].
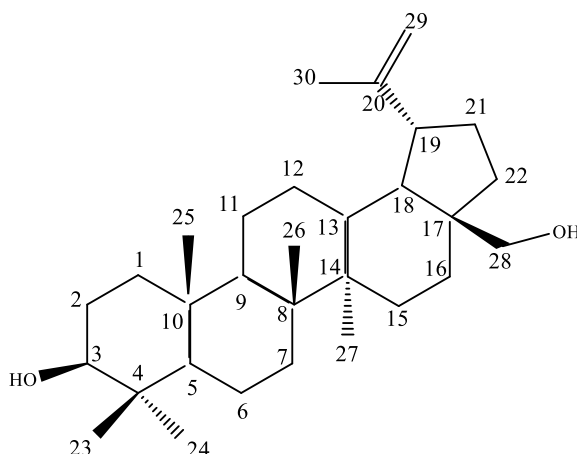
Figure 2.4 Betulin **(3)**

2.2.8 **α**-Glucosidase inhibition of compounds 1-3

Inhibitory activity of isolated compounds (**1-3**) was determined against **α**-glucosidases (Table 2.6).

Table 2.5 α-Glucosidase inhibition of isolated compounds (**1-3**)

Compounds	IC_{50} (**μ**M)[a]		
	Baker's yeast	Rat Intestinal	
		Maltase	Sucrase
1	23.90	NI[b]	1,052.66
2	27.73	NI	1,194.77
3	18.87	NI	1,186.75
Acarbose	103.0	2.1	26.0

[a] Data shown as mean of duplicate experiments.

[b] NI, no inhibition, inhibitory effect less than 30 % at 10 mg/mL.

Compounds **1-3** from *Ceriops tagal* leaves were classified as pentacyclic triterpenoids. In Table 2.6, compounds **1-3** inhibited yeast **α**-glucosidase with IC_{50} values in range of 18.87-27.73 **μ**M. On the other hand, they showed no inhibition toward rat intestine maltase, whereas inhibition of **1-3** against rat intestine sucrose was

weak. To gain insight into the mechanism underlying the inhibitory effects of **1-3**, a kinetic study was also conducted. The lineweaver-Burk plots (Figures 2.5, 2.6 and 2.7, respectively) revealed a linear relationship at each tested concentration of **1-3**. Interestingly, all straight lines have intersected in the x-axis at a single negative value. The analysis demonstrated that V_{max} decreased with increasing concentration of **1-3** while K_m remained constant (Table 2.7), supporting that **1-3** inhibits α-glucosidase in a noncompetitive manner (Ki of 5.95, 2.55 and 1.21 μM, repectively).

Table 2.6 Inhibition mechanism

Type of inhibition	K_m	V_{max}	Intersection
Competitive	increase	unchanged	Y axis, Y > 0
Non-competitive	unchanged	decrease	X axis, X < 0
Uncompetitive	decrease	decrease	no intersection
Mixed	increase	decrease	second quadrant
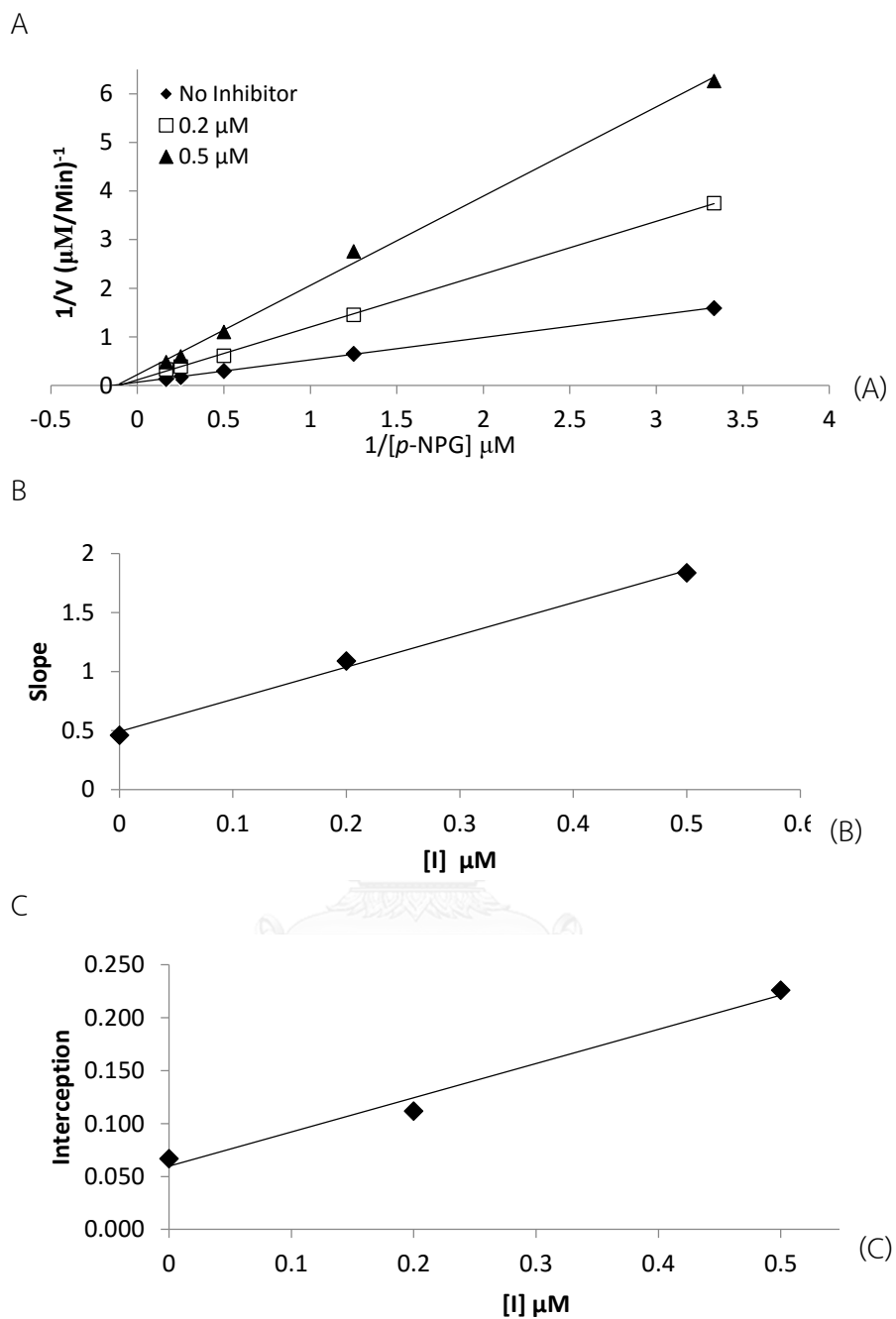
Figure 2.5 (A) Lineweaver-Burk plot of lupeol (1), 1/V against 1/[S]. **(B)** Secondary replot of slope vs. [I] from a primary Lineweaver-Burk plot for the determination of Ki. **(C)** Secondary replot of intercept vs. [I] from a primary Lineweaver-Burk plot for the determination of Ki'.

A

(A)

B

(B)

C

(C)
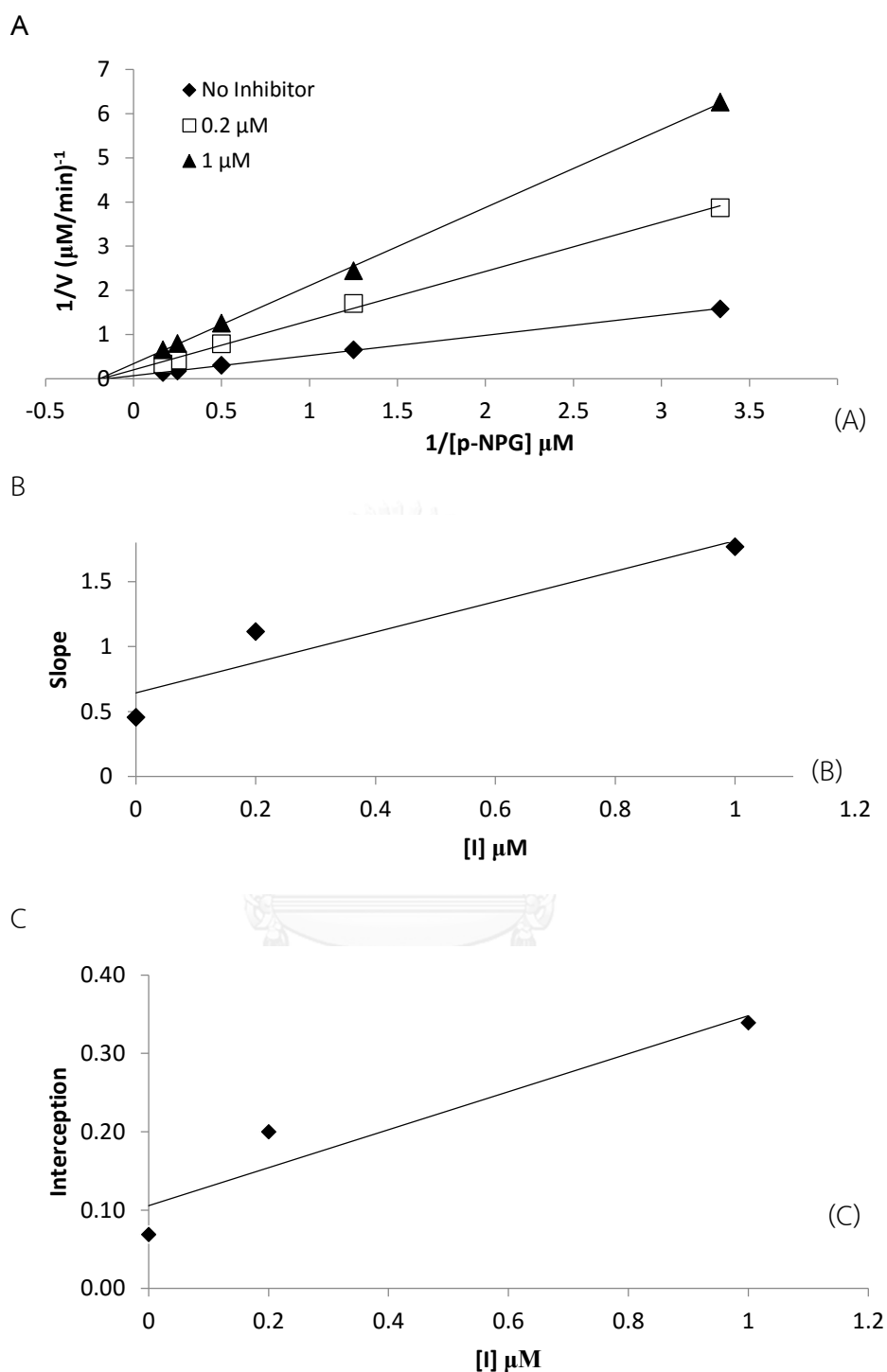
Figure 2.6 (A) Lineweaver-Burk plot of betulone (2), 1/V against 1/[S]. **(B)** Secondary replot of slope *vs.* [I] from a primary Lineweaver-Burk plot for the determination of K_i. **(C)** Secondary replot of intercept *vs.* [I] from a primary Lineweaver-Burk plot for the determination of K_i'.

A

B

C
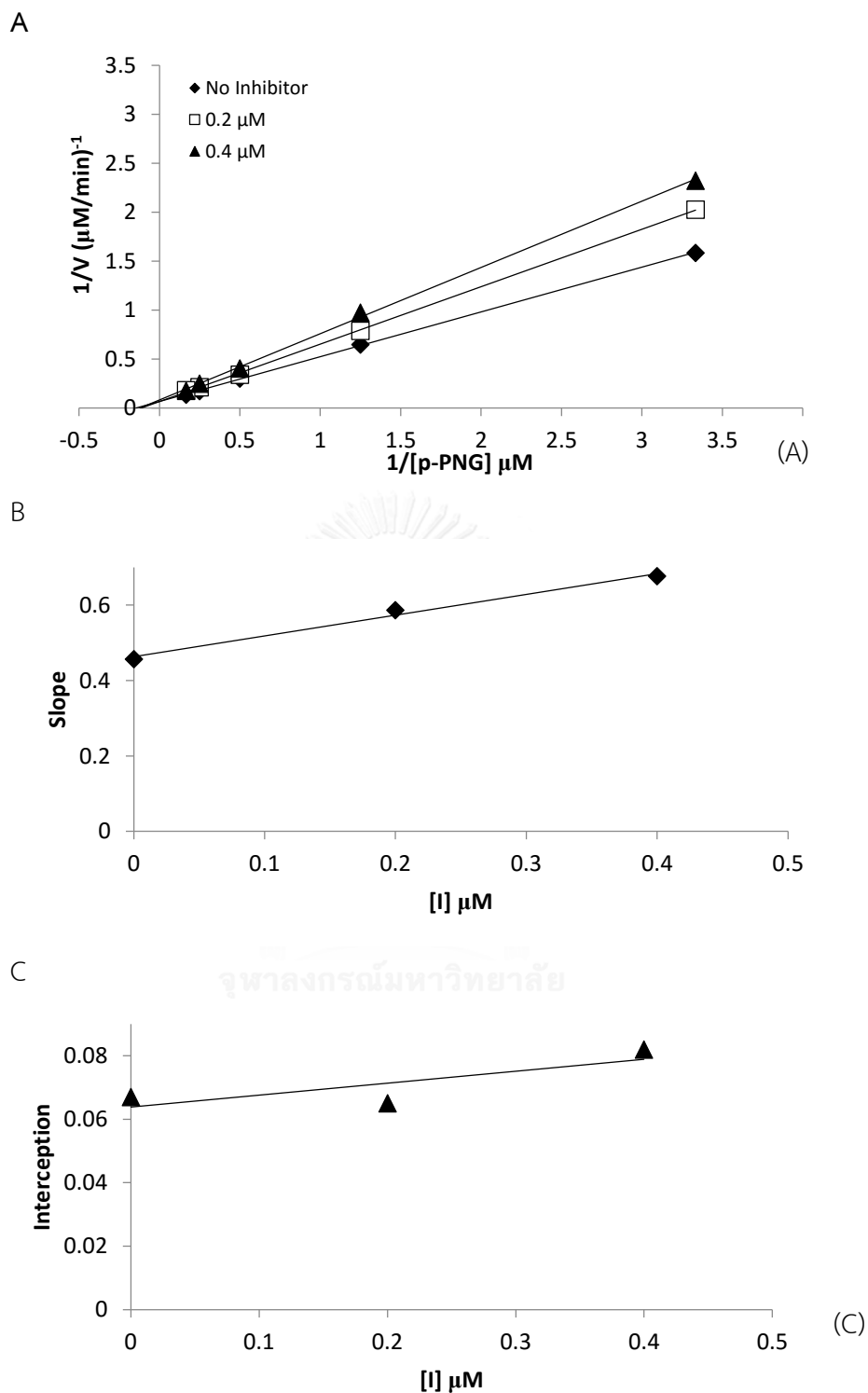
Figure 2.7 (A) Lineweaver-Burk plot of betulin (3), 1/V against 1/[S]. **(B)** Secondary replot of slope *vs.* [I] from a primary Lineweaver-Burk plot for the determination of K_i. **(C)** Secondary replot of intercept *vs.* [I] from a primary Lineweaver-Burk plot for the determination of K_i'

2.3   Experimental section

2.3.1   General experimental procedures

NMR spectra were recorded on a 400 MHz Bruker AVANCE spectrometers. The chemical shifts were reported in ppm as referenced to solvent residues. Chromatography was performed on a Sephadex LH-20, Merck silica gel 60 (70-230 mesh) and TLC was performed on precoated Merck silica gel 60 F_{254} plates (0.25 mm thick layer). 2.2-Diphenyl-1-picrylhydrazyl (DPPH), quercetin, Folin-Ciocalteu reagent, α-Glucosidase (EC 3.2.1.20) from *Saccharomyces cerevisiae* and 4-nitrophenyl-α-D-glucopyranoside (*p*-NPG) were obtained from Sigma-Aldrich (St. Louis, MO, USA). Gallic acid was obtained from Wako Pure Chemical Industries, Japan. Ascorbic acid (Vitamin C), sodium nitrite, aluminium chloride, sodium hydroxide, sulfuric acid, ammonium molybdate, sodium carbonate, sodium acetate, methanol were obtained from Merck, Darmstadt, Germany. Acarbose was obtained from Bayer Vitol Leverkusen, Germany. Rat intestinal acetone powder was supplied by Sigma Aldrich. Spectrophotometric measurements for the α-glucosidase inhibition, antioxidant assay and kinetic study were taken on a Sunrise microplate reader spectrophotometer.

2.3.2   Plant material

Plants were collected from their natural habitat in the rain forest from East Kalimantan, Indonesia. Plant authentication was carried out by Plant Physiology Laboratory at the Mulawarman University. The plant species, with local names and voucher number, used in this study were *Leucaena leucocephala* (seeds) "lamtoro/petai china" (KK-1305-LA001), *Swietenia macrophylla* King (seeds) "Mahoni" (KK-1305-MA001), *Pycnarrhena tumefacta* (leaves) "Daun Apa/Bekai'" (KK-1305-BK001), *Luvunga eleutherandra* (roots) "Seluang Belum" (KK-1305-SE001), *Cresentia cujete* (leaves) "Berenuk" (KK-1305-BR001) and *Ceriops tagal* (leaves) "Tingi" (KK-1305-TI001). All plant specimens have been deposited at the Forest Products Chemistry Laboratory at The Mulawarman University, East Kalimantan, Indonesia.

2.3.3 Extraction and isolation

The air-dried leaves (57.81 g) of *Ceriops tagal* were crushed and extracted with MeOH at room temperature for 48 h. After removing the solvent by evaporation under reduced pressure, the crude extract (24.5 g) was partitioned with *n*-hexane, and obtained methanol (2.76 g) and *n*-hexane (0.2817 g) fractions. The methanol extract (2.76 g) was subjected to quick column chromatography (QCC) by silica gel and eluted with dicloromethane : *n*-hexane as a gradient to afford seven fractions; Fraction A (17 mg); fraction B (30 mg); fraction C (87 mg); fraction D (93 mg); fraction E (141 mg); fraction F (278 mg) and fraction G (387 mg). All the fractions were checked for TLC profile to know character from compounds. Fractions C, D and E showed a good TLC with several profile with several interesting spots. Fraction C (87 mg) was chromatographed on silica gel and eluted with a mixture of 50 % dichloromethane-*n*-hexane to yield lupeol (**1, 60 mg**). Fraction D (93 mg) was chromatographed on Sephadex LH-20 column and eluted with 100 % MeOH. Further purification was also carried out using Sephadex LH-20 and eluted with a mixture of 10:10:80 EtOAc-MeOH-*n*-hexane to give betulone (**2, 7 mg**). Fraction E (141 mg) was first chromatographed on Sephadex LH-20 column (100 % MeOH), followed by silica gel chromatography eluted with a mixture of 10:90 EtOAc:*n*-hexane to give betulin (**3, 19 mg**).

Lupeol (1) white powder, mp 120-122°C; ^{1}H NMR (CDCl$_3$, 400 MHz) δ_H 4.56 (1H, s H-29a), 4.68 (1H, s, H-29b), 3.16 (each 3H, m), 2.37 (1H, m), 0.75, 0.78, 0.82, 0.94, 0.97, 1.02, 1.67 (each 3H, s). ^{13}C NMR (CDCl$_3$) δ_C 150.9 (C-20), 109.3 (C-29), 79.0 (C-3), 55.3 (C-5), 50.4 (C-9), 48.3 (C-19), 47.9 (C-18), 43.0 (C-17), 42.8 (C-14), 40.8 (C-8), 40.0 (C-22), 38.8 (C-4), 38.7 (C-1), 38.1 (C-13), 37.2 (C-10), 35.6 (C-16), 34.3 (C-7), 30.4 (C-21), 28.0 (C-23), 27.4 (C-15), 25.0 (C-12), 20.9 (C-11), 19.3 (C-30), 18.2 (C-6), 18.0 (C-28), 16.1 (C-26), 15.9 (C-25), 15.3 (C-24), 14.5 (C-27).

Betulone (2) white powder, mp 201-2013 °C; ^{1}H NMR (400 MHz CDCl$_3$) δ_H 4.68 (1H, s, H-29a) , 4.58 (1H,s, H-29b), 3.79 (1H, d, *J*= 10.8 Hz, H-28a), 3.34 (1H, d, *J*= 10.8 Hz, H-28b), 2.47 (m, H-2), 2.40 (m, H-19), 1.68 (3H, s, H-30) 1.10, 1.09, 1.05, 1.02, 0.95

(each 3H, s). ^{13}C NMR (CDCl$_3$) δ_C 217.9 (C-3), 150.3 (C-20), 109.7 (C-29), 60.6 (C-28), 54.9 (C-5), 49.7 (C-9), 48.7 (C-18), 47.7(C-17), 47.7 C-19), 47.3 (C-4), 42.8 (C-14), 40.9 (C-8), 39.6 (C-1), 37.4 (C-13), 36.8 (C-10), 34.1 (C-2), 33.9 (C-22), 33.5 (C-7), 29.7 (C-21), 29.1 (C-16), 27.1 (C-15), 26.6 (C-23), 25.2 (C-12), 21.3 (C-11), 21.0 (C-24), 19.6 (C-6), 19.1 (C-30), 15.9 (C-25), 15.8 (C-26), 14.7 (C-27).

Betulin (3) white powder, mp 234-236°C; ^{1}H NMR (400 MHz CDCl$_3$) δ_H 4.68 (1H, s, H-29a), 4.58 (1H, s, H-29b), 3.79 (1H, d, J=10.4 Hz, H-28b), 3.33 (1H, d, J=10.8, H-28a), 3.18 (1H, dd, J=11.0, 4.84, H-3), 1.67 (3H, s, H-30), 0.95, 0.91, 0.82, 0.76 and 0.69 (each 3H, s). δ_C 151.2 (C-20), 109.8 (C-29), 79.2 (C-3), 60.8 (C-28), 55.5 (C-5), 50.6 (C-9), 48.8 (C-18), 47.8 (C-17, C-19), 38.8 (C-4), 38.7   (C-1), 37.4 (C-13), 37.2 (C-10), 34.3 (C-7), 33.9 (C-22), 29.8 (C-21), 29.2 (C-16), 27.9 (C-23), 27.4 (C-2), 27.1 (C-15), 25.3 (C-12), 20.4(C-11), 19.3 (C-30), 18.3 (C-6), 16.1 (C-25), 15.9 (C-26), 15.3 (C-24), 14.7 (C-27).

2.3.4   Chemical screening and Bioactivity

2.3.4. Total phenolic content

A protocol based on the Folin-ciocalteau method described by Orak [64] was employed to detemine the total amount of present phenolic compounds in various extract of plants. The extracts (0.2 mL) at concentration of 30 mg/mL was added to 15.8 mL aquabidest and then was added 1 mL Folin-ciocalteau reagent. Sodium carbonate solution (1 mL) at concentration of 20 % was added to mixture. The mixture was then incubated at 27°C for 2 hours before the absorbance of solutions were measured at 750 nm using a spectrophotometer. Lastly, the total phemolic contents were expressed as a gallic acid equivalent (GAE) besed on Folin-ciocalteau calibration curve using gallic acid as the standard

2.3.4.2 Total flavonoid

The total flavonoid content in extracts was determined according to Choi [65]. Standars solution or samples extract (250 μL) was mixed with 1.25 mL of distilled water and 75 μL of 5 % NaNO$_2$ solution. After incubation for 5 min, 150 μL of 10 % AlCl$_3$.H$_2$O was added. After 6 min, 500 μL of 1 M NaOH and 275 μL of distilled water were added

to the mixture solutions were measured at 500 nm using a spectrophotometer . All determinations were performed in triplicate. Total flavonoid values are expressed in term of catechin equivalents (CE) per gram of plant extracts.

2.3.4.3 Total antioxidant capacity

The total antioxidant content in extract was determined according to Prieto [66]. 100 μL of sample solution (100 μg/mL) was mixed with 1000 μL of reagent (0.6 M sulfuric acid, 28 mM sodium phosphate an 4 mM ammonium molybdate. The mixtures are allowed for 90 min incubation at 95 $^{\circ}$C in boiling water bath and the absorbance was read at 695 nm after cooling in room temperature. Total antioxidant values are expressed in term of gallic acid equivalents (GAE) per gram of plant extracts.

2.3.4.4 Antioxidant activity (DPPH)

The DPPH radical scavenging activities of the each extract were determined by the method of Arung [67] with minor modification. Briefly, 30.3 μL each of the samples at various concentrations was mixed with 469.7 μL methanol and then shake and was mixed with 500 μL of 68 μM DPPH in the methanol. The reaction mixture was then incubated at room temperature in the dark for 30 min. The control contained all reagent without samples, whereas methanol was used as a blank. All measurements were performed in triplicate. DPPH radical scavenging activity was determined by measuring the absorbance at 517 nm.

2.3.4.5 α-glucosidase inhibitory activity from Baker' Yeast

The α-glucosidase inhibition assay was performed according to our previous protocols [68]. The α-glucosidase (0.4 U/mL) and substrate (1 mM p-nitrophenyl-α-D-glucopyranoside) were dissolved in 0.1 M phosphate buffer (pH 6.9). A 10 μL test sample was pre-incubated with yeast α-glucosidase (40 μL) at 37°C for 10 min. A substrate solution (50 μL) was then added to the reaction mixture and incubated at 37°C for an additional 20 min, and terminated by adding 1 M Na_2CO_3 solution (100 μL). The enzymatic hydrolysis of the p-NPG was monitored based on the amount of p-

nitrophenol released into the reaction mixture (Figure 2.8). Enzymatic activity was quantified by measuring the absorbance at 405 nm (Sunrise microplate reader). The percentage inhibition of activity was calculated as follows: % Inhibition = $[(A_0-A_1)/A_0] \times 100$, where: A_0 is the absorbance without the sample; A_1 is the absorbance with the sample. The IC_{50} value was deduced from the plot of % inhibition versus concentration of test sample. Acarbose was used as standard control and the experiment was performed in duplicate.
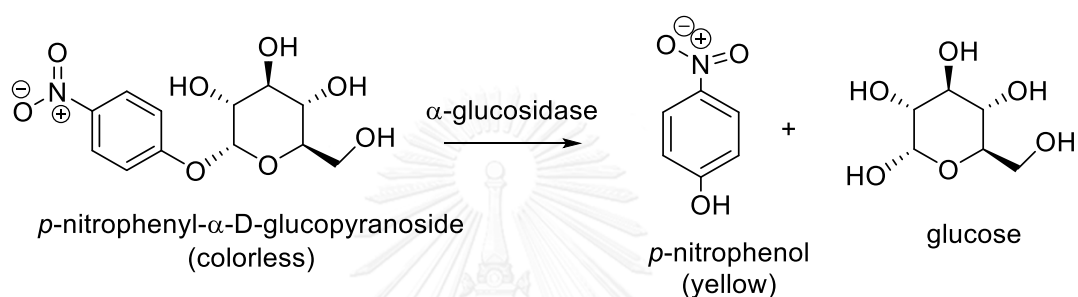
Figure 2.8 Hydrolysis of Baker's yeast **α**-glucosidase

2.3.4.6 **α**-glucosidase inhibitory activity from rat intestine

The inhibition against rat intestinal **α**-glucosidase (maltase and sucrase) was carried out using a similar protocol with baker's yeast. Briefly, 10 μL of the test sample was added to 0.1 M phosphate buffer (pH 6.9, 30 μL), 20 μL of the substrate solution (maltose: 10 mM; sucrose: 100 mM) in 0.1 M phosphate buffer, glucose kit (80 μL) and the crude enzyme solution (20 μL). The reaction mixture was then incubated at 37°C for either 10 min (for maltose) or 40 min (for sucrose). The concentration of glucose released from the reaction mixture was detected by the glucose oxidase method using a glu-kit (Human, Germany) (Figure 2.9). Enzymatic activity was quantified by measuring absorbance at 503 nm.

.

Glucose + H$_2$O + O$_2$ $\xrightarrow{\text{Glucose Oxidase}}$ Gluconic acid + H$_2$O$_2$

2 H$_2$O$_2$ + [4-aminophenazone] + [phenol] $\xrightarrow{\text{Peroxidase}}$ [quinoneimine (pink)] + 4H$_2$O

4-aminophenazone   quinoneimine (pink)
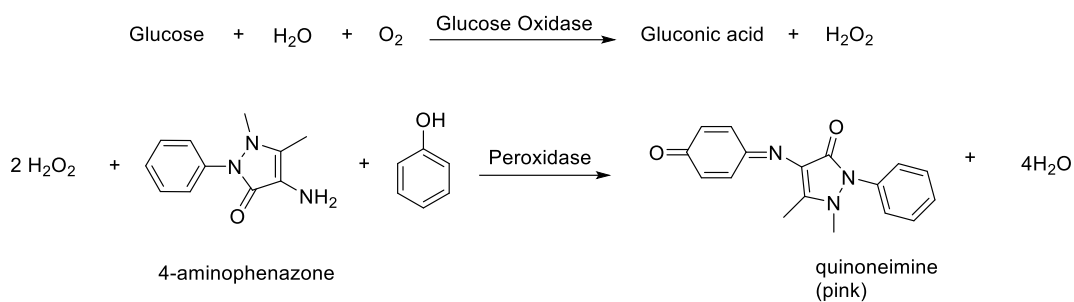
Figure 2.9 The reaction principle of **α**-glucosidase from rat small intestine

2.3.4.7 Kinetic study of **α**-glucosidase inhibition

In order to evaluate the type of inhibition, enzyme kinetic analysis was performed according to the above reaction. The type of inhibition was determined from Lineweaver-Burk plots. The quantity of yeast **α**-glucosidase was maintained at 0.4 U/mL, and the concentrations of each tested (**1-3**) were varied in the range of 0-1 µM. The K_i value was determined from secondary plots of slope *vs*. [I], and the K'_i value was calculated from secondary plots of interception *vs*. [I].

SUPPORTING INFORMATION

Figure 2.10 ^{1}H-NMR spectrum (400 MHz, in CDCl$_3$) of lupeol **(1)**

Figure 2.11 ^{13}C-NMR spectrum (100 MHz, in CDCl$_3$) of lupeol **(1)**

Figure 2.12 ^{1}H-NMR spectrum (400 MHz, in CDCl$_3$) of betulone **(2)**

Figure 2.13 ^{13}C-NMR spectrum (100 MHz, in CDCl$_3$) of betulone **(2)**
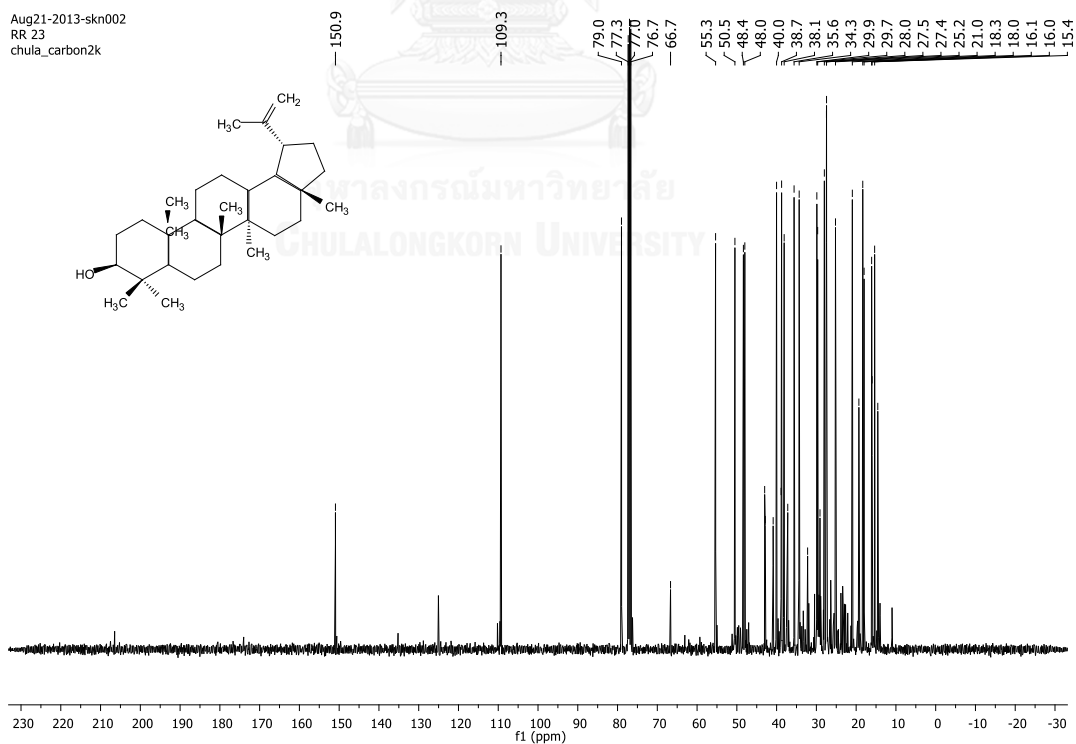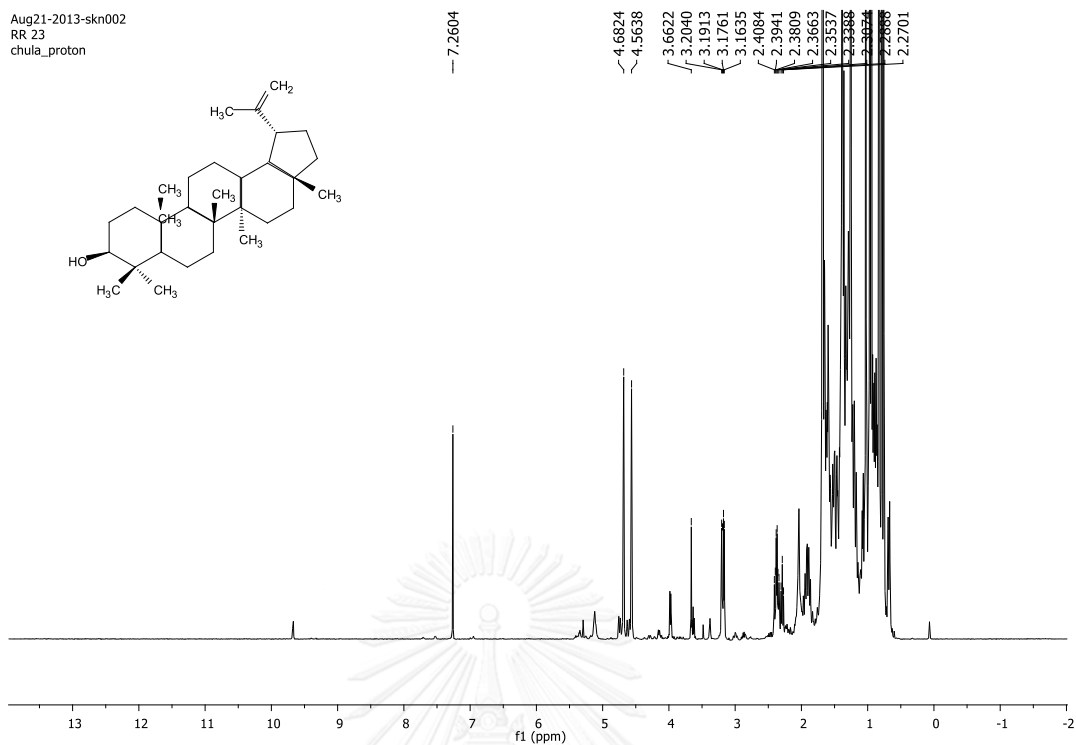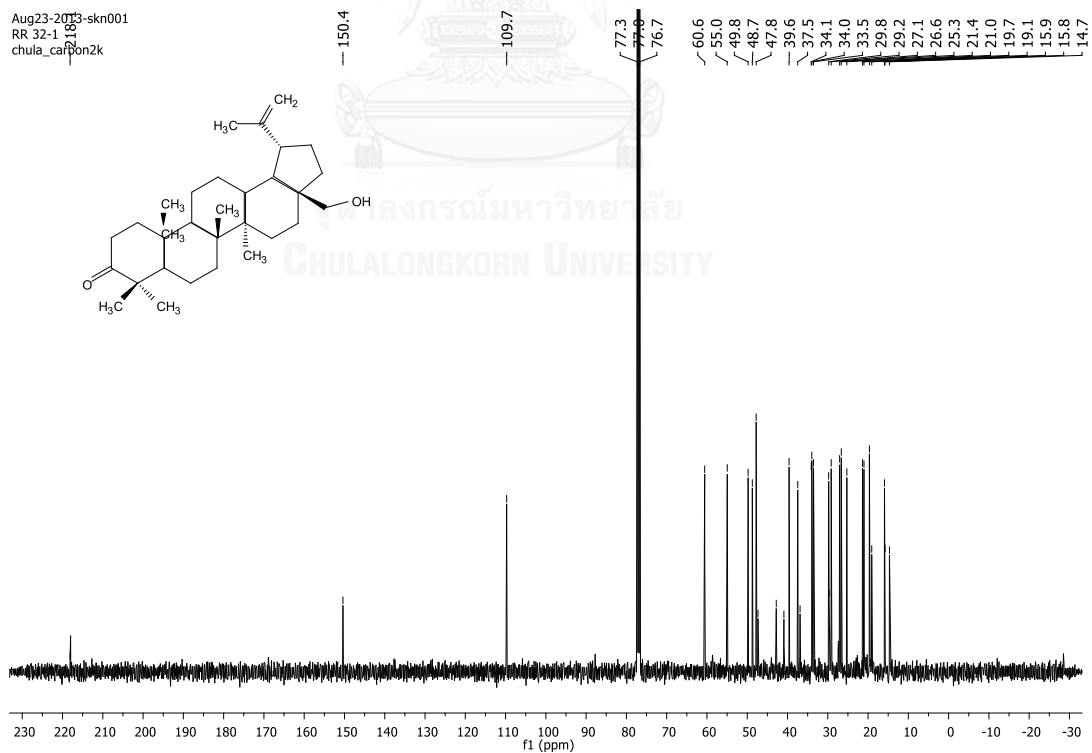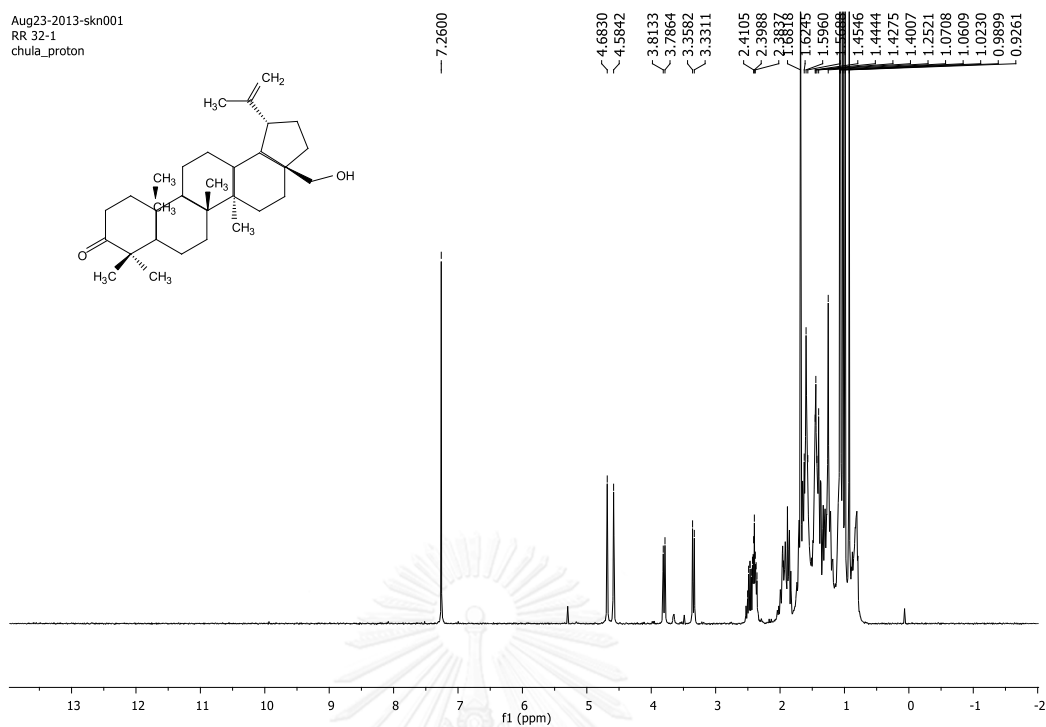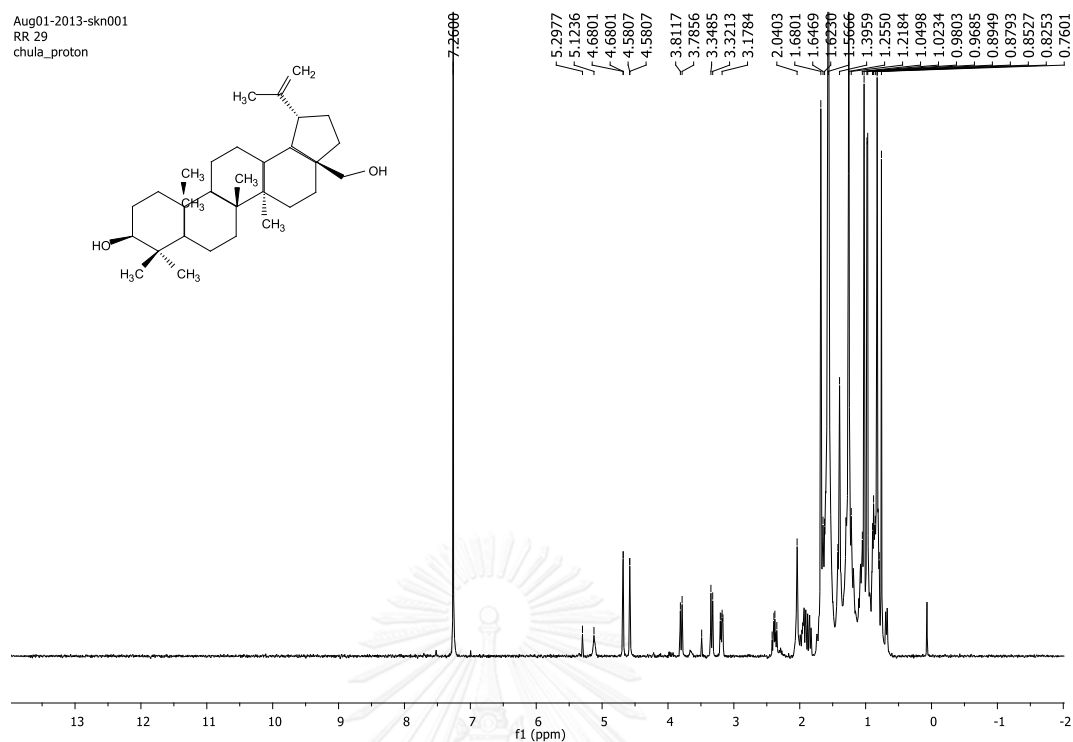
Figure 2.14 ^{1}H-NMR spectrum (400 MHz, in CDCl$_3$) of betulin **(3)**
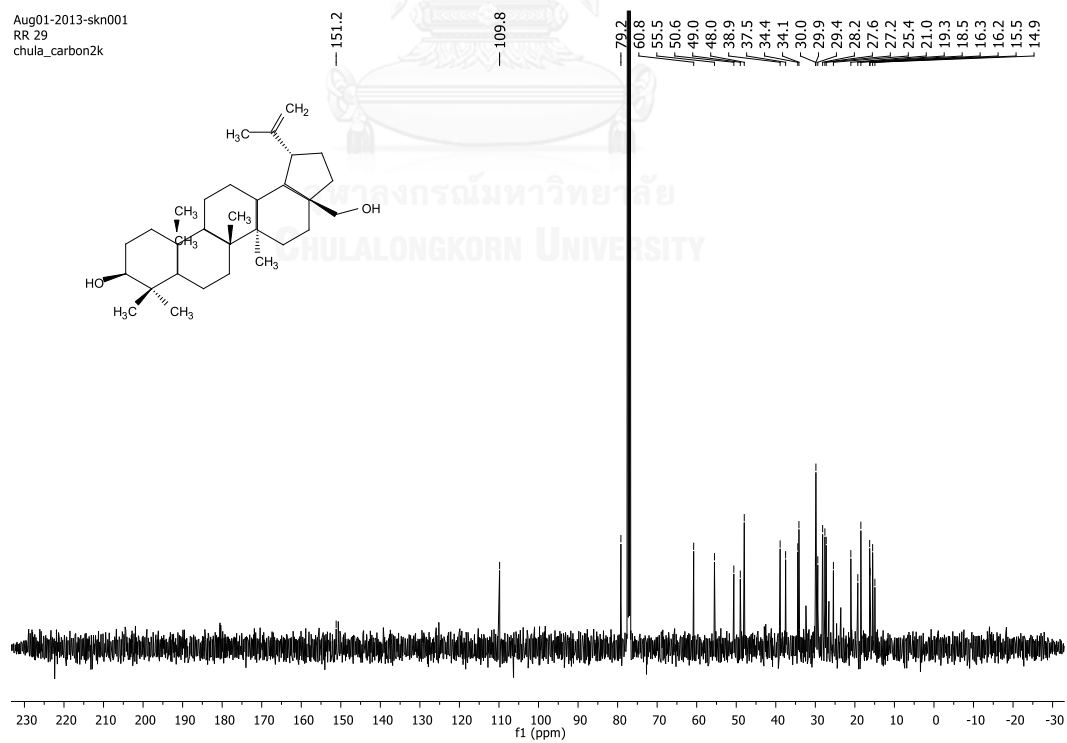
Figure 2.15 ^{13}C-NMR spectrum (100 MHz, in CDCl$_3$) of betulin **(3)**

CHAPTER III

ARYLALKANONES FROM *Horsfieldia macrobotrys* SEED COATS ARE EFFECTIVE ANTIDIABETIC AGENTS ACHIEVED BY α-GLUCOSIDASE INHIBITION AND RADICAL SCAVENGING

3.1 Introduction

3.1.1 Botanical aspect and distribution

The Myristicaceae family found in lowland rainforest in Asian tropics, tropical America, Africa and Madagascar. It consists of about 440 species belonging to 19 different genera. Several genera had been widely explored since the beginning of the 20th century such as Myristica, Horsfiedia, Knema and Virola due to their used in traditional medicine and biological acitivity from several reports [69, 70].

Horsfieldia is the second largest genus after *Myrisctica* in Southeast Asian. A genus of *Horsfieldia* distributed from India to southern China, Southeast Asian and northern of Australia [71]. Represented in Southeast Asia from East Kalimantan by *Horsfieldia* macrobotrys. *Horsfieldia macrobotrys* Merr (syn. *Myristica motley*) is a large tree with a tall straight trunk, brances are crowden on the top of the trunk. The flowers are small and unisexual and the plants are dioecious. The fruits are solitary, supported by a persistent with a brown pericarp that is thick and leathery. For the inside of fruits, the cream colored ovoid seed is inclosed by bright yellow aril [72-74]. The traditional name of *H. macrobotrys* in East Kalimantan is Dara-dara or Deraya. Particular botanical aspects of *H. macrobotrys* are shown in Figure 3.1.
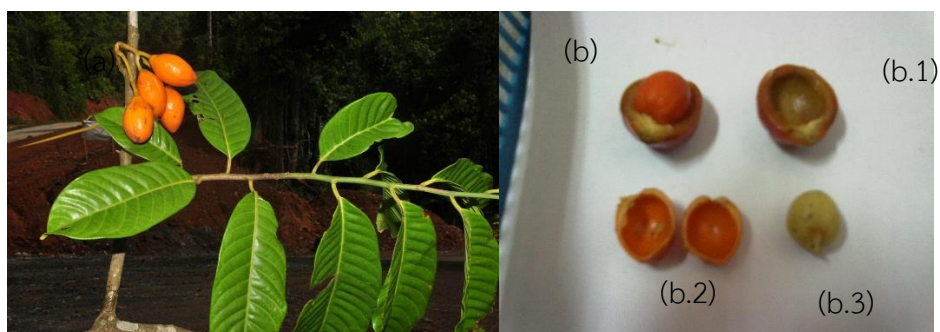
Figure 3.1 Botanical aspects of *Horsfieldia macrobotrys* Merr: (a) seeds and leaves, (b) pericraps (b.1), seed coats (b.2) and seeds (b.3).

3.1.2 Phytochemical and pharmacological investigation

Previous phytochemical studies family of Myristicaceae is known to produce mainly lignans and arylalkanones. A number of lignans, chromones, diarylpropanoids, arylalkanones, procyanidins and neolignans have been described from different *Horsfieldia* species with several bioactivities, such as antidiabetes [75], antimalarial [76], cytotoxicity activity [77], [70], antibacterial [78] and acetylcholinesterase inhibitors [79].

Phytochemical studies of the aerial part of *Horsfieldia glabra* revealed the presence of trymyristin, (+)-asarinin, (-)-dihydrocubebin, 1-(2,6-dihydroxyphenyl)-11-phenylundecan-1-one and 1-(2,4,6-trihydroxyphenyl)-9-phenylnonan-1-one [80]. Other species such as *Horsfieldia iryaghedhi* (syn. *Myristica horsfieldia*) revealed the occurence of myristin acid, lauric acid and dodecanoylphloroglucinol [81, 82].

In addition, other species from *Horsfieldia helwigii* also displayed antimicrobial activity [78]. However, the phytochemical investigation and antidiabetic activity of *Horsfieldia macrobotrys* Merr are reported herein for the first time. Therefore, it is of interest to isolate and identify active compounds using α-glucosidase inhibition and free radical scavenging activity guided isolation.

3.2   Results and discussion

3.2.1   Isolation

Dried seed coats of *Horsfieldia macrobotrys* (300 g) were ground and extracted with methanol (MeOH). The MeOH extract was partitioned with equal volume of *n*-hexane. The methanolic layer was evaporated and fractionated on Sephadex LH-20 using mixtures of MeOH-hexane-CH$_2$Cl$_2$, yielding 14 fractions. Fractions 11 to 14 were combined and purified by Sephadex LH-20 (MeOH:hexane:CH$_2$Cl$_2$) to afford 1-(2,4,6-trihydroxyphenyl)-9-phenylnonan-1-one (**4**). The combined fractions 3 and 4 were purified by silica gel using hexane:CH$_2$Cl$_2$ to afford malabaricone A (**5**). The combined fractions 8 to 10 were further purified by silica gel (ethyl acetate:hexane) to yield 7-hydroxyflavanone (**6**). The isolation procedure is summarized in (Scheme 3.1).
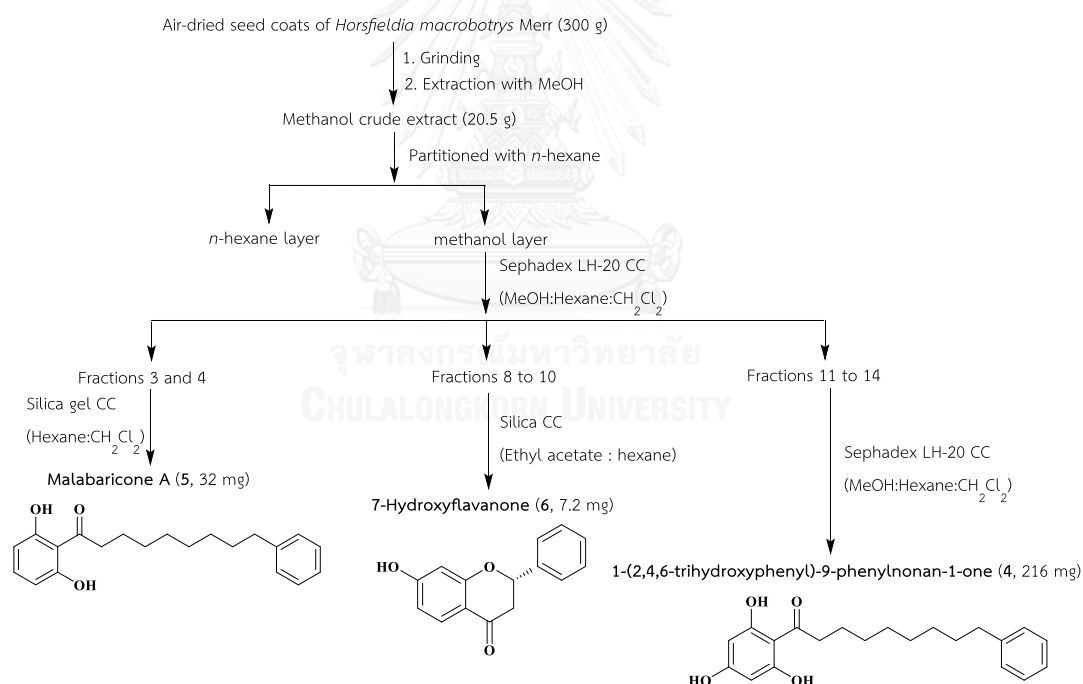
Scheme 3.1 Isolation procedure of isolated compounds from seed coats of *Horsfieldia macrobotrys* Merr.

3.2.2 Structure elucidation of 4

1-(2,4,6-Trihydroxyphenyl)-9-phenylnonan-1-one was obtained as white powder. The positive HRESIMS spectrum of **4** showed $[M + Na]^+$ ion at *m/z* 365.1733 (Calcd 365.1729 for $C_{21}H_{26}NaO_4$) that corresponded with molecular formula of $C_{21}H_{26}O_4$. The ^1H NMR spectrum showed five aromatic protons at δ_H 7.29-7.17 (5H, m, C_6H_5) and two protons at δ_H 5.86 (2H, s, H-3', H-5') were indentical and characteristic of a symmetrical 1', 2', 4', 6'-tetrasubstituted aryl ring. There were eight methylenes; one connecting with carbonyl at δ_H 3.03 (2H, t, *J*= 7.5 Hz) assigned to H-2, six proton signals at δ_H 1.64 (8H, br s) and 1.32 (4H, br s) assigned as long chain and one methylene connecting with others aromatic ring at δ_H 2.59 (2H, t, *J*= 7.7 Hz) assigned as H-9 (Figure 3.2). The ^{13}C NMR spectrum was confirmed. In addition, the NMR data of **4** were consistent with previous report [80].

Figure 3.2 1-(2,4,6-trihydroxyphenyl)-9-phenylnonan-1-one **(4)**

3.2.3 Structure elucidation of 5

1-(2,6-Dihydroxyphenyl)-9-phenylnonan-1-one (malabaricone A) was obtained as white powder. The positive HRESIMS spectrum showed the $[M+Na]^+$ ion at *m/z* 349.1793 (Calcd 349.1780 for $C_{21}H_{26}NaO_3$) which indicated a molecular formula of $C_{21}H_{26}O_3$. The ^1H and ^{13}C NMR spectra of **5** were similar to those of **4** except for the lack of one hydroxyl group at C-4'. Therefore, the structure of 1-(2,6-dimethoxyphenyl)-9-phenylnonan-1-one (malabaricone A) was assigned for compound **5** (Figure 3.3), and its NMR data were consistent with those previously reported [83].
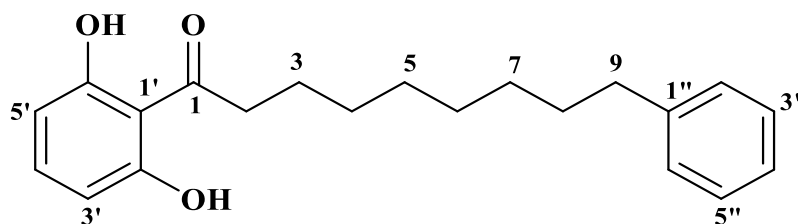
Figure 3.3 1-(2,6-dihydroxyphenyl)-9-phenylnonan-1-one **(5)**

3.2.4 Structure elucidation of 6

7-Hydroxyflavanone was obtained as yellow solid. The ^{1}H NMR spectrum showed proton signals of ring B at δ_H 7.48 (m, 2H), 7.44 (m, 2H) and 7.41 (m, 1H) for H-2' and H-6', H-3' and H-5', and H-4', respectively. Another signals indicative of a flavanone structure at δ_H 5.49 (dd, J_1 = 13.2 Hz, J_2 = 2.9 Hz, H-2), 3.07 (dd, J_1 = 16.8 Hz, J_2 = 13.2 Hz, H-3$_{ax}$) and 2.86 (dd, J_1 = 16.8 Hz, J_2 = 2.9 Hz, H-3$_{eq}$). Two proton signals at δ_H 7.89 (d, J = 8.6 Hz) and 6.57 (dd, J_1 = 8.6 Hz, J_2 = 2.2 Hz) were assigned for H-5 and H-6, respectively. In addition, one proton signal at δ_H 6.49 (d, J = 2.1 Hz) was assigned to H-8. Therefore, the structure of 7-hydroxyflavanone corresponding to those report previously (Figure 3.4) [84].
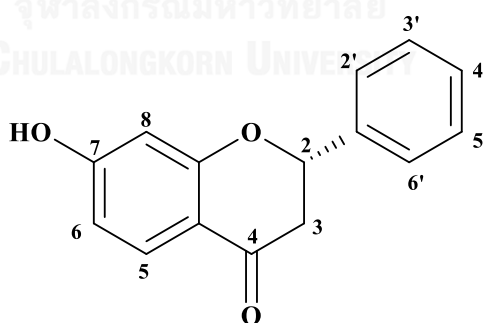
Figure 3.4 7-Hydroxyflavanone **(6)**

3.2.5 Methylation of 4 and 5

To envision a bioactivity change if the hydroxyl groups were replaced by alkoxy groups. Arylalkanones **4** and **5** were separately converted to their corresponding methyl ether analogues (**4a** and **5a**, respectively) by reaction with MeI/K_2CO_3. The synthesized analogues **4a** and **5a** shown in Figure 3.5.
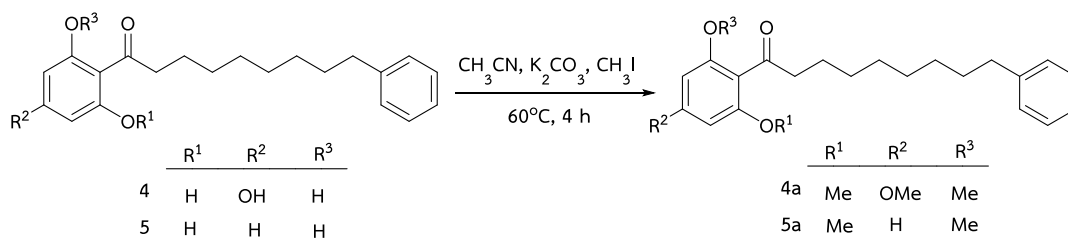
Figure 3.5 Methylation reactions of **4** and **5**

3.2.6 Structure elucidation of 4a

1-(2,4,6-Trimethoxyphenyl)-9-phenylnonan-1-one was obtained as yellow oil. The structure was deduced by ^1H, ^{13}C NMR spectroscopic methods. The ^1H NMR spectrum showed five aromatic protons at δ_H 7.22-7.18 (m, 5H, C_6H_5) and two protons at δ_H 7.11 (s, 1H) and 7.10 (s, 1H) that could be ascribed to H-5′ and H-3′, respectively. In addition, these were methoxy groups at δ_H 3.81 (s, 3H, -OMe), 3.77 (s, 3H, -OMe), 3.74 (s, 3H, OMe) and signals at δ_H 2.92-2.88 (m, 2H) assigned as H-2. Two proton signals at δ_H 2.53 (t, J = 8.0 Hz) indicated the presence of a methylene connected with aromatic ring in position H-9. In addition, twelve proton signals at 1.51 (br s, 6H) and 1.26 (br s, 6H) were assigned to the methylenes protons of long chain hydrocarbons (Figure 3.6). The ^{13}C NMR spectrum also confirmed the identify of product shown below.
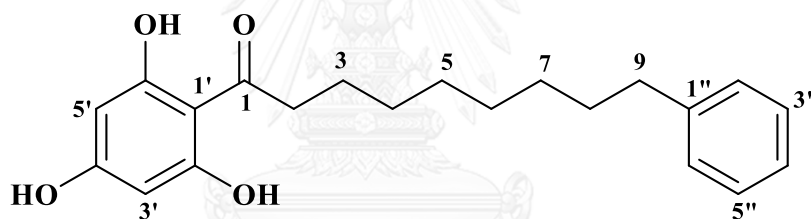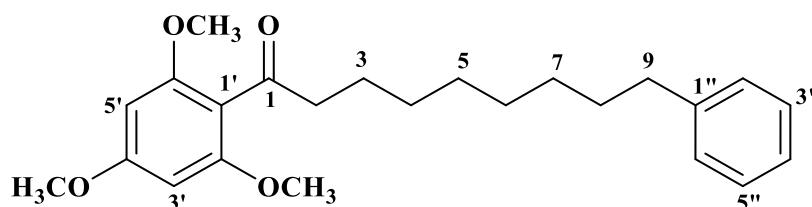

Figure 3.6 1-(2,4,6-Trimethoxyphenyl)-9-phenylnonan-1-one **(4a)**

3.2.7 Structure elucidation of 5a

1-(2,6-Dimethoxyphenyl)-9-phenylnonan-1-one was obtained as yellow oil. The structure was deduced by the results from ^{1}H and ^{13}C NMR spectroscopic methods. The ^{1}H NMR spectra showed 6 aromatic protons at δ_H 7.22 – 7.10 (m, 6H, C$_6$H$_5$ and H-4′), whereas two protons at δ_H 6.47 (d, J = 8.0 Hz, 2H, H-3′ and H-5′) were indentical and characteristic of a symmetrical 1', 2', 6'-trisubstituted aryl ring. Six methoxy proton signals at δ_H 3.70 (br s, 6H, 2×OMe) could be ascribed to OMe-2′ and OMe-6′. In addition, two triplet proton signals at 2.65 (t, J = 8.0 Hz, 2H) and 2.52 (t, J = 8.0 Hz, 2H) were assigned to H-2 and H-9, respectively. Twelve other proton signals at δ_H 1.60-1.51 (m, 4H) and 1.24 (br s, 8H) were assigned as long chain hydrocarbons (Figure 3.7). The ^{13}C NMR spectrum also confirmed the indentify of product shown below. In addition, the data NMR of **5a** were consistent with previous report [85].
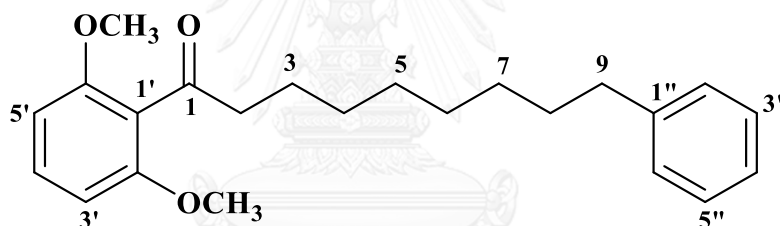
Figure 3.7 1-(2,6-dimethoxyphenyl)-9-phenylnonan-1-one **(5a)**

3.2.8 **α-Glucosidase inhibition and radical scavenging activity of compounds 4-6 and their derivatives**

Inhibitory activity of isolated compounds (**4-6**) and their derivatives (**4a-5a**) was determined against **α**-glucosidases and DPPH (Table 3.1).

Table 3.1 α-Glucosidase inhibition and DPPH radical scavenging activity of isolated compounds and their derivatives

Compounds	IC$_{50}$ (μM)[a]			
	Baker's yeast	Rat Intestinal		DPPH[c]
		Maltase	Sucrase	
4	10.8	84.4	64.0	2.6
4a	163.4	813.3	813.3	23.2
5	304.4	562.8	634.6	6.2
5a	564.6	852.5	528.2	13.9
6	3,363.1	NI	NI	26.6
Acarbose	103.0	2.1	26.0	-
Ascorbic Acid	-	-	-	2.5

[a] Data shown as mean of duplicate experiments.

[b] NI, no inhibition, inhibitory effect less than 30 % at 10 mg/mL.

[c] The values are expressed as SC$_{50}$ (mM).

Compounds **4** and **5** from *Horsfieldia macrobotrys* Merr seed coats were classified as arylalkanones while compound **6** was flavanone, respectively. Arylalkanone **4** displayed bioactivities more potent than those of compound **5** in all bioassays examined (Table 3.1). Interestingly, radical scavenging of **4** (SC$_{50}$ 2.6 mM) was comparable with that of ascorbic acid (SC$_{50}$ 2.5 mM). The inhibitory effects of **4** against α-glucosidases were 7-30 times more pronounced. Notably, the structure of **4** differed from **5** by one additional hydroxyl at C-4$'$. Therefore, it could be generalized that the number of hydroxyl groups on the aryl moiety is critical for exerting radical scavenging and α-glucosidase inhibition.

To envision a bioactivity change if the hydroxyl groups were replaced by alkoxy groups. Arylalkanones **4** and **5** were separately converted to their corresponding methyl ether analogues (**4a** and **5a**, respectively) by reaction with MeI/K$_2CO_3$. The synthesized analogues **4a** and **5a** were examined for radical scavenging and α-glucosidase inhibition (Table 3.1). The replacement of all hydroxyls in **4** by methoxy

groups considerably reduced the bioactivities of **4a**, by approximately 10-16 times. Similar observations were also noticed for **5a**, but were less significant (*ca* 2-times less potent) in relation to **5**. Therefore, the results suggested the critical role of hydroxyls (-OH) in exerting bioactivities, which could not be replaced by the presence of related methyl ether moieties (-OMe) [86].

Table 3.2 Inhibition mechanism

Type of inhibition	K_m	V_{max}	Intersection
Competitive	increase	unchanged	Y axis, Y > 0
Non-competitive	unchanged	decrease	X axis, X < 0
Uncompetitive	decrease	decrease	no intersection
Mixed	increase	decrease	second quadrant

Since compound **4** displayed an intense inhibitory activity against yeast α-glucosidase, mechanism underlying the inhibition of **4** was further determined by Lineweaver-Burk plot (Figure 3.8). A kinetic study of **4**, the most potent inhibitor, was conducted against yeast α-glucosidase. The Lineweaver–Burk plot of **4** displayed a set of straight lines, all of which intersected in the second quadrant. Kinetic analysis revealed that V_{max} decreased with elevated K_m in the presence of increasing concentrations of **4** (Table 3.2). This behavior indicated that the enzyme was inhibited by **4** in mixed manner. This observation could be rationalized by concomitant formation of an enzyme-inhibitor (EI) complex in a competitive manner and an enzyme-substrate-inhibitor (ESI) complex in a noncompetitive manner (Scheme 3.2).

We subsequently investigated the pathway in which arylalkanone **4** preferentially preceded by determining dissociation constants of EI (*Ki*) and ESI (*Ki′*) complexes. The secondary plots in Figure 3.8 (B and C) revealed *Ki* and *Ki′* values of 1.10 and 0.68 mM, respectively, thus suggesting that arylalkanone **4** predominantly formed an ESI complex rather than competitively bound to the enzyme. The proposed inhibitory mechanism is summarized in Scheme 3.2.

$$E \;+\; S \;\rightleftharpoons\; ES \;\longrightarrow\; E \;+\; P$$

$$I \;\big\updownarrow\; K_i \;1.10\ \text{mM} \qquad I \;\big\updownarrow\; K_i' \;0.68\ \text{mM}$$

$$EI \qquad\qquad ESI$$
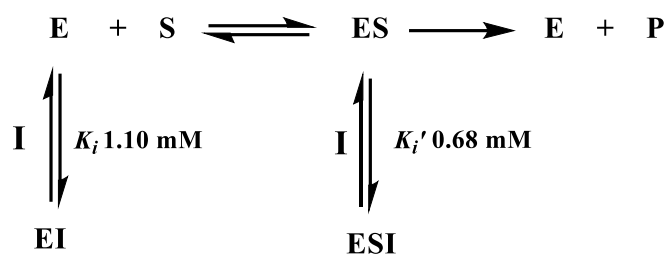
Scheme 3.2 Proposed inhibition mechanism of **4 (I)** against yeast α-glucosidase. E, S and P represent enzyme, *p*-nitrophenyl-α-D-glucopyranoside (substrate) and glucose (P), respectively.

In conclusion, arylalkanone **4** could serve as a new potent antidiabetic agent because it revealed both therapeutic effect by inhibiting α-glucosidase and preventive effect by radical scavenging. In addition, the number of hydroxyl groups on the aryl moiety was crucial for exerting improved bioactivity, which could not be replaced by the presence of methoxy groups in **4a**.
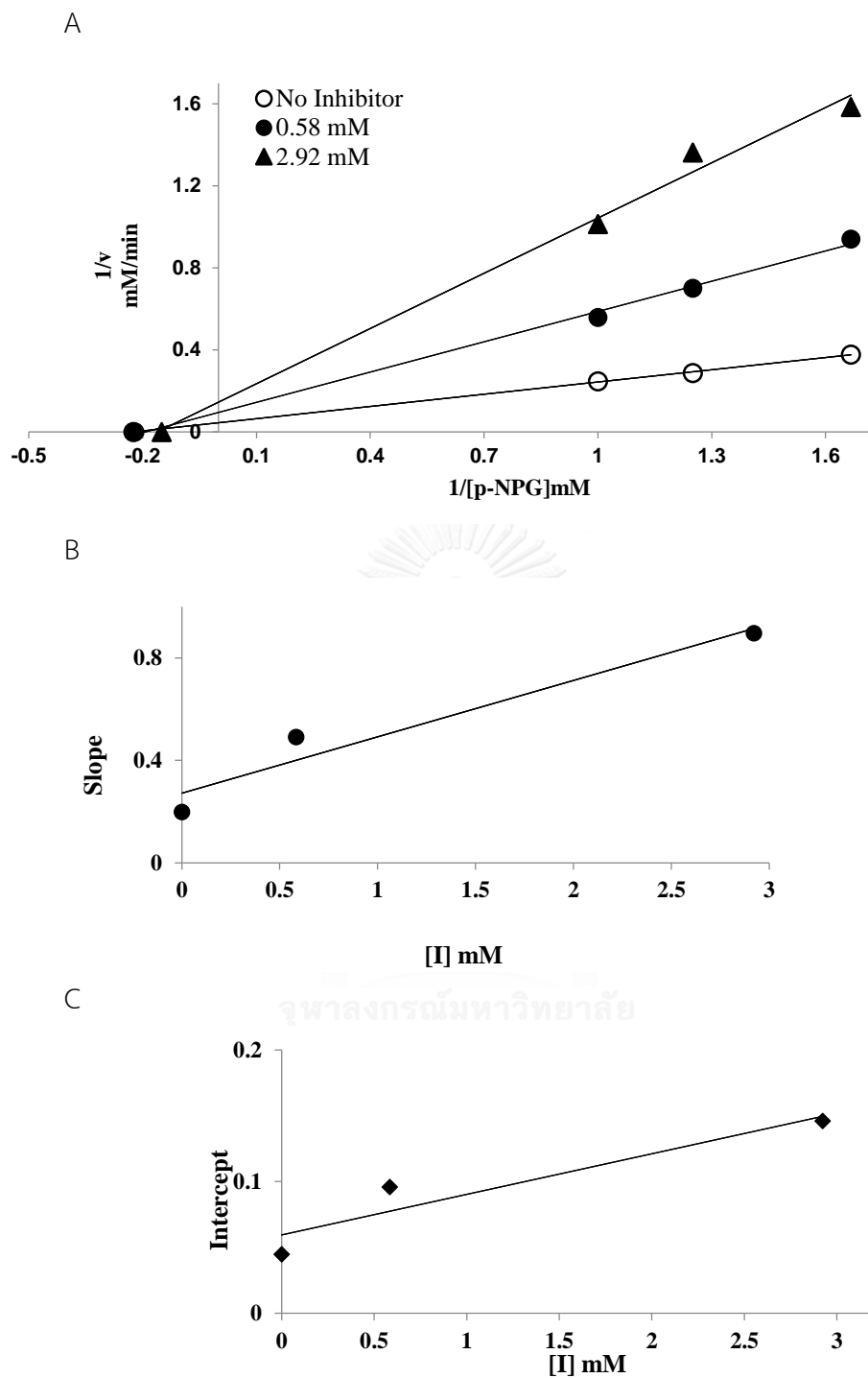
Figure 3.8 (A) Lineweaver-Burk plot of 1-(2,4,6-trimethoxyphenyl)-9-phenylnonan-1-one (4), 1/V against 1/[S]. **(B)** Secondary replot of slope *vs.* [I] from a primary Lineweaver-Burk plot for the determination of K_i. **(C)** Secondary replot of intercept *vs.* [I] from a primary Lineweaver-Burk plot for determination of $K_i{}'$.

3.3   Experimental section

3.3.1   General experimental procedures

The ^{1}H and ^{13}C NMR spectra were recorded on a Bruker 400 AVANCE spectrometer using TMS as an internal reference and the chemical shifts were reported in δ (ppm). TLC was performed using silica gel 60 F_{254} aluminium sheets. Gel filtration chromatography was performed on silica gel and Sephadex LH-20. Spectrophotometric measurements for assay were taken on a Sunrise microplate reader. HR-ESI-MS data were obtained using a Bruker MICROTOF model mass spectrometer.

3.3.2   Plant material

The fruits of *Horsfieldia macrobotrys* Merr were collected from East Kalimantan, Indonesia in May 2013. The plant material was identified by the Research Center for Biology, Indonesian Institute of Sciences, and a voucher specimen (KK-1410-HM001) was deposited at the Forest Products Chemistry Laboratory at the Mulawarman University, East Kalimantan, Indonesia.

3.3.3   Extraction and isolation

The air-dried seed coats of *Horsfieldia macrobotrys* Merr (300 g), obtained after peeling pericarps, were extracted repeatedly with methanol at room temperature. The methanol extract was concentrated *in vacuo* to yield a dried extract (20.5 g). A portion of this (12.8 g) was suspended in methanol and partitioned with *n*-hexane. The methanol soluble fraction was applied to a Sephadex LH-20 column (6:14:80 MeOH-*n*-hexane-CH$_2$Cl$_2$), yielding 14 fractions. The combined fractions 11 to 14 were purified by Sephadex LH-20 (4:16:80 MeOH-*n*-hexane-CH$_2$Cl$_2$) to afford 1-(2,4,6-trihydroxyphenyl)-9-phenylnonan-1-one (**4**, 216 mg). The combined fractions 3 and 4 were further purified by silica gel (40:60 *n*-hexane-CH$_2$Cl$_2$) to afford 1-(2,6-trihydroxyphenyl)-9-phenylnonan-1-one (malabaricone A) (**5**, 32 mg**)**. The combined fractions 8 to 10 was subjected to column chromatography (silica gel, 80% *n*-hexane:ethyl acetate) and re-crytallization to afford 7-hydroxyflavanone (**6**, 7.2 mg).

1-(2,4,6-trihydroxyphenyl)-9-phenylnonan-1-one (4) white powder; ^{1}H NMR (CDCl$_3$, 400 MHz) δ 7.29-7.17 (5H, m, C$_6$H$_5$), 5.86 (2H, s, H-3', H-5'), 3.03 (2H, t, J= 7.5 Hz, H-2), 2.59 (2H, t, J= 7.7 Hz, H-9), 1.64 (8H, br s), 1.32 (4H, br s). ^{13}C NMR (CDCl$_3$, 100 MHz) δ 206.2 (C-1), 164.1 (C-4'), 161.89 (C-2' and C-6'), 143.0 (C-1"), 128.4 (C-3" and C-5"), 128.2 (C-4"), 125.5 (C-2" and C-6"), 105.1 (C-1'), 95.76 (C-3' and C-5') , 77.5 (C-9), 44.0 (C-2), 43.9 (C-8), 35.9 (C-4), 35.51 (C-5), 31.43 (C-6), 29.33 (C-7), 24.59 (C-3). HRESIMS m/z [M+Na]$^+$ 365.1733.

1-(2,6-dihydroxyphenyl)-9-phenylnonan-1-one(malabaricone A) (5) white powder; ^{1}H NMR (CDCl$_3$, 400 MHz) δ 9.61 (br s, 2-OH), 7.32-7.18 (m, 6H), 6.42 (d, J = 8.2 Hz, H-3' and H-5'), 3.14 (t, J = 7.4 Hz, H-2, 2H), 2.63 (t, J = 7.7 Hz, H-9, 2H), 1.72 (br s, 3H), 1.64 (m, 1H), 1.36 (br s, 8H). ^{13}C NMR (CDCl$_3$, 100 MHz) δ 207.9 (C-1), 161.2 (C-2' and C-6'), 142.9 (C-1"), 135.6 (C-4'), 128.4 (C-3" and C-5"), 128.2 (C-4"), 125.5 (C-2" and C-6") , 110.1 (C-1'), 108.4 (C-3' and C-5'), 77.3 (C-9), 46.4 (C-2), 44.7 (C-8), 35.9 (C-4), 31.4 (C-5), 29.7 (C-6), 29.3 (C-7), 24.4 (C-3). HRESIMS m/z [M+Na]$^+$ 349.1793.

7-Hydroxyflavanone (6) yellow oil; ^{1}H NMR (CDCl$_3$, 400 MHz) δ 7.89 (d, J = 8.6 Hz, H-5) 7.48 (m, H-2' and H-6'), 7.44 (m, H-3' and H-5'), 7.41 (m, H-4'), 6.57 (dd, J_1 = 8.6 Hz, J_2 = 2.2 Hz, H-6), 6.49 (d, J = 2.1 Hz, H-8), 5.49 (dd, J_1 = 13.2 Hz, J_2 = 2.9 Hz, H-2), 3.07 (dd, J_1 = 16.8 Hz, J_2 = 13.2 Hz, H-3$_{ax}$), 2.86 (dd, J_1 = 16.8 Hz, J_2 = 2.9 Hz, H-3$_{eq}$). ^{13}C NMR (CDCl$_3$, 100 MHz) δ 190.7 (C-4), 164.0 (C-8), 162.7 (C-6), 138.7 (C-1'), 129.4 (C-4a), 128.8 (C-3' and C-5'), 128.7 (C-4'), 126.2 (C-2' and C-6'), 115.2 (C-8a), 110.6 (C-5), 103.5 (C-7), 79.9 (C-2), 44.3 (C-3).

3.3.4   Chemical modification

To a mixture of **4** (20 mg) and K_2CO_3 (43 mg) dissolved in acetonitrile (1 mL) was added MeI (0.1 mL) dropwise. The reaction mixture was heated at 60°C for 4 h. The solvent was then removed under reduced pressure to obtain the reaction residue, which was purified by silica gel column chromatography (5:95 EtOAc-*n*-hexane) to yield **4a** (6 mg) . The methyl ether analogue **5a** (6 mg) was also prepared using the same protocol starting from **5**.

1-(2,4,6-Trimethoxyphenyl)-9-phenylnonan-1-one (4a) ^{1}H NMR (CDCl$_3$, 400 MHz) δ 7.22-7.18 (m, 5H, C$_6$H$_5$), 7.11 (s, 1H, H-5′), 7.10 (s, 1H, H-3′), 3.81 (s, 3H, -OMe), 3.77 (s, 3H, -OMe), 3.74 (s, 3H, -OMe), 2.92-2.88 (m, 2H, H-2), 2.53 (t, *J* = 8.0 Hz, 2H, H-9), 1.51 (br s, 6H), 1.26 (br s, 6H). ^{13}C NMR (CDCl$_3$, 100 MHz) δ 206.0 (C-1), 167.6 (C-4′), 165.7 (C-2′ and C-6′), 142.90 (C-1″), 128.3 (C-3″ and C-5″), 128.2 (C-2″ and C-6″), 125.5 (C-4″), 105.8 (C-1′), 93.7 (C-3′ and C-5′), 55.4 (3×OMe), 44.4 (C-2), 35.9 (C-9), 31.9 (C-8), 30.3 (C-7), 29.9 (C-6), 29.6 (C-5), 28.9 (C-4), 24.7 (C-3). ESIMS *m/z* [M+Na]$^+$ 407.23.

1-(2,6-Dimethoxyphenyl)-9-phenylnonan-1-one (5a) ^{1}H NMR (CDCl$_3$, 400 MHz) δ 7.22 – 7.10 (m, 6H, C$_6$H$_5$ and H-4′), 6.47 (d, *J* = 8.0 Hz, 2H, H-3′ and H-5′), 3.70 (br s, 6H, 2×OMe), 2.65 (t, *J* = 8.0 Hz, 2H, H-2), 2.52 (t, *J* = 8.0 Hz, 2H, H-9), 1.60-1.51 (m, 4H), 1.24 (br s, 8H). ^{13}C NMR (CDCl$_3$, 100 MHz) δ 205.4 (C-1), 156.7 (C-2′ and C-6′), 142.9 (C-1″), 130.3 (C-4′), 128.3 (C-3″ and C-5″), 128.2 (C-2″ and C-6″), 125.5 (C-4″), 120.8 (C-1′), 104.0 (C-3′ and C-5′), 55.8 (2×OMe), 44.7 (C-2), 35.9 (C-9), 31.4 (C-8), 29.9 (C-7), 29.6 (C-6), 29.3 (C-5), 29.2 (C-4), 23.4 (C-3). ESIMS *m/z* [M+Na]$^+$ 377.49.

3.3.5 α-Glucosidase inhibitory activity and free radicals scavenging

3.3.5.1 Chemical and equipment

The α-glucosidase from Baker's yeast, *p*-nitrophenyl-α-D-glucopyranoside (*p*-NPG), rat intestinal acetone powder and substrate (maltose and sucrose) were purchased from Sigma-Aldrich (St. Louis, MO, USA). Acarbose was obtained from Bayer (Germany). Glucose assay kit was purchased from Human Gesellschaft für Biochemica und Diagnostica mbH (Germany). DPPH (2,2-diphenyl-1-picrylhydrazyl) and ascorbic acid as standard were obtained from Sigma-Aldrich (St. Louis, MO, USA).

3.3.5.2 α-Glucosidase inhibitory activity from baker's yeast

The activity effect of isolated compound were evaluated using the same procedure described in Chapter 2.

3.3.5.3 α-Glucosidase inhibitory activity from rat intestine

The activity effect of isolated compound were evaluated using the same procedure described in Chapter 2.

3.3.5.4 Kinetic study of α-glucosidase inhibition

In order to evaluate the type of inhibition, enzyme kinetic analysis was performed according to the above reaction. The type of inhibition was determined from Lineweaver-Burk plots. The quantity of yeast α-glucosidase was maintained at 0.4 U/mL, and the concentrations of each tested were varied in the range of 0-2.92 mM. The K_i value was determined from secondary plots of slope *vs*. [I], and the K'_i value was calculated from secondary plots of interception *vs*. [I].

3.3.5.5 Free radicals scavenging (DPPH)

The antioxidant activity of the compounds was evaluated through the free radical scavenging effect on 2,2'-diphenyl-1-picrylhydrazyl (DPPH) radical as previously reported [87] with slight modifications. 100 µL of 0.10 mM DPPH methanolic solution was added to 20 µL of the samples with various concentrations. The mixture was thoroughly mixed and kept in the dark for 30 mins. The absorbance was measured at 517 nm using a Sunrise microplate reader spectrophotometer.

SUPPORTING INFORMATION
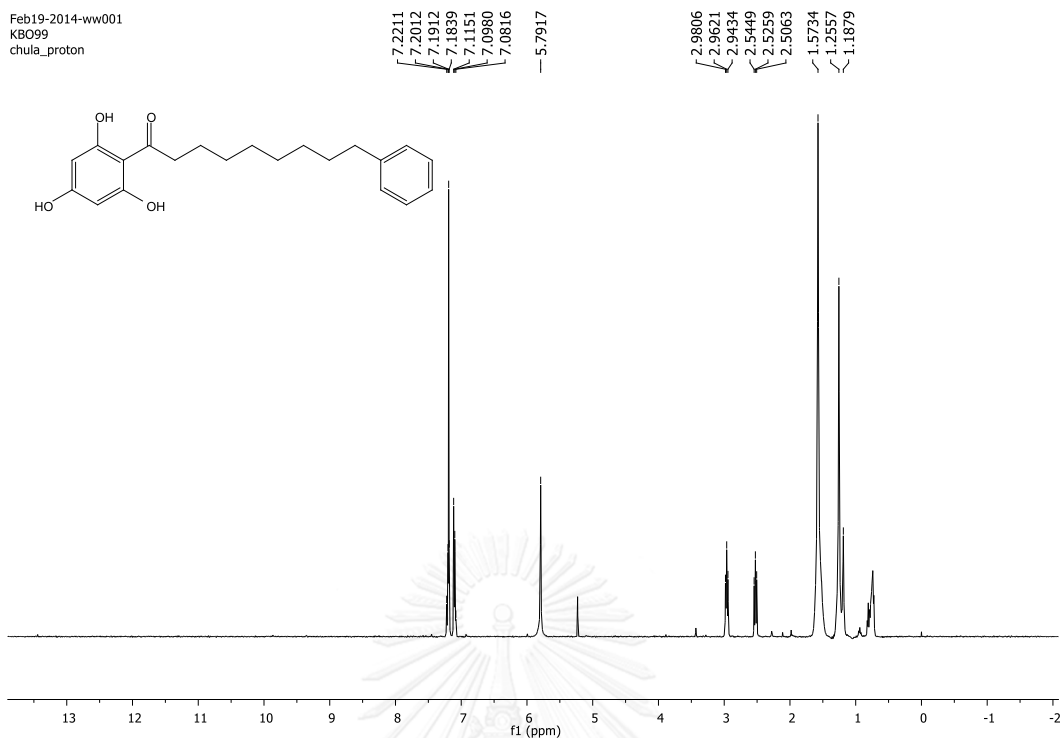
Figure 3.9 ^{1}H-NMR spectrum (400 MHz, in CDCl$_3$) of 1-(2,4,6-trihydroxyphenyl) 9-phenylnonan-1-one **(4)**
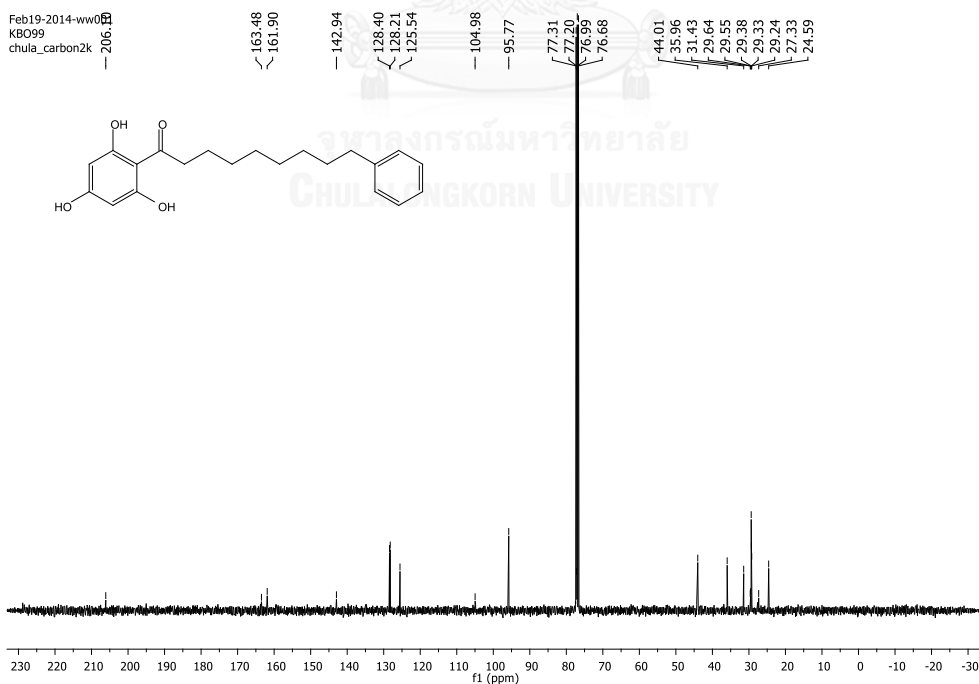
Figure 3.10 ^{13}C-NMR spectrum (100 MHz, in CDCl$_3$) of 1-(2,4,6-trihydroxyphenyl)-9-phenylnonan-1-one **(4)**
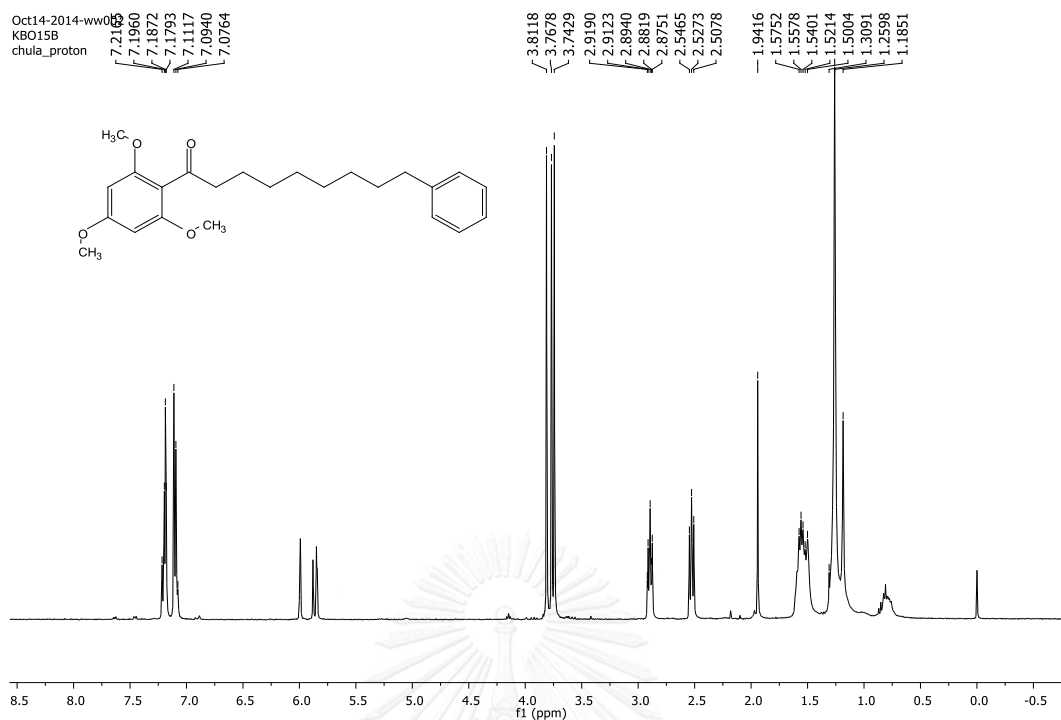
Figure 3.11 ^{1}H-NMR spectrum (400 MHz, in CDCl$_3$) of 1-(2,4,6-trimethoxyphenyl)-9-phenylnonan-1-one **(4a)**
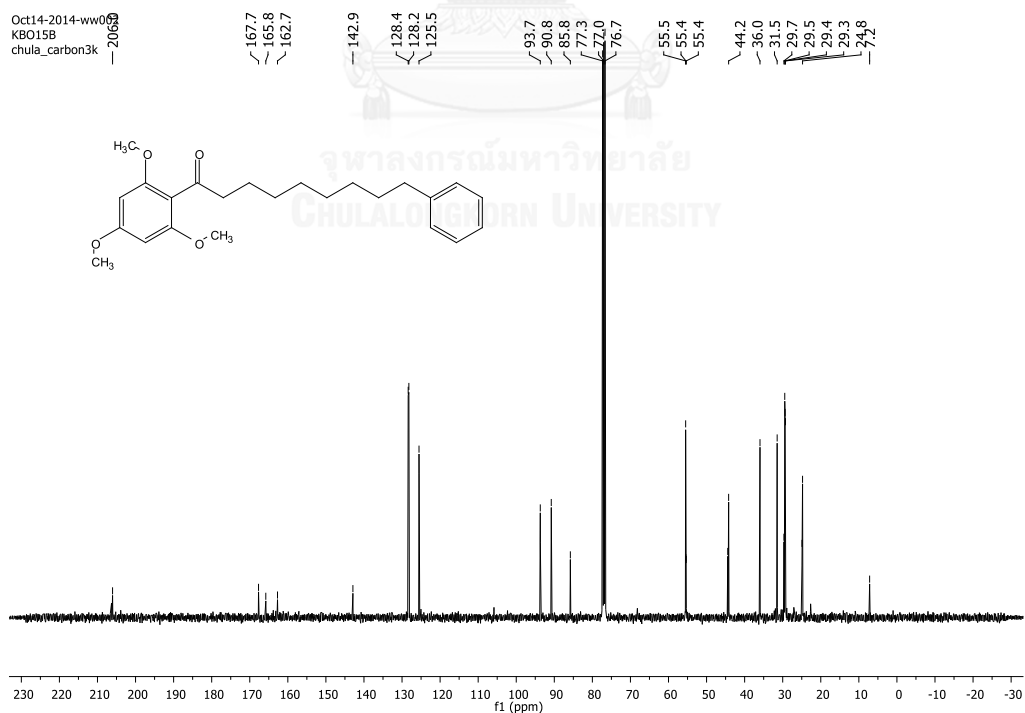
Figure 3.12 ^{13}C-NMR spectrum (100 MHz, in CDCl$_3$) of 1-(2,4,6-trimethoxyphenyl)-9-phenylnonan-1-one **(4a)**
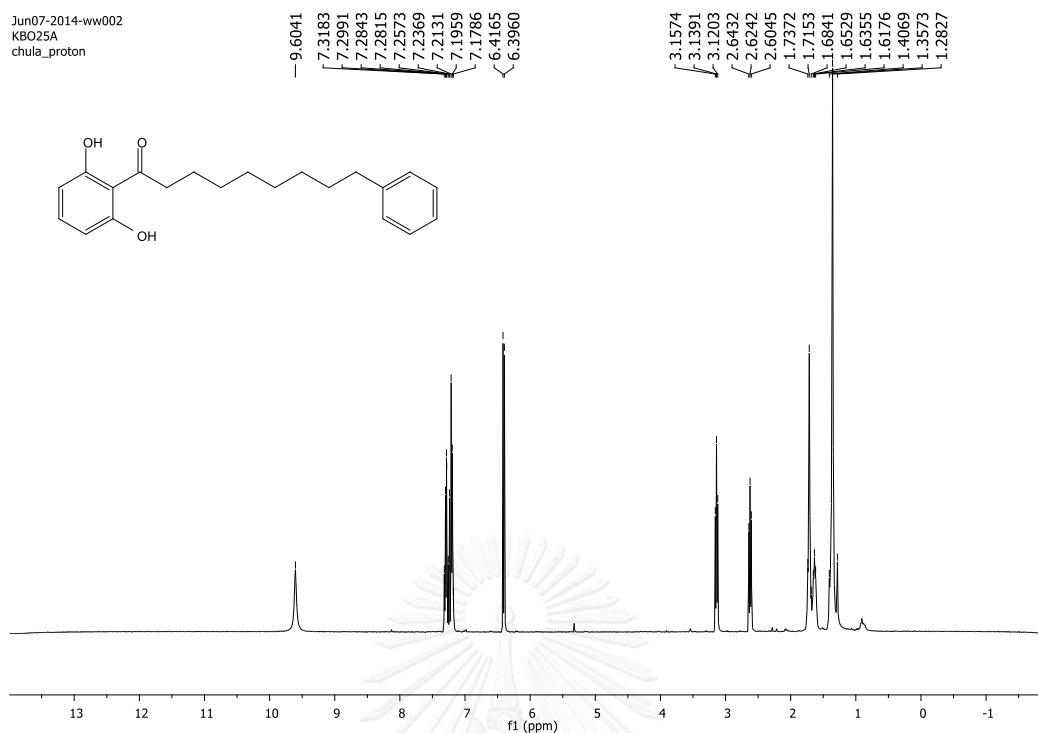
Figure 3.13 ¹H-NMR spectrum (400 MHz, in CDCl₃) of 1-(2,6-dihydroxyphenyl)-9-phenylnonan-1-one (malabaricone A) **(5)**
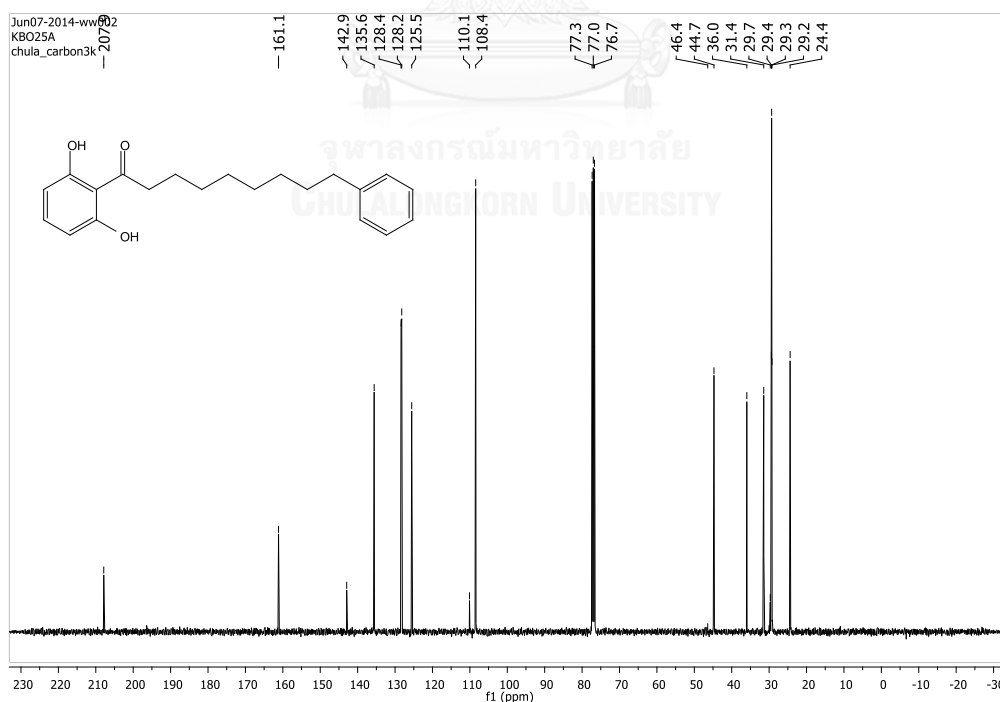
Figure 3.14 ¹³C-NMR spectrum (100 MHz, in CDCl₃) of 1-(2,6-dihydroxyphenyl)-9-phenylnonan-1-one (malabaricone A) **(5)**
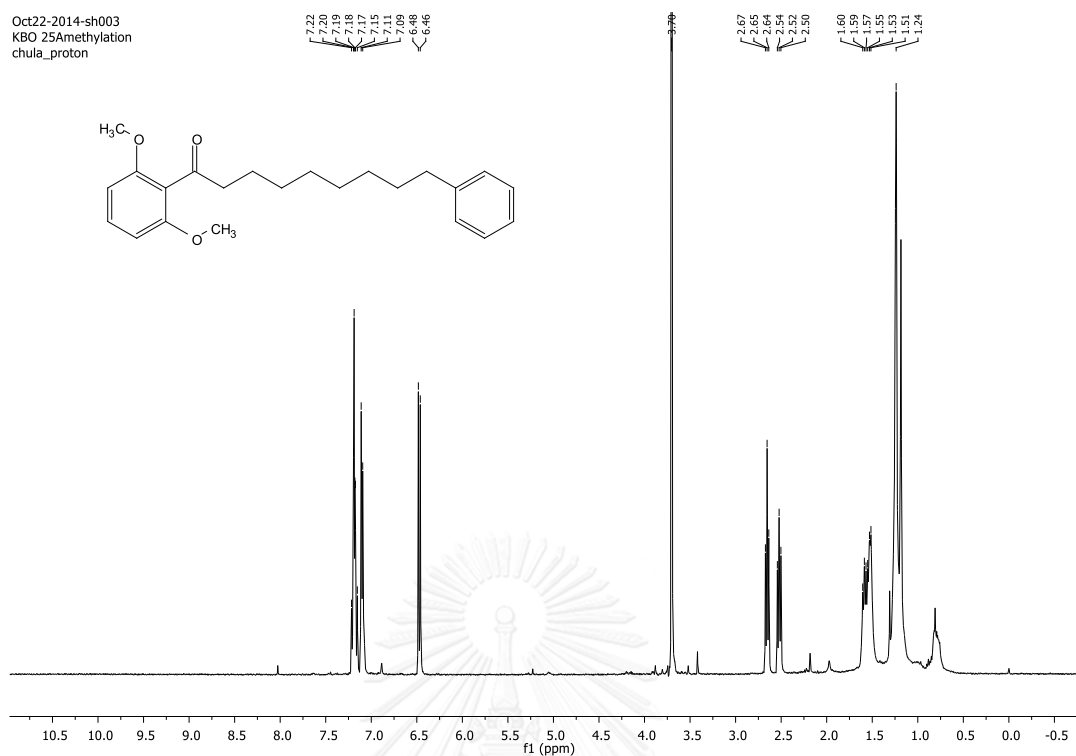
Figure 3.15 ^{1}H-NMR spectrum (400 MHz, in CDCl$_3$) of 1-(2,6-dimethoxyphenyl)-9-phenylnonan-1-one **(5a)**
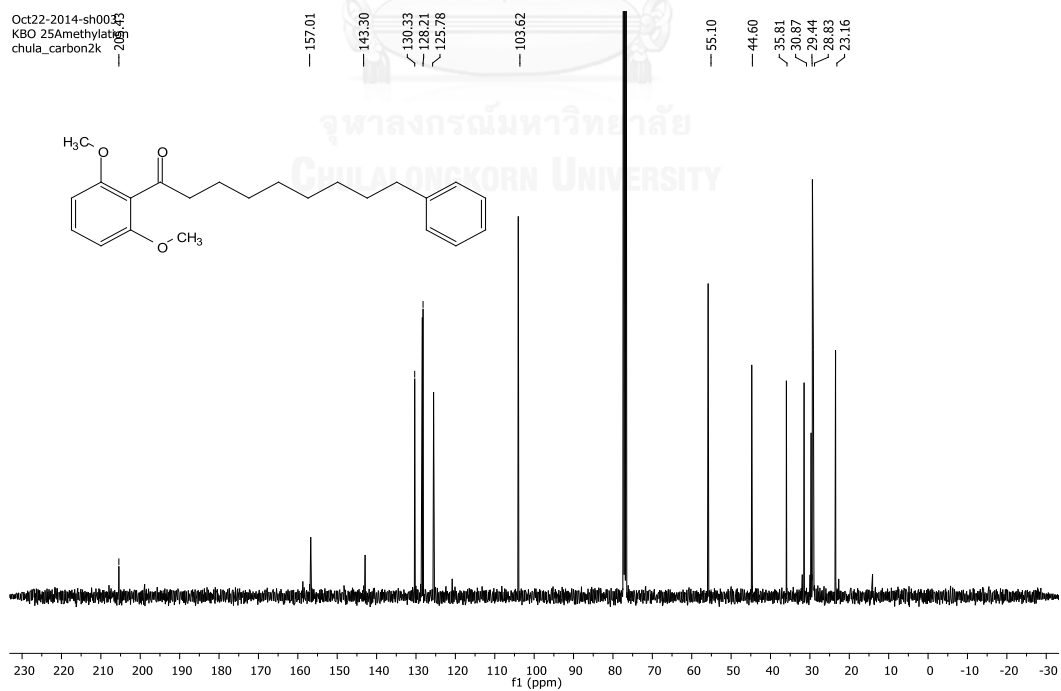
Figure 3.16 ^{13}C-NMR spectrum (100 MHz, in CDCl$_3$) of 1-(2,6-dimethoxyphenyl)-9-phenylnonan-1-one **(5a)**
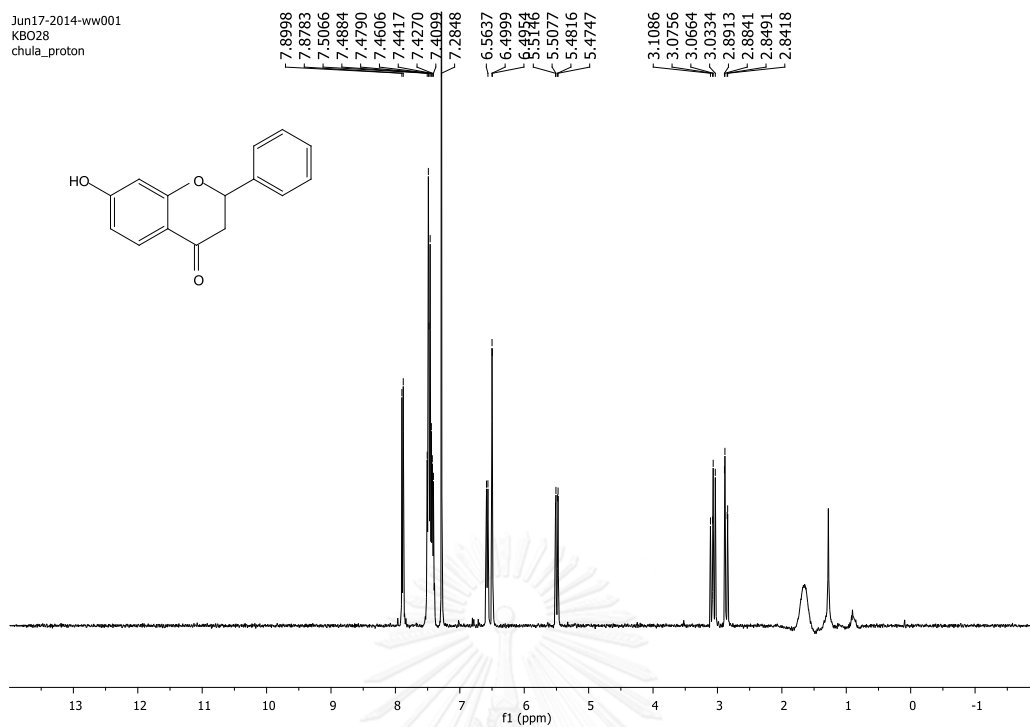
Figure 3.17 ^{1}H-NMR spectrum (400 MHz, in CDCl$_3$) of 7-Hydroxyflavanone **(6)**
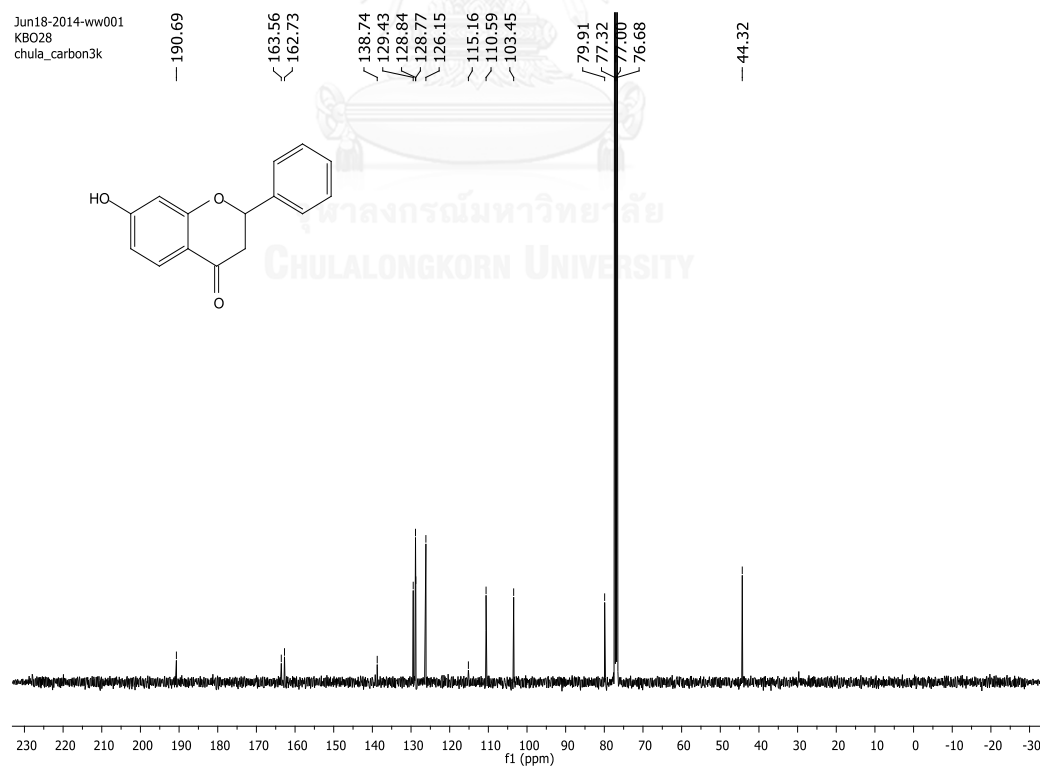
Figure 3.18 ^{13}C-NMR spectrum (100 MHz, in CDCl$_3$) of 7-Hydroxyflavanone **(6)**

CHAPTER IV

NEW ARYLALKANONES AND FLAVONOID GLYCOSIDE FROM *Horsfieldia macrobotrys* STEM BARKS, EFFECTIVE ANTIDIABETIC AGENTS CONCOMITANTLY INHIBITING α-GLUCOSIDASE AND FREE RADICALS

4.1   Introduction

The seed coats of *Horsfieldia macrobotrys* has been reported for the first time in Chapter III as a source of diverse secondary metabolites including arylalkanones and flavonoid. In addition, the isolated arylalkanones, especially 4, revealed a highly inhibitory effect against both DPPH radicals and α-glucosidase [75]. Coupled with ethnopharmacological use of this plant by native people in Kalimantan, not only seed coats were used for treat blood sugar level but also other parts of this plant such as stem barks also were used for treat blood sugar level and antiinflamation.

Several previous studies of Myristicaceae family especially *Horsfieldia* species reported the isolation of arylalkanones, lignans, chromones, diarylpropanoids, procyanidins and neolignans; some of which demonstrated several bioactivities, such as antidiabetes [75], cytotoxicity activity [77], antimalarial [76] and antibacterial [78].

These interesting features inspired us to further investigate secondary metabolites from other parts of this plant such as stem barks, thus leading to the discovery of other active compounds as potent inhibitors against both α-glucosidase and free radicals. In addition, the phytochemical investigation and antidiabetic activity of *H. macrobotrys* Merr from stem barks are reported herein for the first time.

4.2   Results and discussion

4.2.1   Isolation

The dried stem barks of *H. macrobotrys* Merr (2.4 kg) were extracted with MeOH at ambient temperature for 3 days. The concentrated MeOH extract was suspended in water and partitioned with CH_2Cl_2 (3 ✕ 1L) to afford the active CH_2Cl_2 extract, which was chromatographed by vacuum column chromatography (silica gel 60G Merck) column (120 mm ID ✕ 7 cm length) and eluted with six mobile phases of 1:0, 8:2, 6:4, 4:6, 2:8 and 0:1 hexane:EtOAc. The fraction 4 was chromatographed on Sephadex LH-20 using MeOH followed by crystallization (CH_2Cl_2) to afford horsfieldone A (**7,** 420 mg). Subfractions from fraction 4 were separated on Sephadex LH-20 (1:1 CH_2Cl_2-MeOH) to afford maingayone D (**8**, 35 mg). The fraction 6 was chromatographed on Sephadex LH-20 using MeOH to afford 12 subfractions. Subfraction 6 was chromatographed on Sephadex LH-20 (12:80:8 C_6H_{14}-CH_2Cl_2-MeOH) to afford 8-C-β-D-glucopyranosylpinocembrin (**9**, 24 mg). The isolation procedure is summarized in (Scheme 4.1).
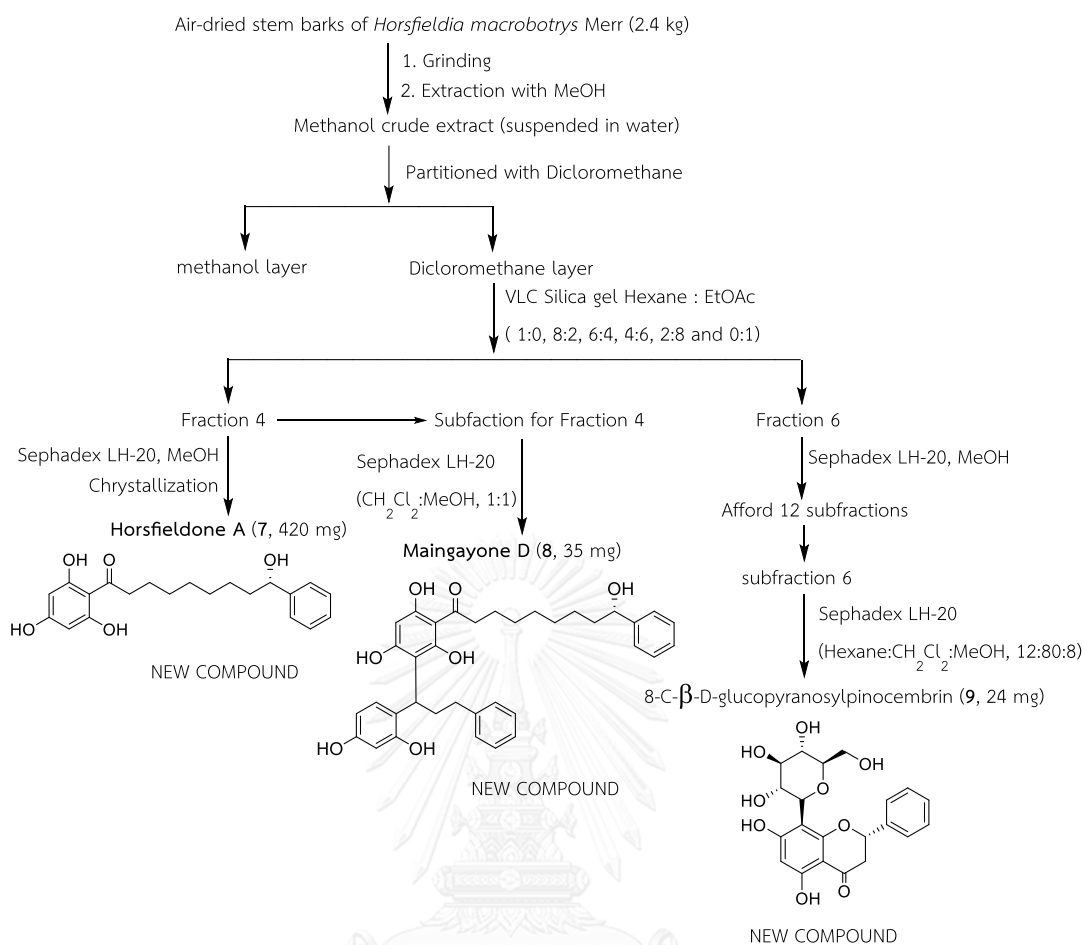
Scheme 4.1 Isolation procedure of isolated compounds from stem barks of *Horsfieldia macrobotrys* Merr.

4.2.2 Structure elucidation of 7

Horsfieldone A (**7**) was obtained as white powder; $[\alpha]_D^{27}$= -4.58 (*c* 1.1, MeOH); UV (MeOH) λ_{max} (log ε): 271 (1.03) nm. The HRESIMS spectrum showed the [M+Na]$^+$ ion at *m/z* 381.1677, which was accounted for the molecular formula of $C_{21}H_{26}O_5$. The ^{1}H NMR spectrum revealed two sets of aromatic protons [δ_H 5.83 (2H, s) and 7.22-7.32 (5H, m)], oxygenated methines (δ_H 4.59) as well as methylene protons in two different regions [δ_H 3.02 (2H) and 1.23-1.71 (*ca* 12H)]. The presence of ketone (δ_C 207.6) and querternary oxygenated carbons (δ_C 166.0 (2×C) and 165.8) were also observed in ^{13}C

NMR spectrum. NMR data analysis including COSY, HSQC and HMBC led to the construction of three separated substructures.

Starting from the aromatic singlet at δ_H 5.83 (2H, H-3′ and H-5′), its HMBC correlations (Figure 4.1) with C-4′ (166.0), C-2′ & C-6′ (165.8), C-1′(105.4) and C-1 (207.6) allowed to establish the acyl substituted 1,3,5-trihydroxybenzene moiety as the first substructure. The second substructure was assigned as monosubstituted benzene linked to a secondary alcohol (δ_H 4.59 (1H) and δ_C 75.3) as evidenced by HMBC crosspeaks of H-9/C-1″ and H-9/C-2″. Subtraction of aforementioned substructures from the molecular formula resulted in seven contiguous methylenes (7✕CH$_2$) as the remaining substructure. Finally, the above two aromatic moieties were flanked by a long chain methylenes, as evidenced from the HMBC correlations of H-2/C-1 and H-8/C-9. Thus, the overall structure of horsfieldone A (**7**) was established as shown.
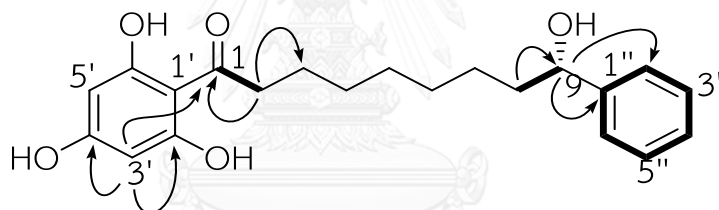
Figure 4.1. Selected COSY (bold line) and HMBC (arrow curve) correlations of **7**

The absolute configuration of C-9 in **7** was addressed by applying Mosher's method [88] (Scheme 4.2). Prior to introducing chiral MPAs, the phenolic groups were methylated with MeI/K$_2$CO$_3$ to avoid undesired ester formation between phenolics and MPA [89], [90]. The obtained methyl ether (**7a**) was subsequently reacted with (*R*)- or (*S*)-MPA acids in the presence *N*-ethyl-*N′*-(3-dimethylaminopropyl)carbodiimide (EDC) as a coupling reagent, yielding the corresponding MPA esters **7b** and **7c**, respectively. The differences in the proton chemical shifts ($\Delta\delta H_{SR}$) between (*S*)- and (*R*)-MPA esters of **7** (Scheme 1) indicated an *S* configuration at C-9.
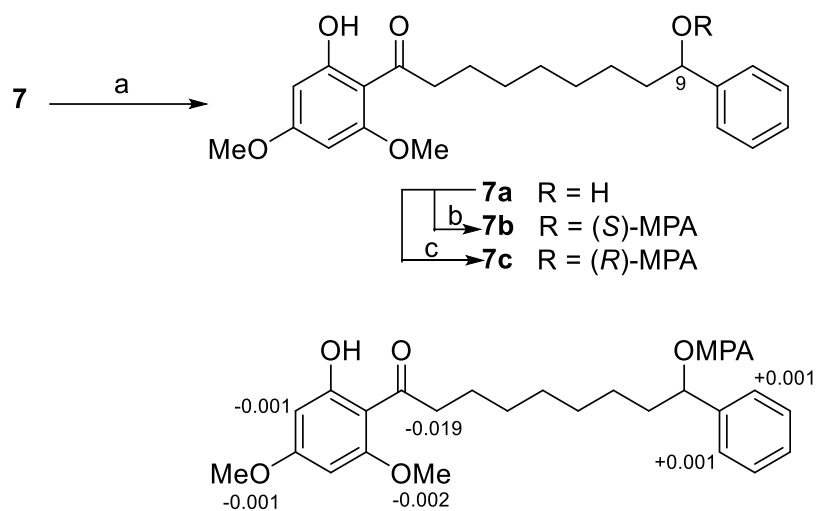
Scheme 4.2 Synthesis of MPA esters of **7** and $\Delta\delta H_{SR}$ distribution, reagent and conditions: (a) MeI, K_2CO_3; (b) (S)-MPA, EDC, DMAP (c) (R)-MPA, EDC, DMAP.

4.2.3 Structure elucidation of 8

Maingayone D (**8**) was obtained as a white powder; $[\alpha]_D^{27}$ = -7.43 (c 1.28, MeOH); UV (MeOH) λ_{max} (log ε): 271 (1.22) nm. Its HRESIMS spectrum showed a peak of $[M+Na]^+$ ion at m/z 607.2655, corresponding to the molecular formula of $C_{36}H_{40}O_7$. Although the ^1H NMR spectrum of **8** was nearly identical to that of **7**, some distinct resonances such as more crowded aromatic protons (δ_H 7.20-7.32, 11H) as well as downfield methylenes (δ_H 2.34-2.64) could be observed. Careful inspection on ^1H and ^{13}C NMR spectra of **8** revealed that all critical signals of **7** were likely to be incorporated in **8**.

The aforementioned findings preliminarily suggested that **8** comprised horsfieldone A core structure (substructure **I**, rings **a**, **b** and long chain methylenes) connected with another smaller arylalkanone residue. The remaining moiety (substructure **II**) was constructed on the basis of COSY and HMBC correlations (Figure 4.2). The propylene moiety (H-1′→H-3′), established from COSY data, was linked to a substituted 1,3-dihydroxybenzene (ring **b′**) and monosubstituted benzene (ring **a′**), on the basis of HMBC correlations of H-1′ to C-11′ (131.0) and C-15′ (156.2) together with those of H-3′ to C-4′ (144.2) and C-5′ (129.2). The newly established substructure **II** was accommodated to substructure **I** through the linkage between C-1′ and C-20 (ring

b) as evidenced by the crosspeaks of H-1′ to C-19, C-20 and C-21. Therefore, the gross structure of **8** was established as shown. The configuration of chiral C-9 was proposed to be identical to that of **7** on the basis of similar chemical shift, multiplicity pattern and biosynthetic point of view whereas the stereochemistry of chiral C-1′ remained undetermined.
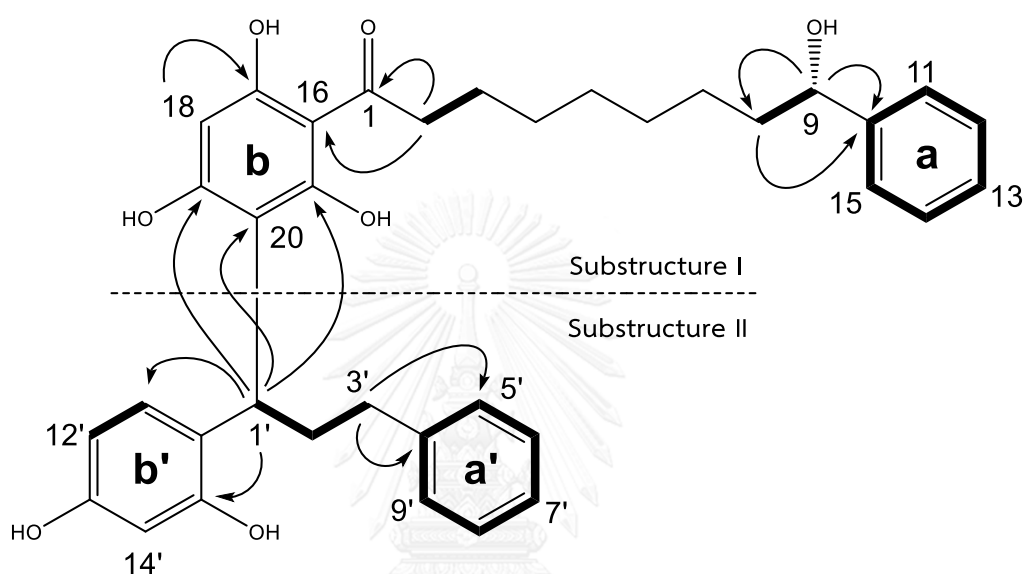
Figure 4.2 Selected COSY (bold line) and HMBC (arrow curve) correlations of **8**

4.2.4 Structure elucidation of 9

8-C-β-D-glucopyranosylpinocembrin (**9**) was obtained as a yellowish oil; $[\alpha]_D^{27}$= -74.28 (*c* 0.9, MeOH); UV (MeOH) λ_{max} (log ε): 271 (1.21) nm. The molecular formula of $C_{21}H_{22}O_9$ was established by the observation of $[M+Na]^+$ ion peak at *m/z* 441.1161 in HRESIMS spectrum. The ^{1}H NMR spectrum contained signals corresponding to characteristic of a flavanone structure at δ_H 5.54 (dd, *J* =12.8, 2.4 Hz, H-2), 2.99 (dd, *J* =16.9, 13.2 Hz, H-3) and 2.81 (dd, *J* =17.0, 3.0 Hz, H-3), in addition to monosubstituted (δ_H 7.36-7.59, 5H) and pentasubstituted (δ_H 5.98, s, 1H) benzenes. The downfield signal of typical 5-OH (δ_H 12.20, s) in conjunction with HMBC correlations from H-6 to C-5 (163.2), C-7 (167.3) and C-8 (105.3) suggested the substitution pattern of ring A as shown (Figure 4.3). A typical coupling pattern among H-2, H-3$_{ax}$ and H-3$_{eq}$ suggested an *S-*

configuration for C-2 of **9**, which is common among natural flavanones [91], [92], [93], [94].

The presence of a sugar moiety was noticed by anomeric proton (H-1″) at δ_H 4.81 along with a series of contiguous oxygenated methines (δ_H 4.07, 3.71, 3.41 and 3.32) and methylene (δ_H 3.90). Analysis of NMR chemical shifts and coupling constants allowed to assign this sugar as glucosyl moiety, whose β-orientation was proved by a large coupling constant (9.8 Hz) of H-1″. Finally, the gross structure of **9** was established by assembling the flavanone and glucose moieties through *C*-glycosidic bond from C-8 to C-1″ as evidenced from relatively upfield shift of anomeric C-1″ (δ_C 75.4) along with HMBC crosspeaks from H-1″ to C-7, C-8 and C-8a. The absolute D-configuration for glucose was assigned from the natural occurrence of this sugar in flavanone glycosides.

9
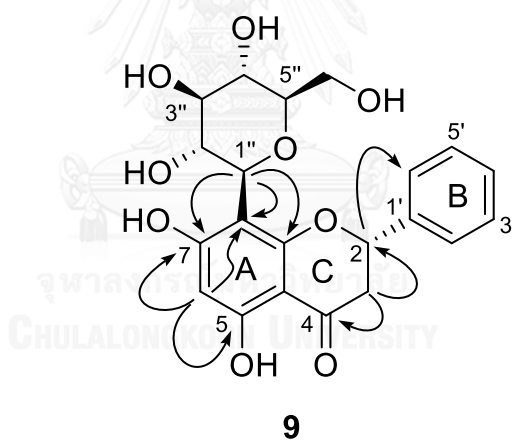
Figure 4.3. Selected HMBC correlations of **9**

4.2.5 α-Glucosidase inhibition and radical scavenging activity of compounds 7-9 and their derivatives

Inhibitory activity of isolated compounds (**7-9**) was determined against α-glucosidases and DPPH (Table 4.1).

Table 4.1 α-Glucosidase inhibition and DPPH radical scavenging activity of isolated compounds

Compounds	IC_{50} (μM)[a]			DPPH[c]
	Baker's yeast	Rat Intestinal		
		Maltase	Sucrase	
7	22.61	47.18	94.93	1.60
8	5.65	33.89	47.41	0.43
9	528.56	1,851.16	NI[b]	6.76
Acarbose	103.0	2.1	26.0	-
Ascorbic Acid	-	-	-	2.45

[a] Data shown as mean of duplicate experiments.

[b] NI, no inhibition, inhibitory effect less than 30 % at 10 mg/mL.

[c] The values are expressed as SC_{50} (mM).

Compounds **7-9** were evaluated for antioxidant activity and inhibitory effect against α-glucosidase from two different sources, Baker's yeast (type I) and rat intestine (type II as maltase and sucrase) (Table 4.1). Of tested compounds, arylalkanones **7** and **8** showed strikingly potent activity, compared with flavanone glycoside **9**, in all bioassays examined. Maingayone D (**8**) displayed significantly more potent bioactivity (4 times) than **7**, toward DPPH radical (IC_{50} 0.42 μM) and yeast α-glucosidases (IC_{50} 5.65 μM). However, the inhibition of **8** against maltase and sucrase was slightly improved (1-2 times) than that of **7**. These observations suggested that the presence of additional phenolic moieties in **8** somewhat enhanced inhibitory effect against free radical and α-glucosidase.

To gain insight into the mechanism underlying inhibitory effect of arylalkanones **7** and **8** toward rat intestinal α-glucosidases, their kinetic study was performed. The Linewaever-Burk plot of **7** against maltase (Figure 4.4a) showed a series of straight lines; all of which intersected in the second quadrant. Kinetic analysis showed that V_{max} decreased with elevated K_m in the presence of increasing concentrations of **7**. This behavior suggested that maltase could be inhibited by **7** in two opposite pathways, competitive and noncompetitive manners. The observed resulted could be elaborated by simultaneous formation of enzyme-inhibitor (EI) and enzyme-substrate-inhibitor (ESI) complexs in competitive and noncompetive manners, respectively (Scheme 4.3).

A

B
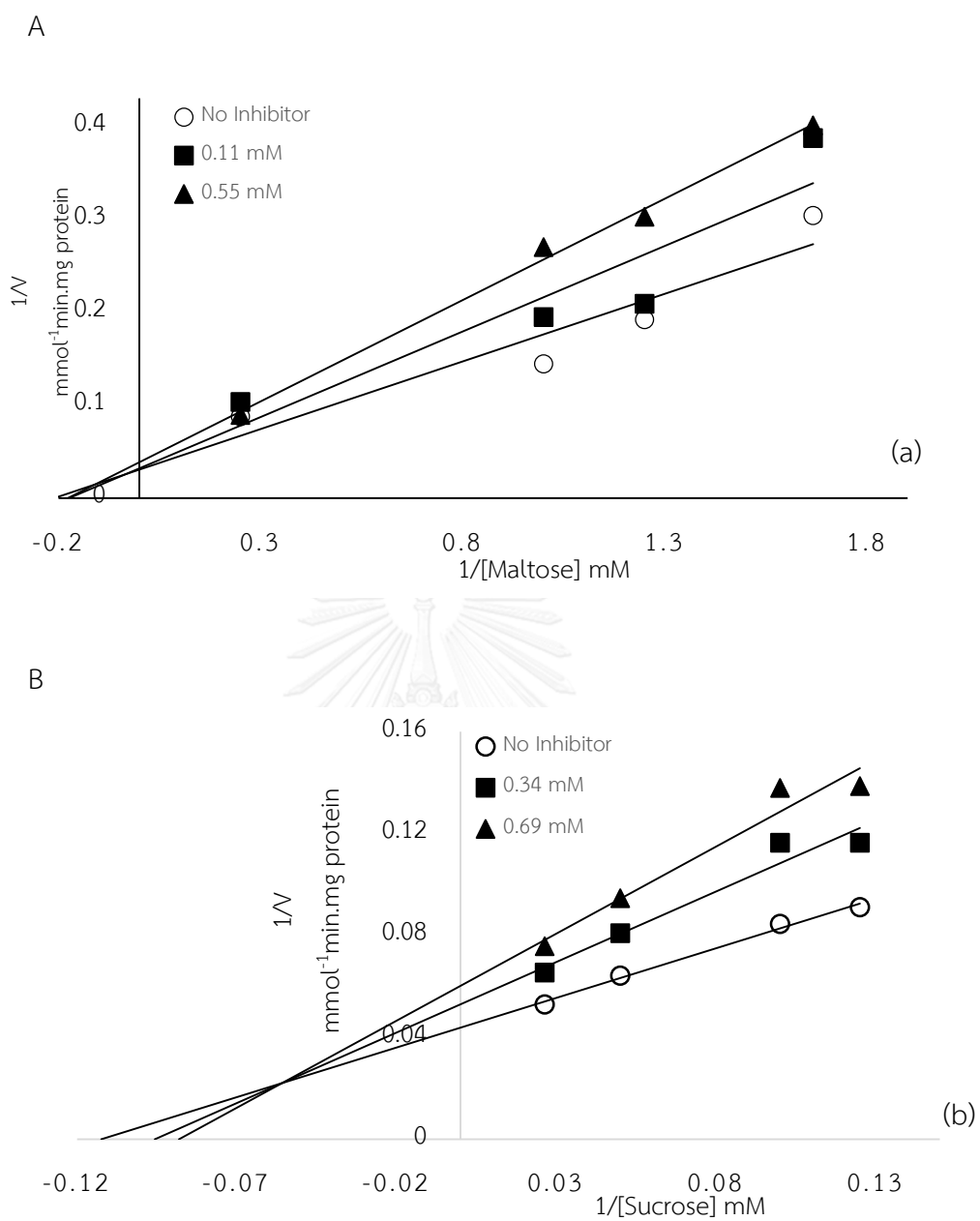
Figure 3.4 Lineweaver-Burk plot analysis of **7** against rat intestinal **(a)** maltase and **(b)** sucrase.

A

(a)

B

(b)
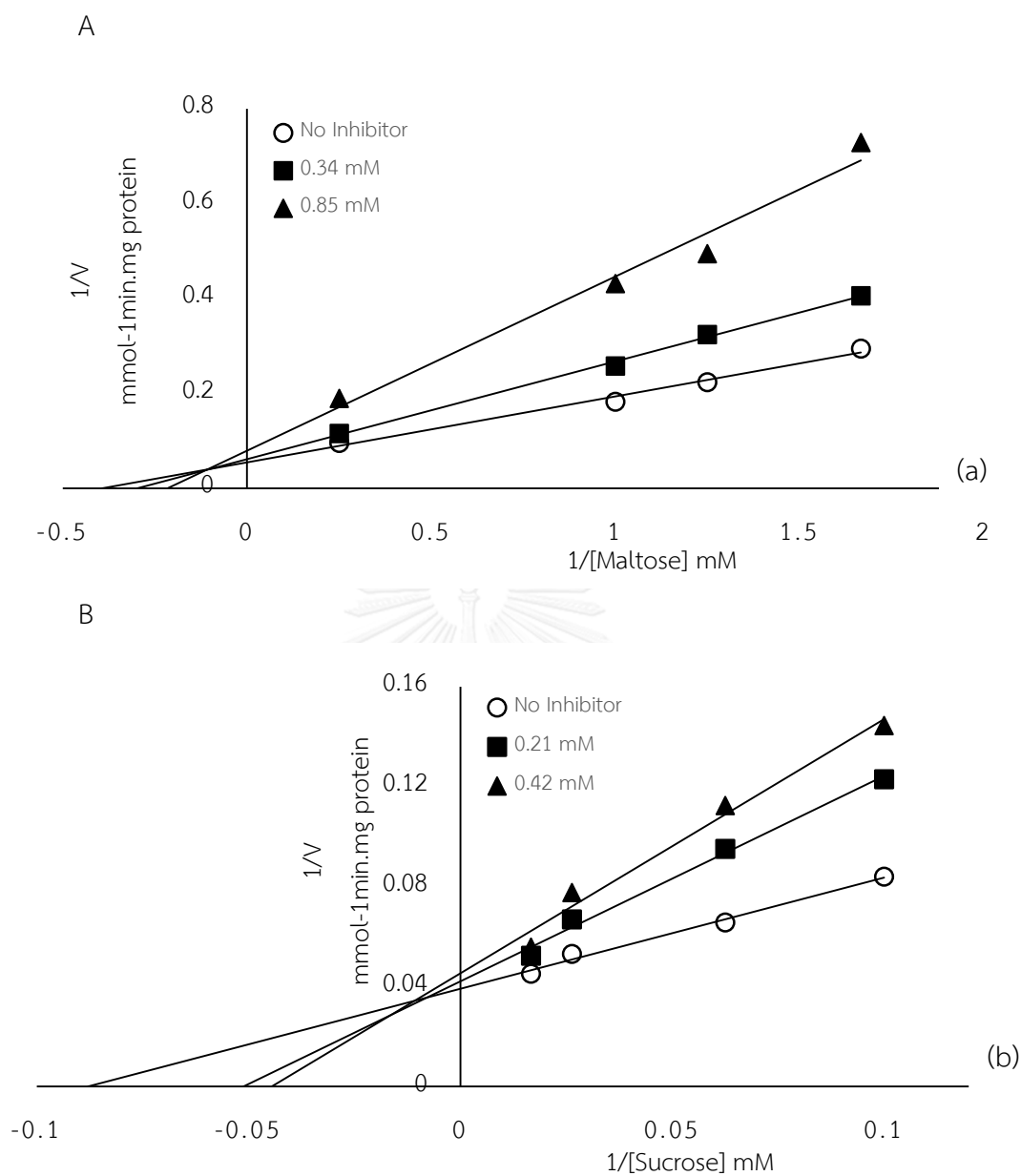
Figure 4.5. Lineweaver-Burk plot analysis of **8** against rat intestinal **(a)** maltase and **(b)** sucrase.

We further investigate the pathway in which **7** preferentially preceded by determining dissociation constants of EI (K_i) and ESI (K_i') complexes (Table 4). Apparently, the secondary plot demonstrated K_i and K_i' values of 1.64 and 0.48 mM, respectively, therefore indicting that **7** predominantly formed an ESI complex rather

than directly bound to maltase (EI). The putative inhibitory mechanism is summarized in Scheme 4.3.
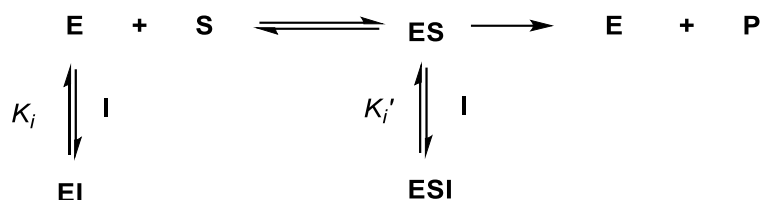
Scheme 4.3. Putative inhibitory mechanism of **7** and **8** against rat intestinal α-glucosidases. E, S, I and P represent enzyme, substrates, (maltose and sucrose), inhibitors (**7** and **8**) and glucose, respectively.

The inhibitory mechanism of **7** against sucrase (Figure 4.4b) together with that of **8** toward maltase (Figure 4.5a) and sucrase (Figure 4.5b) were also examined using the above methodology. Apparently, they inhibited these α-glucosidases by both competitive and noncompetitive manners (mixed-type inhibition). All kinetic factors are summarized in Table 4.2.

Table 4.2 Kinetic factors of **7** and **8** for inhibition against rat intestinal α-glucosidases

Compounds	Maltase			Sucrase		
	K_i (mM)	K_i' (mM)	Inhibition type	K_i (mM)	K_i' (mM)	Inhibition type
7	1.64	0.48	mixed	1.09	0.54	mixed
8	1.96	0.53	mixed	3.07	0.38	mixed

In summary, a new series of effective antibiabetic agents having both therapeutic and preventive effects were identified. Of isolated metabolites, maingayone D (**8**) is of great interest in terms of structural feature and inhibitory potency. To our knowledge, there have been a few dimeric arylalkanones reported so far. In fact, maingayone has been collectively applied for the dimer containing identical monomers connected each other through sp^2C-sp^3C bonding, while giganteone is

another collective name applied for dimeric arylalkanones having similar monomers coupled each other via sp^2C-sp^2C linkage (Figure 4.6) [70, 79]

However, the structure of maingayone D (**8**) is quite distinct among others maingayones in that it comprises two different moieties, the C_6-C_{10}-C_6 arylalkanone and C_6-C_3-C_6 phenolic; whereas other maingayones were biosynthesized from two identical C_6-C_{10}-C_6 residues. The occurrence of maingayone D (**8**) suggested plausible cross couplings among phenolic compounds, therefore producing a variety of diverse skeletons.

The highly potent antioxidant activity and α-glucosidase inhibition of **8** would be beneficial in diabetes therapy and preventing the onset of its complications. In addition, the mechanism underlying the inhibition of **8** suggested that it could be used as either single antidiabetic agent or combination with competive antidiabetic drugs such as acarbose.
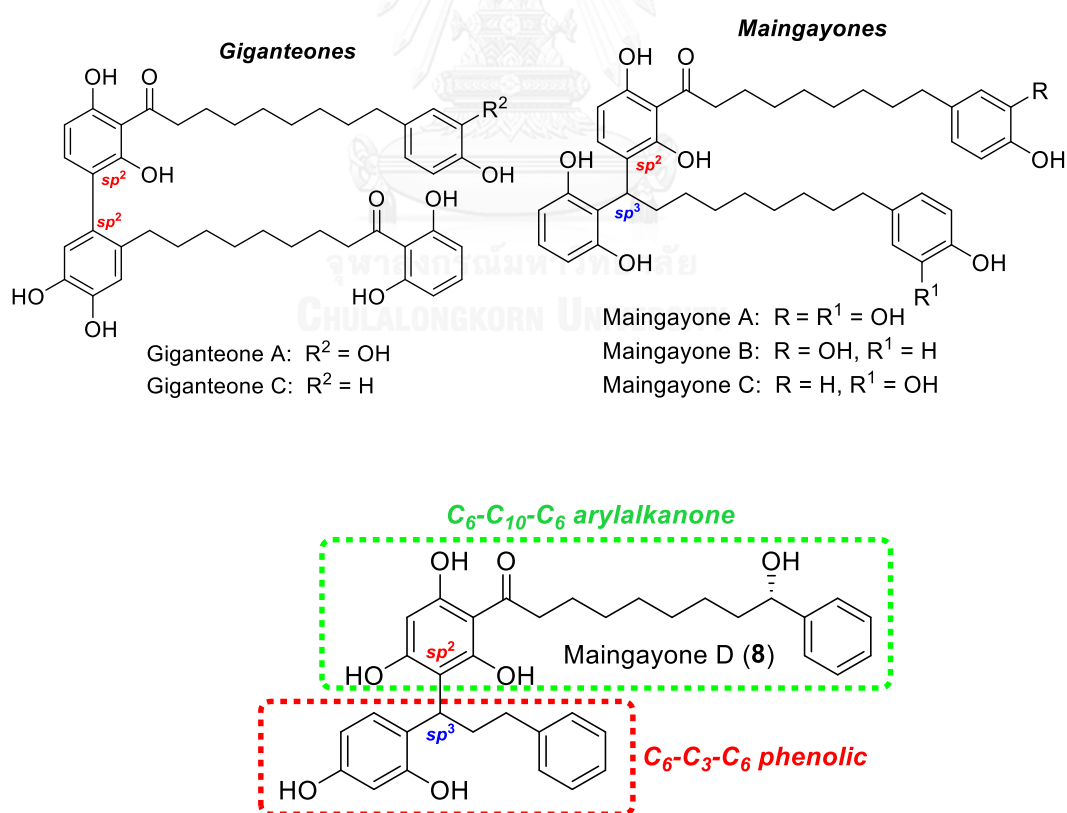

Figure 4.6. Structures of giganteone and maingayone dimeric arylalkanones

4.3   Experimental section

4.3.1   General experimental procedures

1D and 2D NMR spectra were recorded on a 400 MHz Bruker AVANCE spectrometers. The chemical shifts were reported in ppm as referenced to solvent residues (CD$_3$OD, δ_H 3.30 ppm and δ_C 49.0 ppm). UV spectra were measured with a UV-7504 spectrophotometer. Optical rotations were determined on a Perkin-Elmer 341 polarimeter using a cell with a 0.3-mL capacity and a 1 cm path length. High resolution mass spectra were acquired using Bruker micrOTOF mass spectrometer, equipped with an electrospray ionization (ESI) ion source. Chromatography was performed on a Sephadex LH-20, Merck silica gel 60 (70-230 mesh) and TLC was performed on precoated Merck silica gel 60 F$_{254}$ plates (0.25 mm thick layer). α-Glucosidase (EC 3.2.1.20) from *Saccharomyces cerevisiae* and 4-nitrophenyl-α-D-glucopyranoside (*p*-NPG) were obtained from Sigma-Aldrich (St. Louis, MO, USA). Acarbose was obtained from Bayer Vitol Leverkusen, Germany. Rat intestinal acetone powder was supplied by Sigma Aldrich. Spectrophotometric measurements for the α-glucosidase inhibition, antioxidant assay and kinetic study were taken on a Sunrise microplate reader spectrophotometer.

4.3.2 Plant material

The stem barks of *H. macrobotrys* Merr were collected from East Kalimantan, Indonesia in May 2013. Plant authentication was carried out by The Research Center for Biology, Indonesian Institute of Sciences. A voucher specimen (KK-1410-HM002) has been deposited at the Forest Products Chemistry Laboratory at The Mulawarman University, East Kalimantan, Indonesia.

4.3.3   Extraction and isolation

The dried stem bark of *H. macrobotrys* Merr (2.4 kg) were extracted with MeOH at ambient temperature for 3 days. The concentrated MeOH extract was suspended in water and partitioned with CH$_2$Cl$_2$ (3 $\times$ 1L) to afford the active CH$_2$Cl$_2$ extract, which was chromatographed by Vacuum column chromatography (silica gel 60G Merck)

column (120 mm ID X 7 cm length) and eluted with six mobile phases of 1:0, 8:2, 6:4, 4:6, 2:8 and 0:1 hexane:EtOAc. The fraction 4 was chromatographed on Sephadex LH-20 using MeOH followed by crystallization (CH_2Cl_2) to afford horsfieldone A (**7,** 420 mg). Subfractions from fraction 4 were separated on Sephadex LH-20 (1:1 CH_2Cl_2-MeOH) to afford maingayone D (**8**, 35 mg). The fraction 6 was chromatographed on Sephadex LH-20 using MeOH to afford 12 subfractions. Subfraction 6 was chromatographed on Sephadex LH-20 (12:80:8 C_6H_{14}-CH_2Cl_2-MeOH) to afford 8-C-***β***-D-glucopyranosylpinocembrin (**9**, 24 mg).

Horsfieldone A **(7)** white powder, $[α]_D^{27}$= -4.58 (*c* 1.1, MeOH); UV (MeOH) $λ_{max}$ (log $ε$): 271 (1.03) nm; ^{1}H NMR (CD$_3$OD, 400 MHz) $δ$ 7.32 (2H, m, H-3" and H-5"), 7.31 (2H, m, H-2" and H-6"), 7.22 (1H, m, H-4"), 5.83 (2H, s, H-3'and H-5'), 4.59 (1H, t, *J* = 6.7 Hz, H-9), 3.02 (1H, t, *J* = 7.9 Hz, H-2), 1.71 (1H, m, H-8), 1.62 (1H, m, H-7), 1.62 (1H, m, H-3), 1.40 (1H, m, H-6), 1.32 (1H, m, H-5), 1.23 (1H, m, H-4). ^{13}C NMR (CD$_3$OD, 100 MHz) $δ$ 207.6 (C-1), 166.0 (C-4'), 165.8 (C-2' and C-6'), 146.5 (C-1"), 129.2 (C-3" and C-5"), 128.2 (C-4"), 127.1 (C-2" and C-6"), 105.4 (C-1'), 95.8 (C-3' and C-5'), 75.3 (C-9), 44.8 (C-2), 40.2 (C-8), 30.5 (C-3, C-4 and C-5), 26.3 (C-7), 26.2 (C-3). HRESIMS *m/z* [M+Na]$^+$ 381.1677.

Maingayone D **(8)** white powder, $[α]_D^{27}$= -7.43 (*c* 1.28, MeOH); UV (MeOH) $λ_{max}$ (log $ε$): 271 (1.22) nm; ^{1}H NMR (CD$_3$OD, 400 MHz) **Substructure I** $δ$ 7.32 (3H, m, H-12, H-13 and H-14), 7.31 (2H, m, H-11 and H-15), 5.93 (1H, s, H-18), 4.59 (1H, t, *J* = 6.7 Hz, H-9), 3.02 (1H, t, *J* = 7.4 Hz, H-2), 1.70 (1H, m, H-8), 1.65 (1H, m, H-7), 1.63 (1H, m, H-3), 1.32 (1H, m, H-5), 1.31 (1H, m, H-4), 1.23 (1H, m, H-6). ^{13}C NMR (CDCl$_3$, 100 MHz) $δ$ 208.0 (C-1), 164.9 (C-21), 164.1 (C-17), 162.0 (C-19), 146.5 (C-10), 128.1 (C-14 and C-12), 127.1 (C-11 and C-15), 126.4 (C-13), 110.0 (C-20), 105.5 (C-16), 95.9 (C-18), 75.3 (C-9), 44.9 (C-2), 40.2 (C-8), 30.5 (C-4), 30.4 (C-5 and C-6), 26.8 (C-7), 26.3 (C-3). **Substructure II** $δ$ 7.31 (1H, m, H-11'), 7.21 (1H, m, H-7'), 7.20 (2H, m, H-5' and H-9'), 7.20 (2H, m, H-6' and H-8'), 6.25 (1H, dd, J_1 = 10.8 Hz; J_2 = 2.5 Hz, H-12'), 6.24 (1H, d, *J* = 2.4 Hz, H-14'), 4.44 (1H, dd, J_1= 8.9 Hz; J_2 = 6.8 Hz, H-1'), 2.50 (1H, t, *J* = 7.7 Hz, H-3'), 2.34; 2.64 (1H, m, H-2'). ^{13}C NMR (CDCl$_3$, 100 MHz) $δ$ 157.1 (C-13'), 156.2 (C-15'), 144.2 (C-4'), 131.0 (C-11'), 129.5

(C-7'), 129.2 (C-5' and C-9'), 129.1 (C-6' and C-8'), 122.8 (C-10'), 107.8 (C-12'), 103.4 (C-14'), 36.0 (C-3'), 34.9 (C-2'), 34.5 (C-1'). HRESIMS m/z [M+Na]$^+$ 607.2655.

8-C-β-D-Glucopyranosylpinocembrin **(9)** yellow oil, $[\alpha]_D^{27}$= -74.28 (*c* 0.9, MeOH); UV (MeOH) λ_{max} (log ε): 271 (1.21) nm; ^{1}H NMR (CD$_3$OD, 400 MHz) δ 12.20 (s, 5-OH), 7.59 (2H, d, *J* = 7.4 Hz, H-2' and H-6'), 7.43 (2H, t, *J* = 7.4 Hz, H-3' and H-5'), 7.36 (1H, t, *J* = 7.3 Hz, H-4'), 5.98 (1H, s, H-6), 5.54 (1H, dd, J_1 = 12.8 Hz; J_2 = 2.4 Hz, H-2), 4.81 (1H, d, , *J* = 9.8 Hz, H-1"), 4.07 (1H, dd, J_1 = 9.2 Hz; J_2 = 9.2 Hz, H-2"), 3.90 (1H, d, *J* = 11.9 Hz, H-6"), 3.71 (1H, m, H-3"), 3.41 (1H, m, H-4"), 3.32 (1H, m, H-5"), 2.99 (dd, J_1 = 16.9 Hz, J_2 = 13.2 Hz, H-3$_{ax}$), 2.81 (dd, J_1 = 17.0 Hz, J_2 = 3.0 Hz, H-3$_{eq}$). ^{13}C NMR (CD$_3$OD, 100 MHz) δ 197.8 (C-4), 167.3 (C-7), 164.9 (C-8a), 163.2 (C-5), 140.7 (C-1'), 129.5 (C-2' and C-6'), 129.3 (C-4'), 127.0 (C-3' and C-5'), 105.3 (C-8), 103.6 (C-4a), 97.3 (C-6), 82.3 (C-5"), 80.2 (C-3"), 80.1 (C-2), 75.4 (C-1"), 73.9 (C-4"), 71.0 (C-2"), 63.2 (C-6"), 44.4 (C-3). HRESIMS m/z [M+Na]$^+$ 441.1161.

4.3.4 α-Glucosidase inhibitory activity and free radicals scavenging

4.3.4.1 Chemical and equipment

The chemical and equipment for bioassay using the same reagents and enzymes described in Chapter 2.

4.3.4.2 α-Glucosidase inhibitory activity from Baker's yeast

The activity effect of isolated compound were evaluated using the same procedure described in Chapter 2.

4.3.4.3 α-Glucosidase inhibitory activity from rat intestine

The activity effect of isolated compound were evaluated using the same procedure described in Chapter 2.

4.3.4.4 Kinetic study of **α-glucosidase inhibition**

In order to evaluate the type of inhibition, a kinetic analysis of maltase and sucrase was carried out according to the above reaction. The quantity of maltase and sucrase was maintaned in crude rat intestinal enzymes, while the concentrations of **7** and **8** for kinetic analysis of maltase were varied in the range of 0-0.55 mM and 0-0.85 mM, respectively. The concentration of **7** and **8** for for kinetic analysis of sucrase were varied in the range of 0-0.69 mM and 0-0.42 mM, respectively. The K_i value was determined from secondary plots of slope *vs.* [I], and the K'_i value was calculated from secondary plots of interception *vs.* [I].

.

4.3.4.5 Free radicals scavenging (DPPH)

The activity effect of isolated compound were evaluated using the same procedure described in Chapter 3.

4.3.5   Modified Methoxytrifluoromethylphenylacetic Acid (MTPA) Reaction of 7

A solution of **7** (60 mg, 0.167 mmol) in acetonitrile (1 mL) was added MeI (100 μL, 0.835 mmol) in the presence of K_2CO_3 (115 mg) at room temperature overnight. The reaction mixture was evaporated to dryness and purified by silica gel column chromatography using 5:95 EtOAc-hexane to yield dimethyl ether analogue **7a** (16 mg) as a major product. A solution of **7a** (9 mg, 0.026 mmol) in anhydrous CH_2Cl_2 (1 mL) was added *S*-MPA acid (6.43 mg, 0.0387 mmol), EDC (19 mg, 0.0645 mmol) and DMAP (catalytic quantity). After stirred at room temperature overnight, the reaction mixture was quenched with water and extracted twice with CH_2Cl_2. The combined organic layer was dried over anhydrous Na_2SO_4, and the solvent was removed under reduced pressure. The residue was purified by silica gel column chromatography eluted with a 1:9 EtOAc-hexane to yield *S*-MPA ester **7b**. In a similar manner, the *R*-MPA ester **7c** was also prepared. ^{1}H NMR spectra of *S*-MPA ester **7b** and *R*-MPA ester **7c** are showed in Figures **4.25** and **4.26**, respectively.
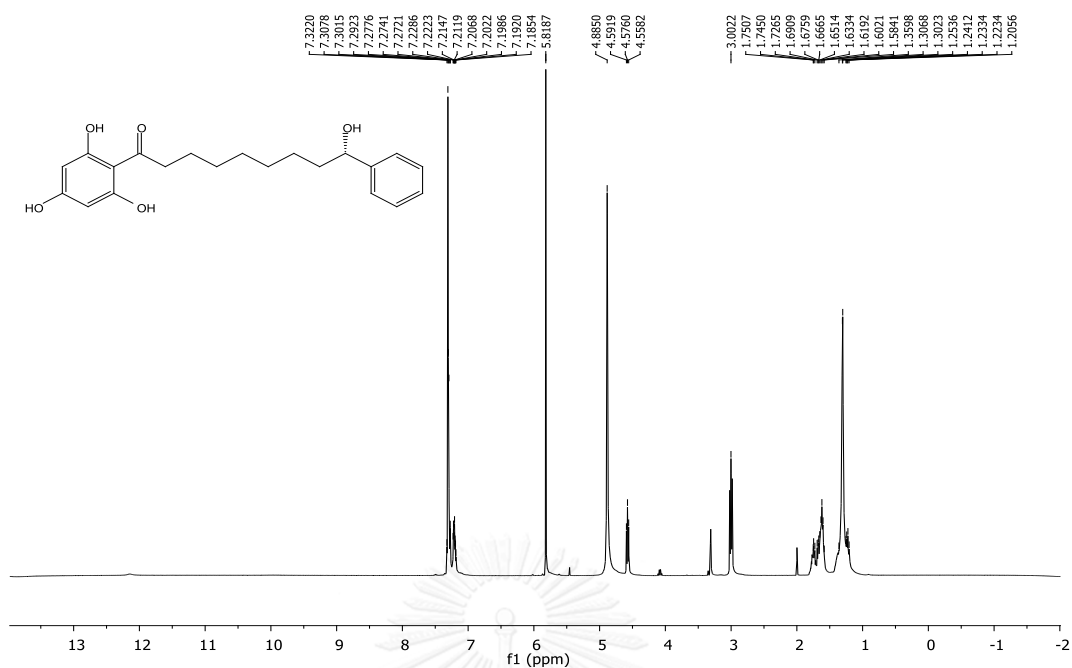
SUPPORTING INFORMATION

Figure 4.7 ^{1}H-NMR spectrum (400 MHz, in CD$_3$OD) of **7**
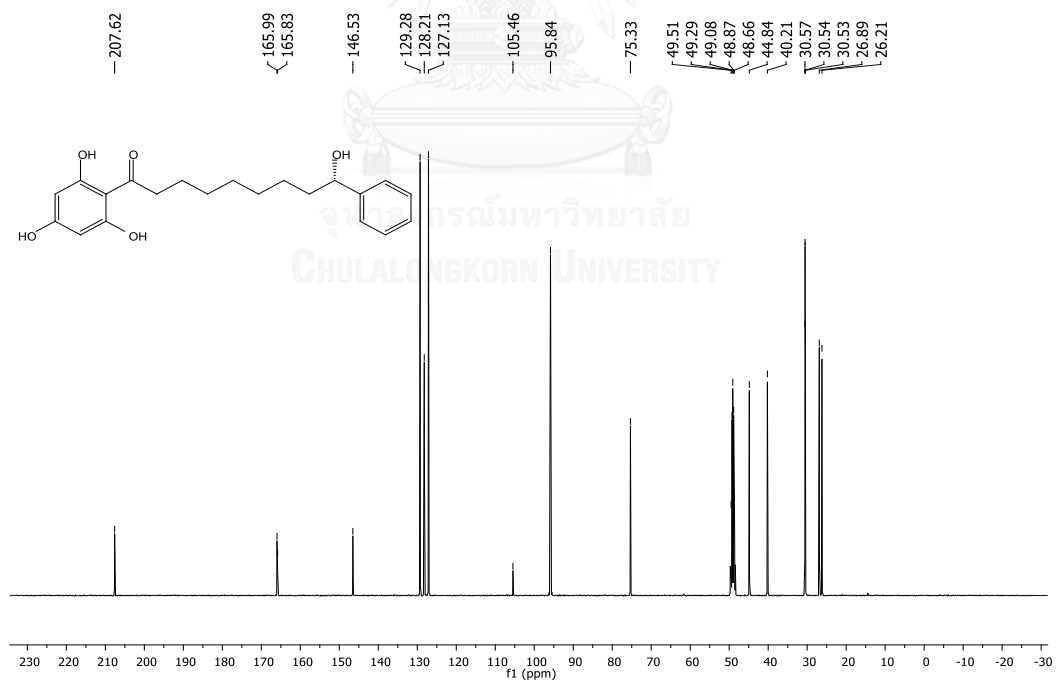
Figure 4.8 ^{13}C-NMR spectrum (100 MHz, in CD$_3$OD) of **7**
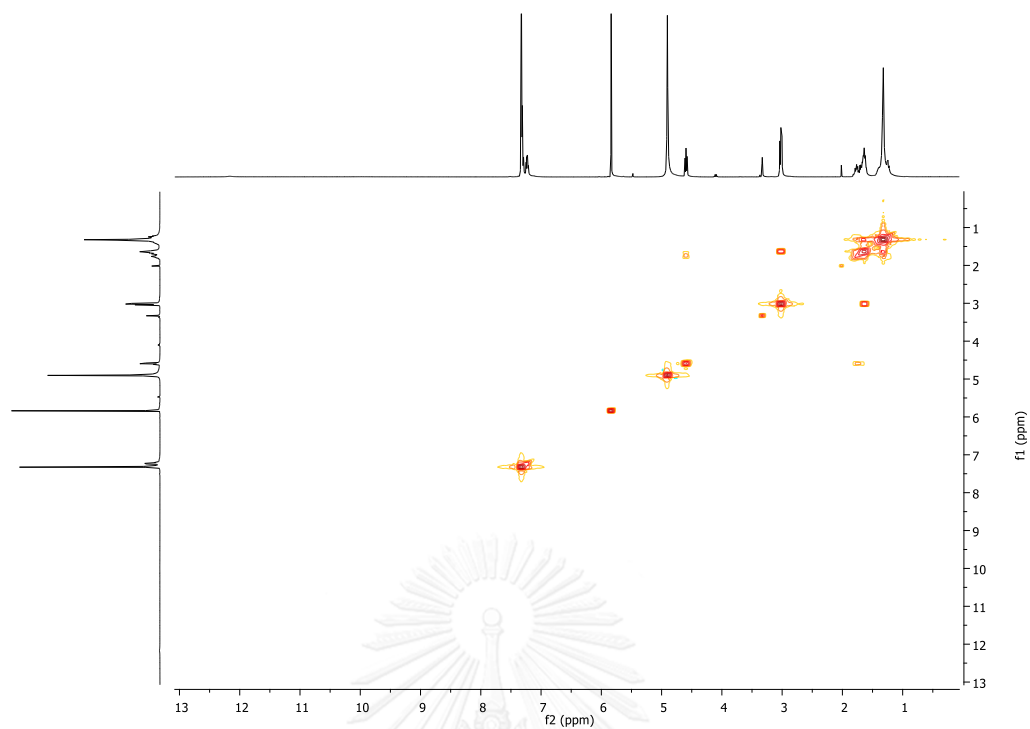
Figure 4.9 COSY spectrum of **7**
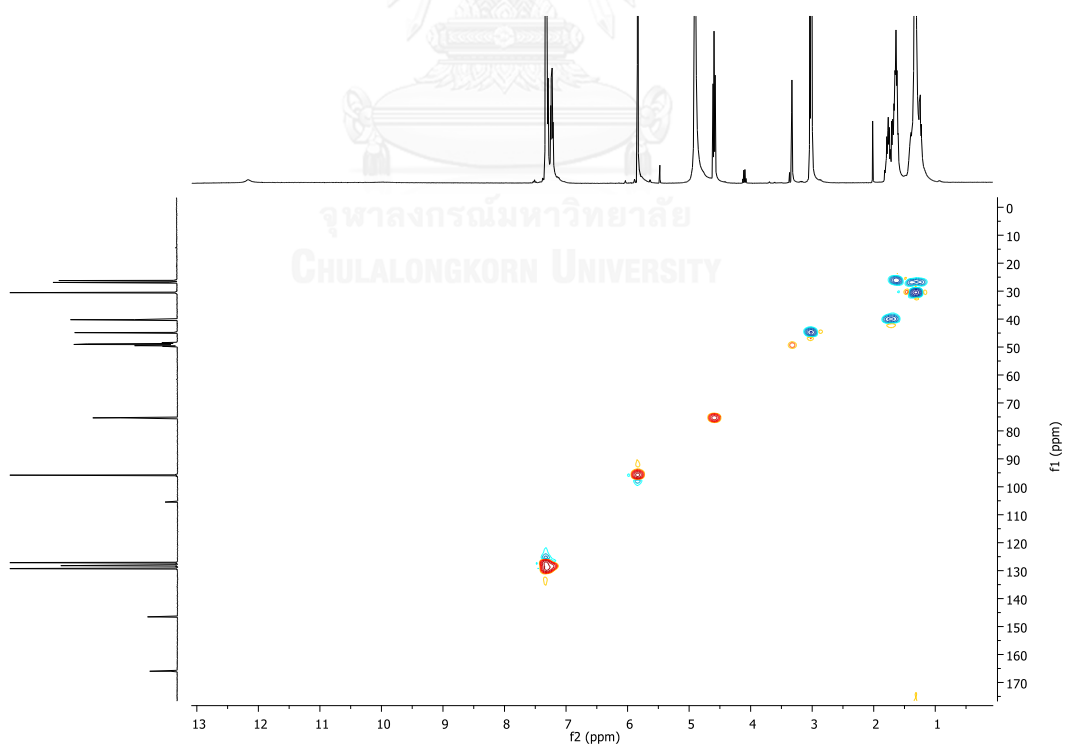
Figure 4.10 HSQC NMR spectrum of **7**
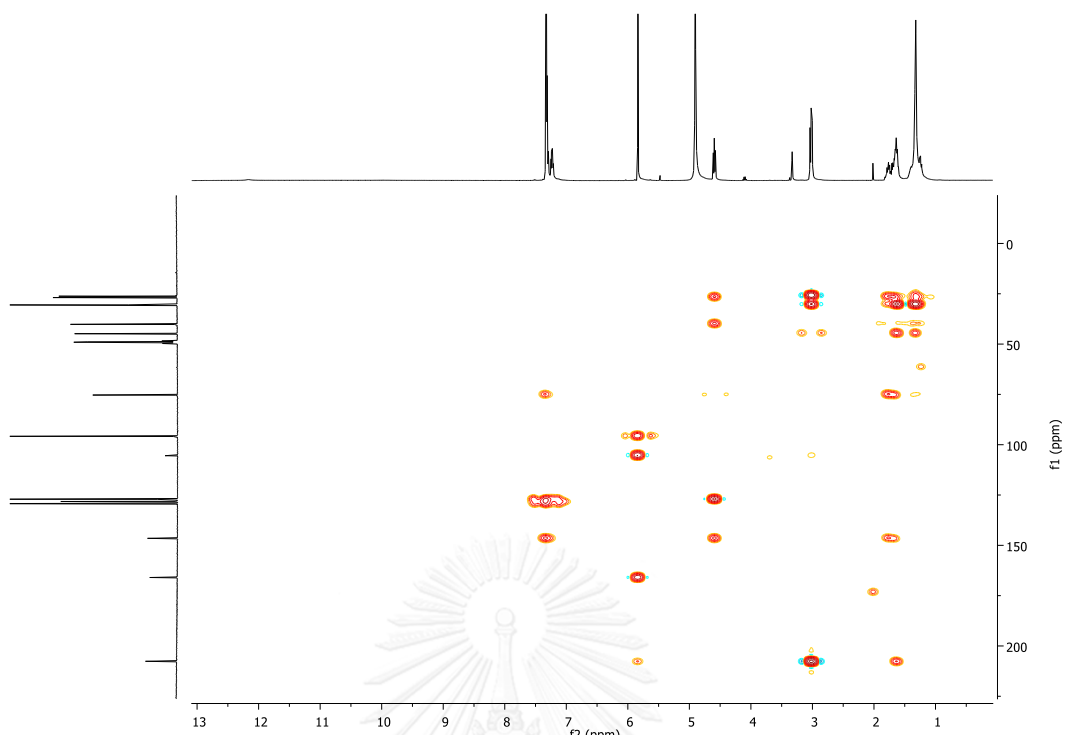
Figure 4.11 HMBC spectrum of **7**

Mass Spectrum List Report

Analysis Info

Analysis Name	OSCULKG571201001.d	Acquisition Date	12/1/2014 12:18:42 PM
Method	MKE_tune_wide_20130204.m	Operator	Administrator
Sample Name	WH14	Instrument	micrOTOF 72
	WH14		

Acquisition Parameter

				Set Corrector Fill	79 V
Source Type	ESI	Ion Polarity	Positive	Set Pulsar Pull	406 V
Scan Range	n/a	Capillary Exit	200.0 V	Set Pulsar Push	388 V
Scan Begin	50 m/z	Hexapole RF	400.0 V	Set Reflector	1300 V
Scan End	3000 m/z	Skimmer 1	45.0 V	Set Flight Tube	9000 V
		Hexapole 1	25.0 V	Set Detector TOF	1910 V
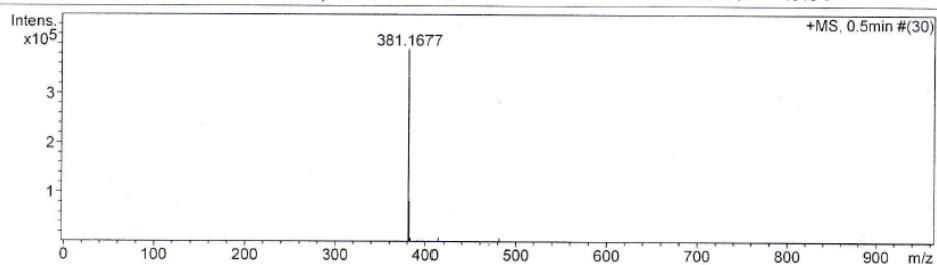
Figure 4.12 HRESIMS spectrum of **7**
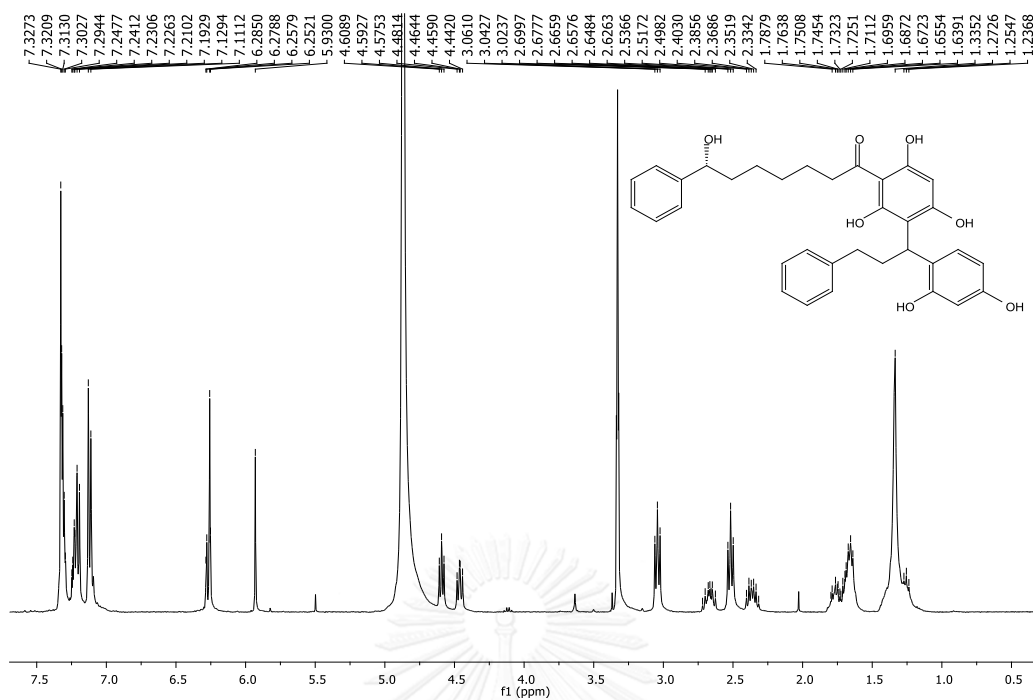
Figure 4.13 ^{1}H NMR spectrum of **8 (**400 MHz, in CD$_3$OD)
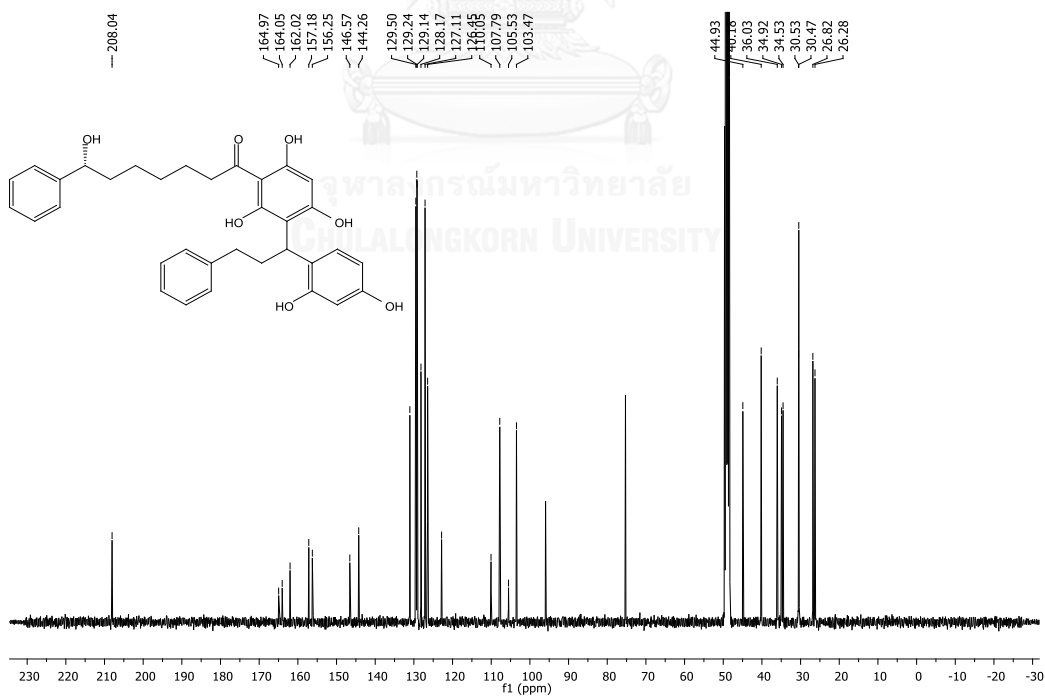
Figure 4.14 ^{13}C NMR spectrum of **8** (100 MHz, in CD$_3$OD)
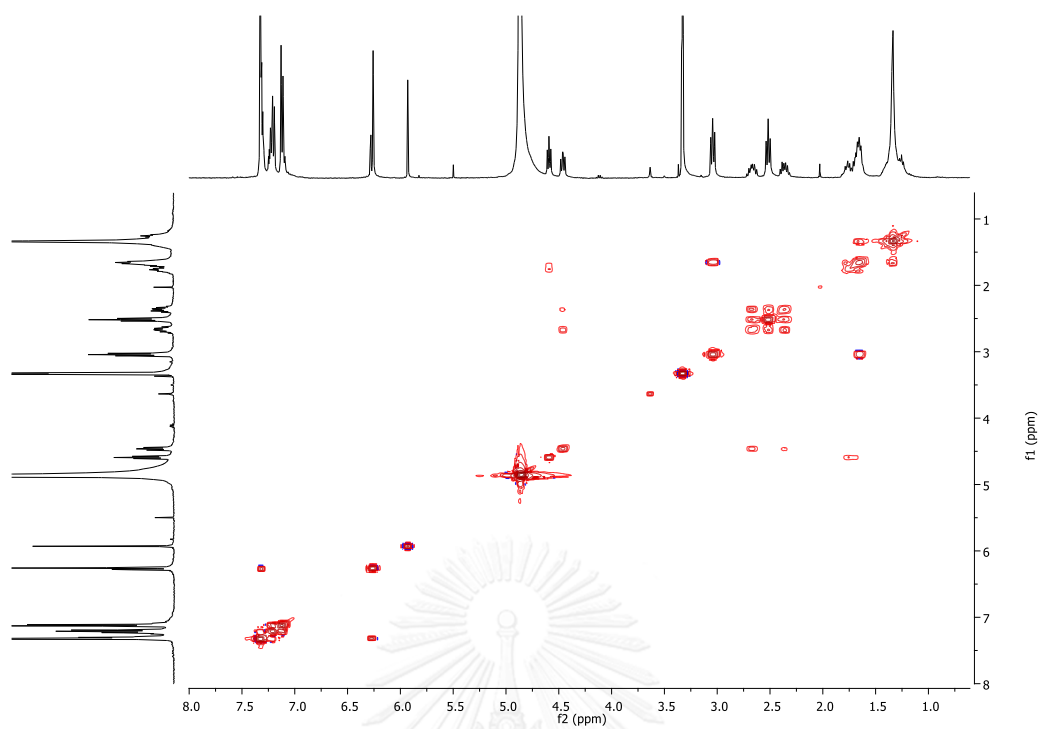
Figure 4.15 COSY spectrum of **8** (CD₃OD**)**
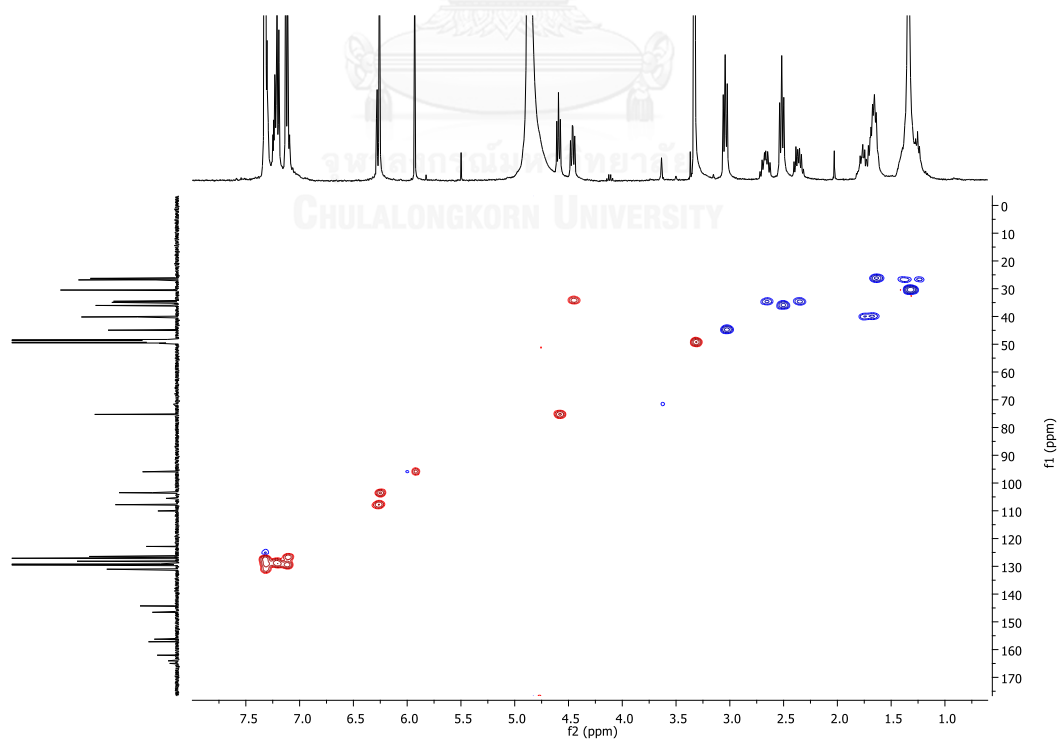
Figure 4.16 HSQC spectrum of **8** (CD₃OD)
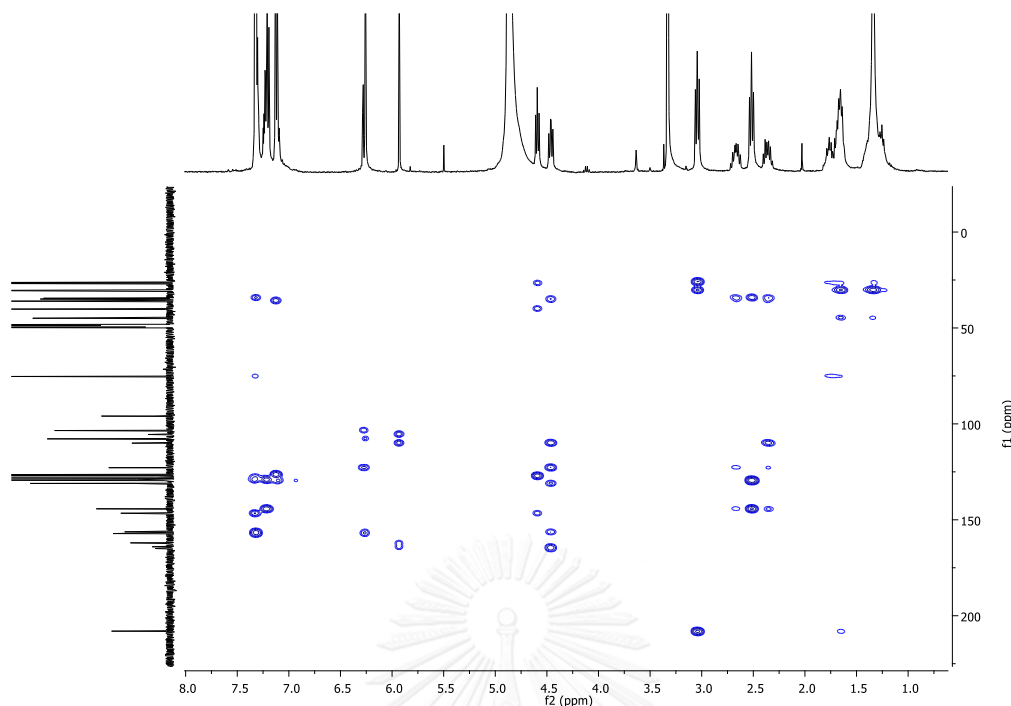
Figure 4.17 HMBC spectrum of **8** (CD₃OD)
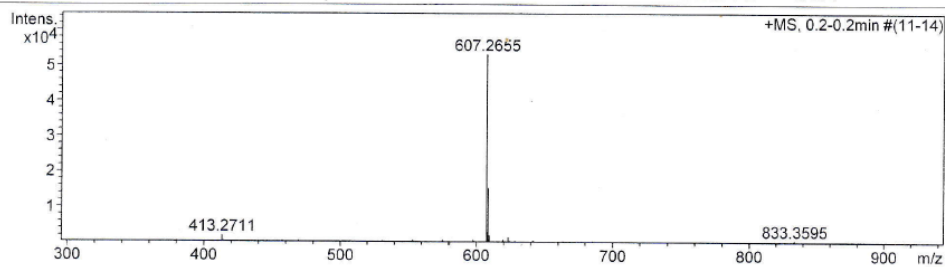
Figure 4.18 HRESIMS spectrum of **8**
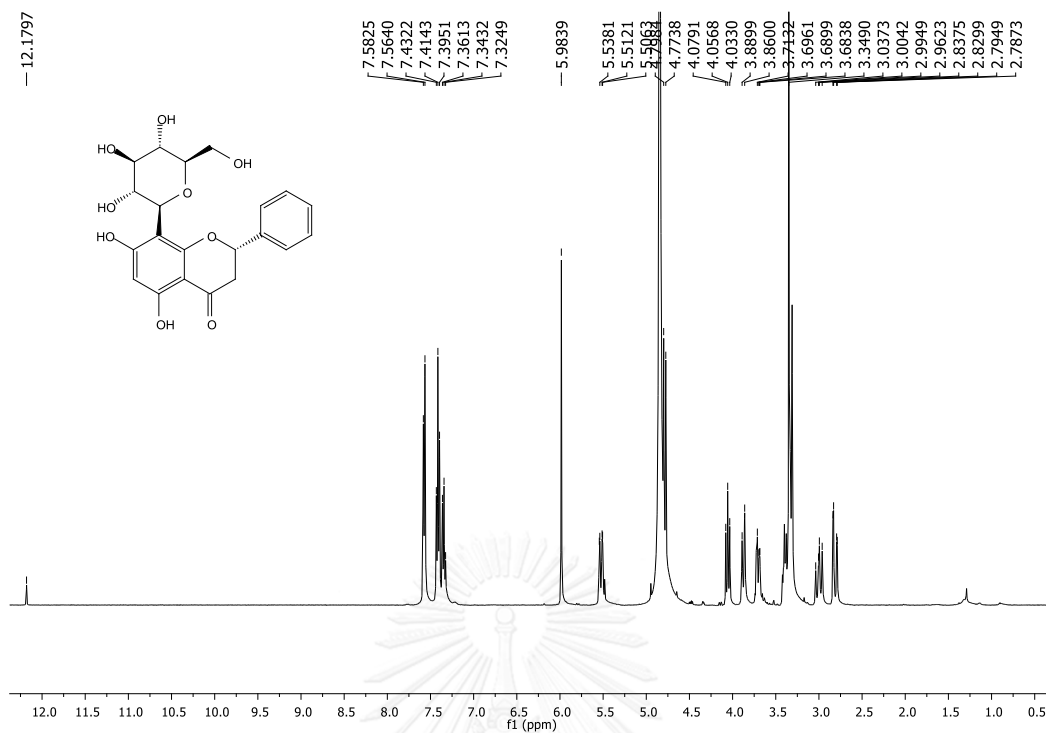
Figure 4.19 ^{1}H NMR spectrum of **9** (400 MHz, in CD$_3$OD)
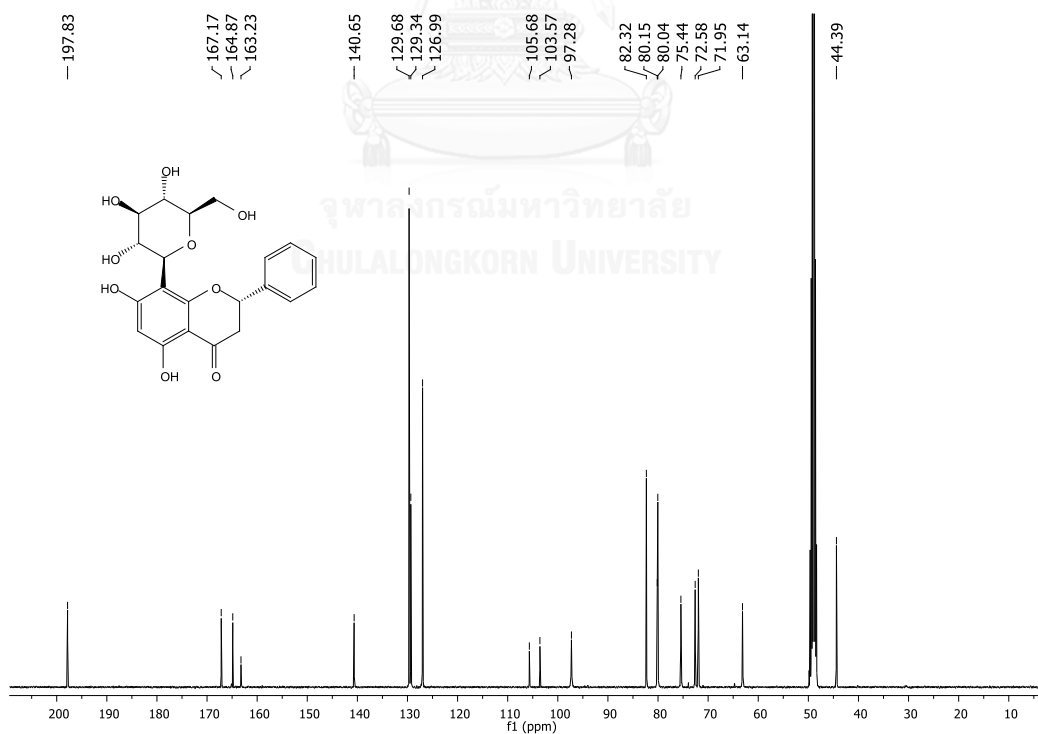
Figure 4.20 ^{13}C NMR spectrum of **9** (100 MHz, in CD$_3$OD)
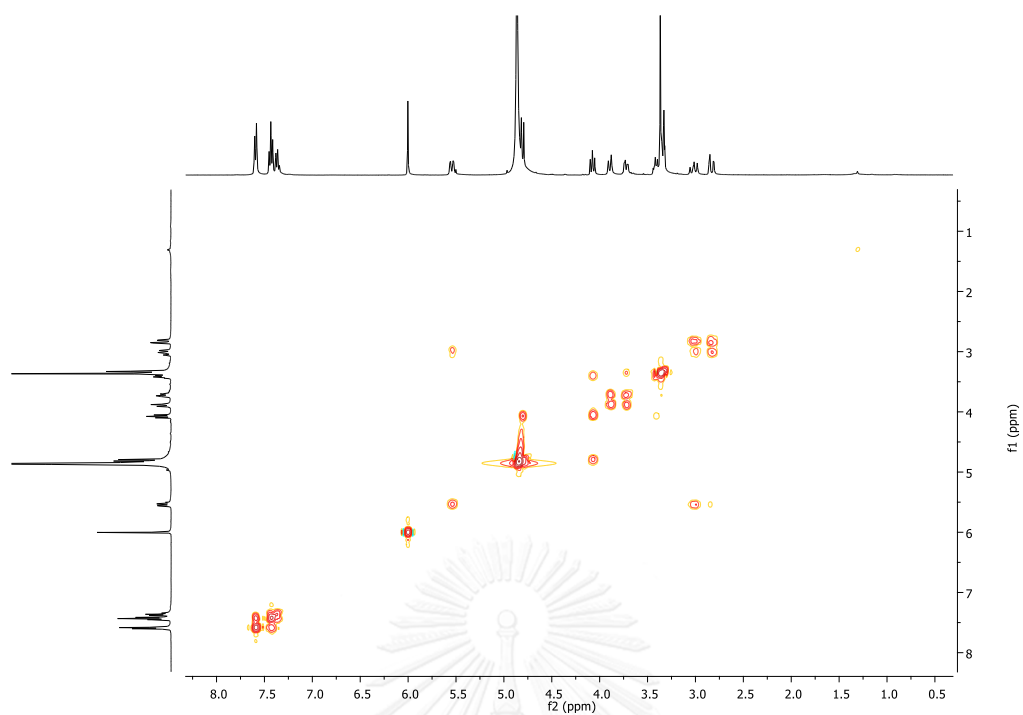
Figure 4.21 COSY spectrum of **9** (CD₃OD)
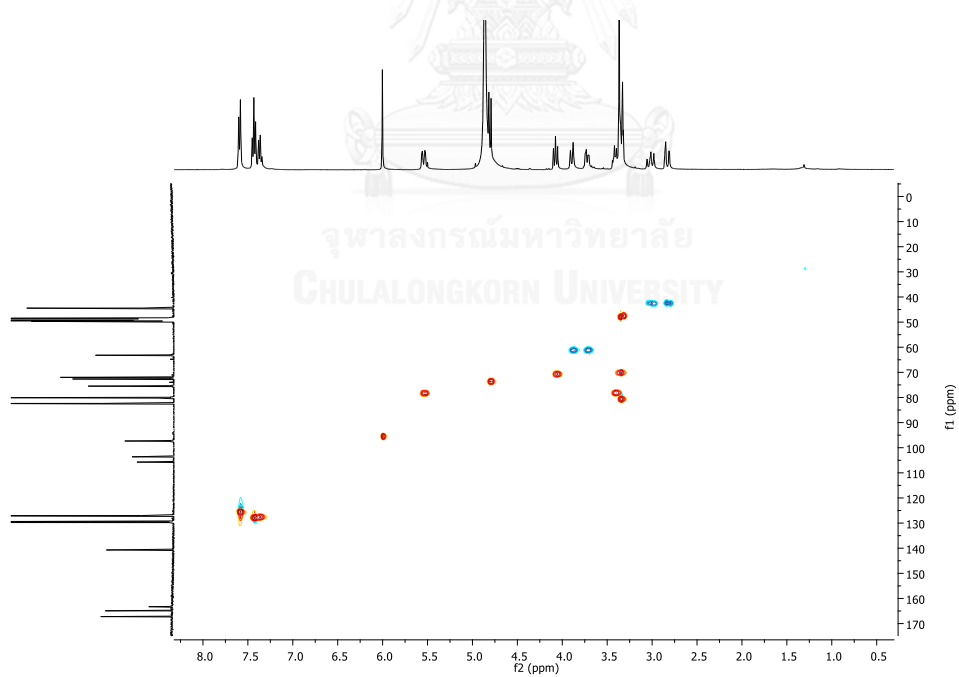
Figure 4.22 HSQC spectrum of **9** (CD₃OD)
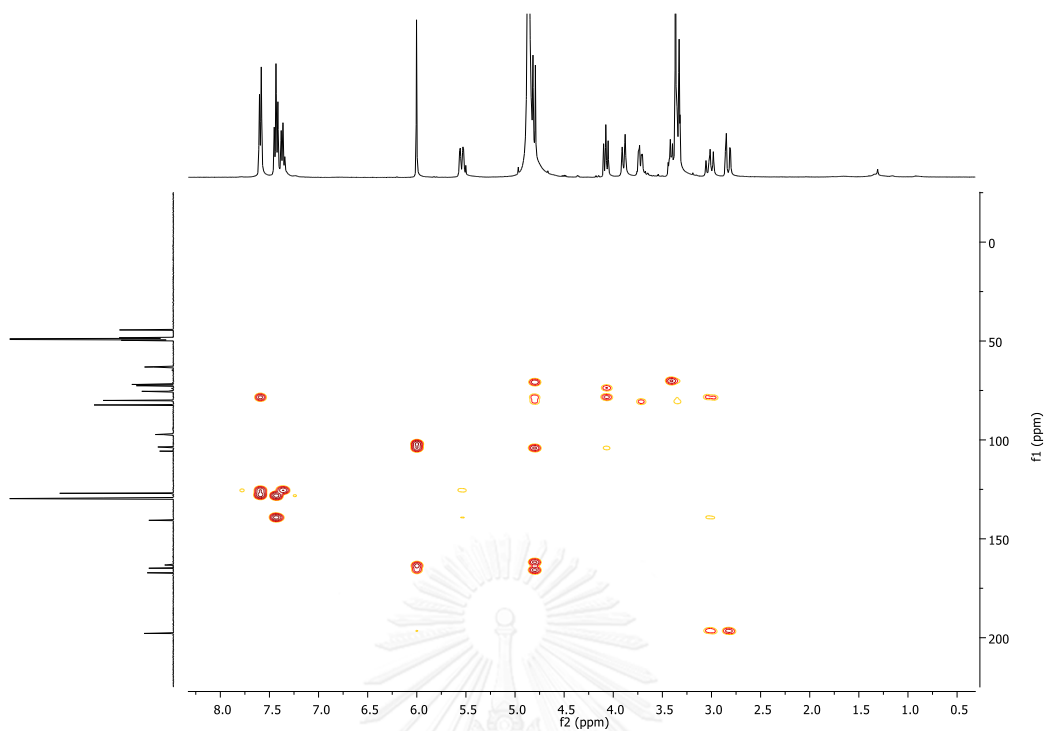
Figure 4.23 HMBC spectrum of **9** (CD$_3$OD)

Figure 4.24 HRESIMS spectrum of **9**
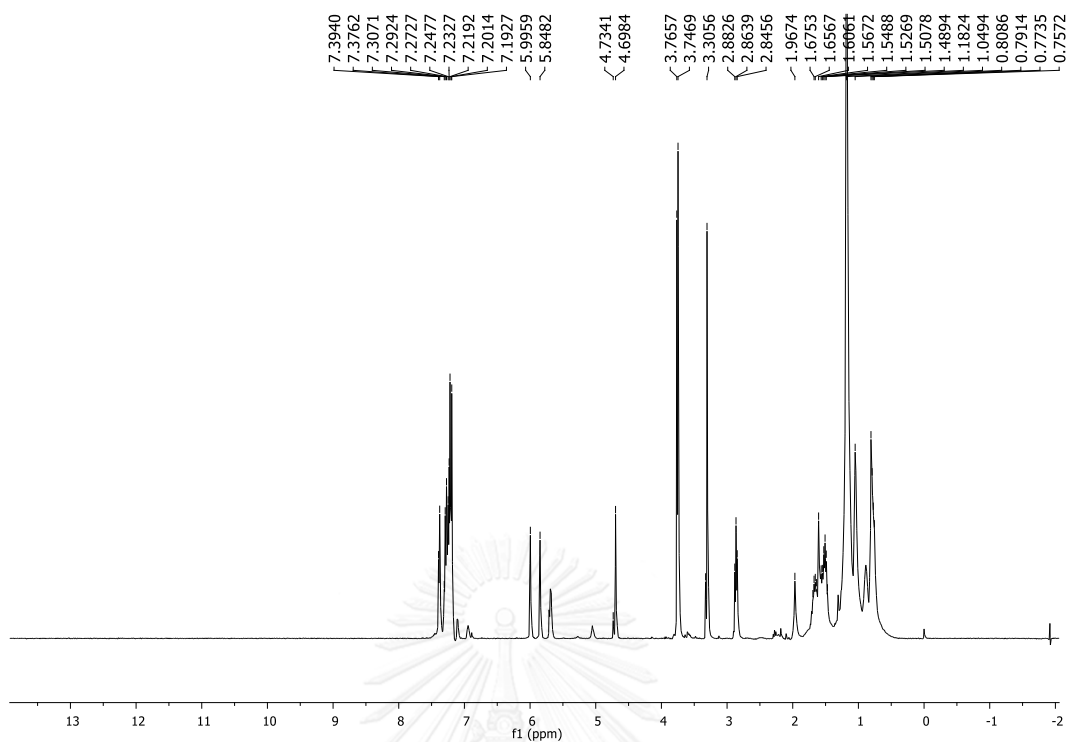
Figure 4.25 ¹H NMR spectrum of *S*-MPA ester (**7b**, 400 MHz, in CDCl₃)
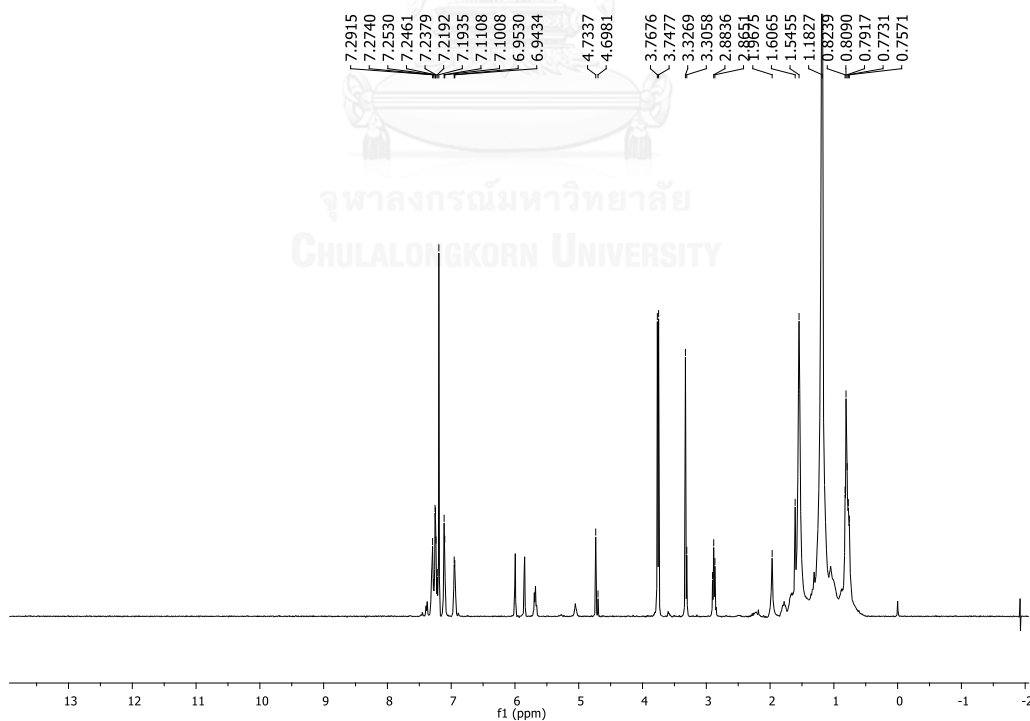
Figure 4.26 ¹H NMR spectrum of *R*-MPA ester (**7c**, 400 MHz, in CDCl₃)

CHAPTER V
CONCLUSION

In the present investigation, seven plants were reported to be used in traditional treatment for diabetes theraphy by Dayak people in East Kalimantan, Indonesia. Ethnopharmacological knowledge conducted in East Kalimantan revealed that the medicinal plants including *Leucaena leucocephala*, *Swietenia macrcophylla*, *Pycnarrhena tumefacta*, *Luvunga eleutherandra*, *Crescentia cujete*, *Ceriops tagal* and *Horsfieldia macrobotrys* possibly contain bioactive compounds that can be used for diabetes theraphy. On the basis of ethnopharmacological knowledge together with biological and chemical screening, they inspired us to develop medicinal plants responsible for antidiabetic and antioxidant activity. Furthermore, phytochemical analyses are currently underway in bioassay-guided isolation of the active components responsible for antidiabetic and antioxidant activity. In this work, we have used quick column chromatography in fractionation step and spectroscopic methods such as NMR, 2D-NMR and MS to confirm the structures of isolated compounds. In addition, inhibitory activity against α-glucosidase from baker's yeast and rat intestine (maltase and sucrase) and antioxidant activity of extract and isolated compounds from selected plants were also evaluated.

The MeOH extracts from *Ceriop tagal* leaves displayed more potent antioxidant and yeast α-glucosidase inhibition than those of others selected plants. Three compounds named lupeol (**1**), betulone (**2**) and betulin (**3**) (Figure 5.1) were isolated from the active fractions.
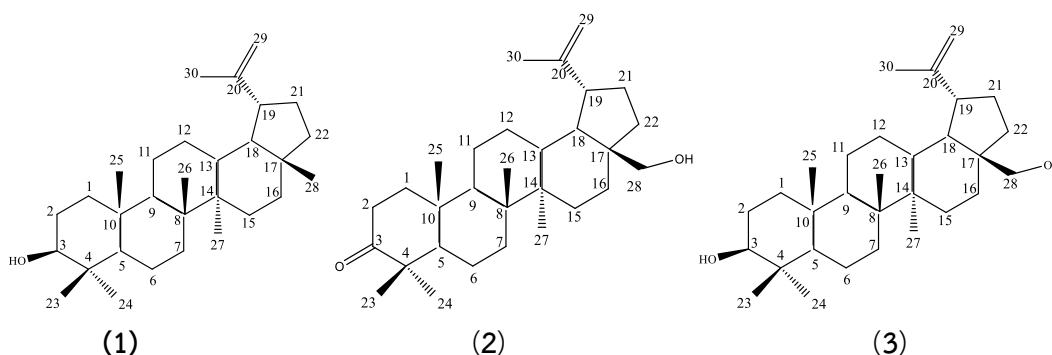
Figure 5.1 The chemical structures of isolated compounds from *Ceriops tagal* leaves

The isolated compounds from *C. tagal* (**1**, **2**, and **3**) were assayed toward α-glucosidase from baker's yeast and rat intestine (maltase and sucrase). As a results, **3** showed highest inhibition against baker's yeast α-glucosidase activity (IC_{50} 18.87 μM) followed by **1** and **2**, respectively. In rat intestine, **1, 2** and **3** showed no inhibition toward maltase (less than 30%), whereas **1**, **2** and **3** showed weak inhibition against sucrase. In addition, the kinetic of **1**, **2** and **3** was carries out using Lineweaver-Burk plots. Interestingly, all of **1**-**3** showed noncompetitive inhibition against baker's yeast α-glucosidase.

In addition, two known arylalkanones named 1-(2,4,6-Trihydroxyphenyl)-9-phenylnonan-1-one (**4**) and malabaricone A (**5**) together with a flavanone named 7-hydroxyflavanone (**6**) (Figure 5.2) were isolated from MeOH extracts of *Horsfieldia macrobotrys* seed coats. Furthermore, **4** and **5** were separately converted to their corresponding methyl ether analogues (**4a** and **5a**, respectively) by reaction with MeI/$K_2C_2O_3$ (Figure 5.2). As a result, **4** showed more potent bioactivities than those of all isolated compounds, in radical scavenging (IC_{50} 2.6 mM) and baker's yeast α-glucosidase inhibition (IC_{50} 10.8 μM). Interestingly, the number of hydroxyl groups (-OH) on the aryl moieties of **4** was critical for exerting radical scavenging and α-glucosidase inhibition. Thus, the replacement of all hydroxyl in **4** and **5** by methoxy groups considerably reduced the bioactivities.
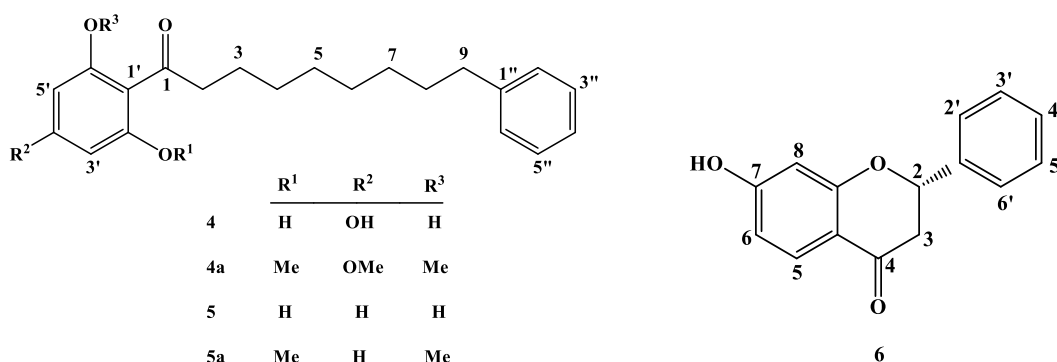
Figure 5.2 The chemical structures of isolated compounds and their synthetic methyl ethers from *Horsfieldia macrobotrys* seed coats

Furthermore, the mechanism underlying inhibition of **4** was investigated. Compound **4** inhibited baker's yeast α-glucosidase through mixed inhibition. The results for **4** is a good starting point for new dual function antidiabetic agent not only for prevent diabetes mellitus but also for preventive effect of diabetes complications.

Since promising bioactivity of isolated arylalkanones from seed coats part of *Horsfieldia macrobotrys*, it inspired us to further investigate other parts of this plant. Bioassay-guided isolation of stem bark extract resulted in two new arylalkanones named horsfieldone A (**7**) and maingayone D (**8**) together with a new flavanone-C-glycoside named 8-C-β-D-glucopyranosylpinocembrin (**9**) (Figure 5.3).

7 (new compound)   **8** (new compound)

9 (new compound)
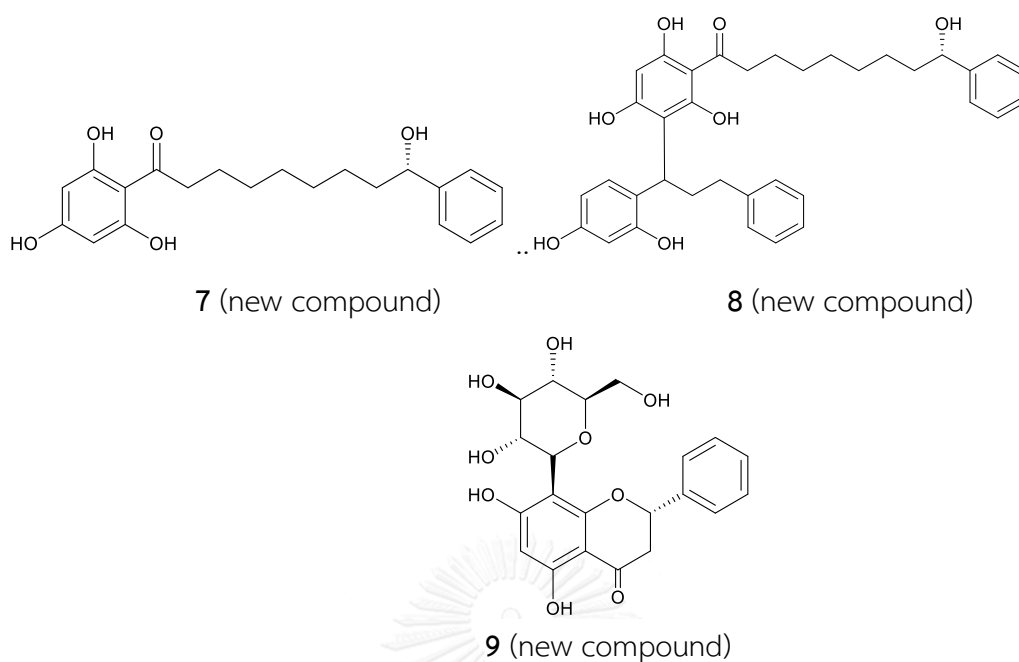
Figure 5.3 The chemical structures of isolated compounds from *Horsfieldia macrobotrys* stem bark.

The isolated compounds were assayed toward α-glucosidase inhibition and scavenging free radicals. As a result, **7** and **8** displayed most potent activity compared with **9** in all bioassay examined. Compound **8** displayed significantly more potent than **7**, toward DPPH radicals (IC$_{50}$ 0.43 mM) and baker's yeast α-glucosidase (IC$_{50}$ 5.65 μM). However, the inhibition of **8** against rat intestine (maltase and sucrase) was slightly improved than **7**. These result showed that the presence of additional phenolic moieties in **8** is critical for exerting radical scavenging and α-glucosidase inhibition. Therefore, to understand mechanism underlying inhibition of **7** and **8**, their kinetic study was carried out using Lineweaver-Burk plots. Apparently, they showed mixed inhibition against rat intestinal maltase and sucrase.

In conclusion, this study demonstrated that ethnopharmacological knowledge from Dayak people together with biological and chemical screenings provide a successful strategy to discover potent antidiabetic agents. Furthermore, this study is also useful for the scientific approach, which could lead to the transfer of natural wealth from traditional knowledge to the scientific evaluation of the potential properties of selected plants. Moreover, this study is imperative to conserve this

cultural heritage such ethnopharmacological knowledge by scientifically evaluating the biological activities of selected plants from East Kalimantan flora.

REFERENCES

[1]   Ali, H., Houghton, P.J., and Soumyanath, A. α-Amylase inhibitory activity of some Malaysian plants used to treat diabetes; with particular reference to *Phyllanthus amarus*. Journal of Ethnopharmacology 107(3) (2006): 449-455.

[2]   Nabeel, M.A., Kathiresan, K., and Manivannan, S. Antidiabetic activity of the mangrove species *Ceriops decandra* in alloxan-induced diabetic rats. Journal of Diabetes 2(2) (2010): 97-103.

[3]   Ortiz-Andrade, R.R., García-Jiménez, S., Castillo-España, P., Ramírez-Ávila, G., Villalobos-Molina, R., and Estrada-Soto, S. α-Glucosidase inhibitory activity of the methanolic extract from *Tournefortia hartwegiana*: An anti-hyperglycemic agent. Journal of Ethnopharmacology 109(1) (2007): 48-53.

[4]   Wild, S., Roglic, G., Green, A., Sicree, R., and King, H. Global prevalence of diabetes estimates for the year 2000 and projections for 2030. Diabetes Care 27(5) (2004): 1047-1053.

[5]   Vetrichelvan, T., Jegadeesan, M., and Devi, B.A.U. Anti-diabetic activity of alcoholic extract of *Celosia argentea* Linn. seeds in rats. Biological and Pharmaceutical Bulletin 25(4) (2002): 526-528.

[6]   Hossain, P., Kawar, B., and El Nahas, M. Obesity and diabetes in the developing world—a growing challenge. New England Journal of Medicine 356(3) (2007): 213-215.

[7]   Lawag, I.L., Aguinaldo, A.M., Naheed, S., and Mosihuzzaman, M. α-Glucosidase inhibitory activity of selected Philippine plants. Journal of Ethnopharmacology 144(1) (2012): 217-219.

[8]   Association, A.D. Diagnosis and classification of diabetes mellitus. Diabetes Care 33(Supplement 1) (2010): S62-S69.

[9]   Devendra, D., Liu, E., and Eisenbarth, G.S. Type 1 diabetes: recent developments. British Medical Journal 328(7442) (2004): 750-754.

[10]   Chauhan, A., Sharma, P., Srivastava, P., Kumar, N., and Dudhe, R. Plants having potential antidiabetic activity: a review. Der Pharmacia Lettre 2(3) (2010): 369-387.

[11]   American Diabetes, A. Diagnosis and Classification of Diabetes Mellitus. Diabetes Care 35(Suppl 1) (2012): S64-S71.

[12]   Hwang, I.G., Kim, H.Y., Woo, K.S., Hong, J.T., Hwang, B.Y., Jung, J.K., Lee, J., and Jeong, H.S. Isolation and characterisation of an α-glucosidase inhibitory substance from fructose–tyrosine Maillard reaction products. Food Chemistry 127(1) (2011): 122-126.

[13]   Kelley, D., Mokan, M., and Veneman, T. Impaired postprandial glucose utilization in non-insulin-dependent diabetes mellitus. Metabolism 43(12) (1994): 1549-1557.

[14]   Stumvoll, M., Goldstein, B.J., and van Haeften, T.W. Type 2 diabetes: principles of pathogenesis and therapy. The Lancet 365(9467) (2005): 1333-1346.

[15]   Rosak, C. and Mertes, G. Critical evaluation of the role of acarbose in the treatment of diabetes: patient considerations. Diabetes, Metabolic Syndrome and Obesity: Targets and Therapy 5 (2012): 357-367.

[16]   Krentz, A.J. and Bailey, C.J. Oral antidiabetic agents. Drugs 65(3) (2005): 385-411.

[17]   Luna, B. and Feinglos, M.N. Oral agents in the management of type 2 diabetes mellitus. American Family Physician 63(9) (2001): 1747-1756.

[18]   Schwientek, P., Szczepanowski, R., Rückert, C., Kalinowski, J., Klein, A., Selber, K., Wehmeier, U.F., Stoye, J., and Pühler, A. The complete genome sequence of the acarbose producer Actinoplanes sp. SE50/110. BioMed Central Genomics 13(1) (2012): 112.

[19]   Yoshikawa, T. and Naito, Y. What is oxidative stress? Japan Medical Association Journal 45(7) (2002): 271-276.

[20] Johansen, J.S., Harris, A.K., Rychly, D.J., and Ergul, A. Oxidative stress and the use of antioxidants in diabetes: linking basic science to clinical practice. <u>Cardiovascular Diabetology</u> 4(1) (2005): 5.

[21] Chen, K. and Keaney Jr, J.F. Evolving concepts of oxidative stress and reactive oxygen species in cardiovascular disease. <u>Current Atherosclerosis Reports</u> 14(5) (2012): 476-483.

[22] Scheibmeir, H.D., Christensen, K., Whitaker, S.H., Jegaethesan, J., Clancy, R., and Pierce, J.D. A review of free radicals and antioxidants for critical care nurses. <u>Intensive and Critical Care Nursing</u> 21(1) (2005): 24-28.

[23] Rahimi, R., Nikfar, S., Larijani, B., and Abdollahi, M. A review on the role of antioxidants in the management of diabetes and its complications. <u>Biomedicine & Pharmacotherapy</u> 59(7) (2005): 365-373.

[24] Baynes, J.W. Role of oxidative stress in development of complications in diabetes. <u>Diabetes</u> 40(4) (1991): 405-412.

[25] Broich, M., Hansen, M.C., Potapov, P., Adusei, B., Lindquist, E., and Stehman, S.V. Time-series analysis of multi-resolution optical imagery for quantifying forest cover loss in Sumatra and Kalimantan, Indonesia. <u>International Journal of Applied Earth Observation and Geoinformation</u> 13(2) (2011): 277-291.

[26] Joshi, L., Wijaya, K., Sirait, M., and Mulyoutami, E. Indigenous systems and ecological knowledge among Dayak people in Kutai Barat, East Kalimantan–a preliminary report. 2004, <u>ICRAF Southeast Asia Working Paper</u>.

[27] De Jong, W. Developing swidden agriculture and the threat of biodiversity loss. <u>Agriculture, Ecosystems & Environment</u> 62(2) (1997): 187-197.

[28] Heinrich, M., Edwards, S., Moerman, D.E., and Leonti, M. Ethnopharmacological field studies: a critical assessment of their conceptual basis and methods. <u>Journal of Ethnopharmacology</u> 124(1) (2009): 1-17.

[29]   Slish, D.F., Ueda, H., Arvigo, R., and Balick, M.J. Ethnobotany in the search for vasoactive herbal medicines. Journal of Ethnopharmacology 66(2) (1999): 159-165.

[30]   Arung, E.T., Matsubara, E., Kusuma, I.W., Sukaton, E., Shimizu, K., and Kondo, R. Inhibitory components from the buds of clove (*Syzygium aromaticum*) on melanin formation in B16 melanoma cells. Fitoterapia 82(2) (2011): 198-202.

[31]   Arung, E.T., Kuspradini, H., Kusuma, I.W., Shimizu, K., and Kondo, R. Validation of *Eupatorium triplinerve* Vahl leaves, a skin care herb from East Kalimantan, using a melanin biosynthesis assay. Journal of Acupuncture and Meridian Studies 5(2) (2012): 87-92.

[32]   Kusuma, I.W., Arung, E.T., Rosamah, E., Purwatiningsih, S., Kuspradini, H., Syafrizal, Astuti, J., Kim, J.U., and Shimizu, K. Antidermatophyte and antimelanogenesis compound from *Eleutherine americana* grown in Indonesia. Journal of Natural Medicines 64(2) (2010): 223-226.

[33]   Jang, D.S., Cuendet, M., Pawlus, A.D., Kardono, L.B.S., Kawanishi, K., Farnsworth, N.R., Fong, H.H.S., Pezutto, J.M., and Kinghorn, A.D. Potential cancer chemopreventive constituents of the leaves of *Macaranga triloba.* Phytochemistry 65(3) (2004): 345-350.

[34]   Mudianta, I.W. and Garson, M.J. Isolation and absolute configuration of boehmenan from *Durio affinis* Becc. Records of Natural Products 8(2) (2014): 195-198.

[35]   Rudiyansyah and Garson, M.J. Secondary Metabolites from the Wood Bark of *Durio. zibethinus* and *Durio kutejensis.* Journal of Natural Products 69(8) (2006): 1218-1221.

[36]   Lambert, L.K. and Garson, M.J. Lignans and triterpenes from the bark of *Durio carinatus* and *Durio oxleyanus.* Journal of Natural Products 73(10) (2010): 1649-1654.

[37]   Babu, P.A., Suneetha, G., Boddepalli, R., Laskhmi, V.V., Rani, T.S., Rambabu, Y., and Srinivas, K.A. A database of 389 medicinal plants for diabetes. Bioinformation 1(4) (2006): 130.

[38]   Kuntorini, E. and Nugroho, L.H. Structural Development And Bioactive Content Of Red Bulb Plant (*Eleutherine americana*) A Traditional Medicines For Local Kalimantan People. Biodiversitas 11(2) (2009): 102-106.

[39]   Oyedemi, S., Bradley, G., and Afolayan, A. Ethnobotanical survey of medicinal plants used for the management of diabetes mellitus in the Nkonkobe municipality of South Africa. Journal of Medicinal Plants Research 3(12) (2010): 1040-1044.

[40]   Shibano, M., Kakutani, K., Taniguchi, M., Yasuda, M., and Baba, K. Antioxidant constituents in the dayflower (*Commelina communis* L.) and their α-glucosidase-inhibitory activity. Journal of Natural Medicines 62(3) (2008): 349-353.

[41]   Ames, B.N. Dietary carcinogens and anticarcinogens oxygen radicals and degenerative diseases. Science 221(4617) (1983): 1256-1264.

[42]   Sumino, M., Sekine, T., Ruangrungsi, N., Igarashi, K., and Ikegami, F. Ardisiphenols and other antioxidant principles from the fruits of *Ardisia colorata*. Chemical and Pharmaceutical Bulletin 50(11) (2002): 1484-1487.

[43]   Fukuda, T., Ito, H., and Yoshida, T. Effect of the walnut polyphenol fraction on oxidative stress in type 2 diabetes mice. Biofactors 21(1-4) (2004): 251-254.

[44]   Kuppusamy, U.R., Arumugam, B., Azaman, N., and Jen Wai, C. *Leucaena leucocephala* Fruit Aqueous Extract Stimulates Adipogenesis, Lipolysis, and Glucose Uptake in Primary Rat Adipocytes. The Scientific World Journal 2014 (2014).

[45]   Utami, M., Wowor, M.P., and Mambo, C. Effects of Usage a *Leucaena leucocephala* againts blood sugar level of mice wistar (*Rattus norvegicus*) with induced alloxan. Journal of Biomedic 3(1) (2015): 363-367.

[46]   Hashim, M.A., Yam, M.F., Hor, S.Y., Lim, C.P., Asmawi, M.Z., and Sadikun, A. Anti-hyperglycaemic activity of *Swietenia macrophylla* king

(meliaceae) seed extracts in normoglycaemic rats undergoing glucose tolerance tests. <u>Chinese Medicine</u> 8(1) (2013): 1-8.

[47]   Moghadamtousi, S.Z., Goh, B.H., Chan, C.K., Shabab, T., and Kadir, H.A. Biological activities and phytochemicals of *Swietenia macrophylla* king. <u>Molecules</u> 18(9) (2013): 10465-10483.

[48]   De, D., Chatterjee, K., Ali, K.M., Bera, T.K., and Ghosh, D. Antidiabetic potentiality of the aqueous-methanolic extract of seed of *Swietenia mahagoni* (L.) Jacq. in streptozotocin-induced diabetic male albino rat: a correlative and evidence-based approach with antioxidative and antihyperlipidemic activities. <u>Evidence-Based Complementary and Alternative Medicine</u> 2011 (2011): 1-11.

[49]   Wibowo, M.A., Ardiningsih, P., and Purba, D.M. Antioxidant activity and cytotoxicity of methanol extracts of Sengkubak leaves (*Pycnarrhena cauliflora* Diels). <u>Journal of Equator Chemistry</u> 3(2) (2014): 7-12.

[50]   Setyowati, F.M. Etnopharmacology and usage of medicinal plant in Dayak Tunjung tribe, East Kalimantan. <u>Medium of Research and Development Health</u> 20(3) (2010): 104-112.

[51]   Abouchacra, M.-L., Leboeuf, M., Guinaudeau, H., Cavé, A., and Cabalion, P. The bisbenzylisoquinoline alkaloids of *Pycnarrhena ozantha*. <u>Journal of Natural Products</u> 50(3) (1987): 375-380.

[52]   Lien, T.P., Kamperdick, C., Schmidt, J., Adam, G., and Van Sung, T. Apotirucallane triterpenoids from *Luvunga sarmentosa* (Rutaceae). <u>Phytochemistry</u> 60(7) (2002): 747-754.

[53]   Kamperdick, C., Lien, T.P., Adam, G., and Sung, T.V. Apotirucallane and Tirucallane Triterpenoids from *Luvunga sarmentosa*. <u>Journal of Natural Products</u> 66(5) (2003): 675-678.

[54]   Al-Zikri, P.N.H., et al. Cytotoxic tirucallane triterpenes from the stem of *Luvunga scandens*. <u>Revista Brasileira de Farmacognosia</u> 24(5) (2014): 561-564.

[55]   Noorcahyati., Arifin, Z., and Ningsih, K. Ethnobotany potency of Kalimantan as a source medicinal plants. Proceeding of Seminar Results Research in BPTKSDA Samboja (2012): 27-37.

[56]   Koffi, N., Konan Edouard, K., and Kouassi, K. Ethnobotanical study of plants used to treat diabetes, in traditional medicine, by Abbey and Krobou people of Agboville (Côte-d'Ivoire). American Journal of Scientific Research 4 (2009): 45-58.

[57]   Shastry, C. and Aswathanarayana, B. Antivenom activity of ethanolic extract of *Crescentia cujete* fruit. International Journal of Phytomedicine 4(1) (2012): 108.

[58]   Das, N., Islam, M.E., Jahan, N., Islam, M.S., Khan, A., Islam, M.R., and Parvin, M.S. Antioxidant activities of ethanol extracts and fractions of *Crescentia cujete* leaves and stem bark and the involvement of phenolic compounds. BMC Complementary and Alternative Medicine 14(1) (2014): 1-9.

[59]   Tiwari, P., Tamrakar, A.K., Ahmad, R., Srivastva, M.N., Kumar, R., Laskhmi, V., and Srivastava, A.K. Antihyperglycaemic activity of *Ceriops tagal* in normoglycaemic and streptozotocin-induced diabetic rats. Medicinal Chemistry Research 17(2-7) (2008): 74-84.

[60]   Chen, J.-D., Yi, R.-Z., Lin, Y.-M., Feng, D.-Q., Zhou, H.-C., and Wang, Z.-C. Characterization of Terpenoids from the Root of *Ceriops tagal* with Antifouling Activity. International Journal of Molecular Sciences 12(10) (2011): 6517-6528.

[61]   Jamal, A., Yaacob, W., and Din, L.B. A chemical study on *Phyllanthus reticulatus*. Journal of Physical Science 19(2) (2008): 45-50.

[62]   Liu, M., Yang, S., Jin, L., Hu, D., Wu, Z., and Yang, S. Chemical constituents of the ethyl acetate extract of *Belamcanda chinensis* (L.) DC roots and their antitumor activities. Molecules 17(5) (2012): 6156-6169.

[63]   Tijjani, A., Ndukwe, I., and Ayo, R. Isolation and Characterization of Lup-20 (29)-ene-3, 28-diol (Betulin) from the Stem-Bark of *Adenium obesum*

(Apocynaceae). <u>Tropical Journal of Pharmaceutical Research</u> 11(2) (2012): 259-262.

[64]   Orak, H.H. Total antioxidant activities, phenolics, anthocyanins, polyphenoloxidase activities of selected red grape cultivars and their correlations. <u>Scientia Horticulturae</u> 111(3) (2007): 235-241.

[65]   Choi, Y., Lee, S., Chun, J., Lee, H., and Lee, J. Influence of heat treatment on the antioxidant activities and polyphenolic compounds of Shiitake (*Lentinus edodes*) mushroom. <u>Food Chemistry</u> 99(2) (2006): 381-387.

[66]   Prieto, P., Pineda, M., and Aguilar, M. Spectrophotometric quantitation of antioxidant capacity through the formation of a phosphomolybdenum complex: specific application to the determination of vitamin E. <u>Analytical Biochemistry</u> 269(2) (1999): 337-341.

[67]   Arung, E.T., Shimizu, K., and Kondo, R. Inhibitory effect of artocarpanone from *Artocarpus heterophyllus* on melanin biosynthesis. <u>Biological and Pharmaceutical Bulletin</u> 29(9) (2006): 1966-1969.

[68]   Thanakosai, W. and Phuwapraisirisan, P. First identification of α-glucosidase inhibitors from okra (*Abelmoschus esculentus*) seeds. <u>Natural Product Communications</u> 8(8) (2013): 1085-1088.

[69]   Gonzalez, M.J., Pinto, M.M.M., Kijjoa, A., Kengthong, S., Mondanondra, I., Silva, A.M.S., Eaton, G., and Herz, W. 5, 7-Dihydroxychromones and 8-hydroxytetrahydrochromones from *Horsfieldia irya*. <u>Phytochemistry</u> 61(8) (2002): 995-998.

[70]   Pham, V.C., Jossang, A., Sévenet, T., and Bodo, B. Novel cytotoxic acylphenol dimers of *Myristica gigantea*; enzymatic synthesis of giganteones A and B. <u>Tetrahedron</u> 58(28) (2002): 5709-5714.

[71]   Dunlop, C., Leach, G., and Cowie, I. Flora of the Darwin Region Vol. 2. <u>Northern Territory Botanical Bulletin</u> 20 (1995): 1-5.

[72]   Datta, A. and Rane, A. Phenology, seed dispersal and regeneration patterns of *Horsfieldia kingii*, a rare wild nutmeg. <u>Tropical Conservation Science</u> 6(5) (2013): 674-689.

[73]   Sidiyasa, K. Tree diversity in the rain forest of Kalimantan. Proceedings of The Balance Between Biodiversity Conservation and Sustainable Use of Tropical Rain Forest (2001).

[74]   Xu, F., and Ronse De Craene, L.P. Floral ontogeny of *Knema* and *Horsfieldia* (Myristicaceae): evidence for a complex androecial evolution. Botanical Journal of the Linnean Society 164(1) (2010): 42-52.

[75]   Ramadhan, R. and Phuwapraisirisan, P. Arylalkanones from *Horsfieldia macrobotrys* are effective antidiabetic agents achieved by α-glucosidase inhibition and radical scavenging. Natural Product Communications 10(2) (2015): 325-328.

[76]   Lu, Z., Wagoner, R.M.V., Pond, C.D., Pole, A.R., Blankenship, D., Grimberg, B.T., Kiapranis, R., Matainaho, T.K., Barrows, L.R and Ireland, C.M. Myristicyclins A and B: antimalarial procyanidins from *Horsfieldia spicata* from Papua New Guinea. Organic Letters 16(2) (2013): 346-349.

[77]   Ma, Q., Min, K., Li, H.L., Jiang, J.H., Liu, Y., Zhan, R., and Chen, Y.G. Horsfiequinones A-F, dimeric diarylpropanoids from *Horsfieldia tetratepala*. Planta Medica 80(8-9) (2014): 688-694.

[78]   Khan, M., Kihara, M., and Omoloso, A. Antimicrobial activity of *Horsfieldia helwigii* and *Melia azedarach*. Fitoterapia 72(4) (2001): 423-427.

[79]   Maia, A., Afonso, I.S., Martin, M.T., Awang, K., Laprévote, O., Guëritte, F., and Litaudon, M. Acylphenols from *Myristica crassa* as new acetylcholinesterase inhibitors. Planta Medica 74(12) (2008): 1457-1462.

[80]   Pinto, M.M., Kijjoa, A., Tantisewiet, B., Yoshida, M., and Gottlieb, O.R. Arylalkanones from *Horsfieldia glabra*. Phytochemistry 27(12) (1988): 3988-3989.

[81]   Gunatilaka, A.L., De Silva, A.J., Sotheeswaran, S., and Tillekeratne, L. Horsfieldin, a lignan and other constituents from *Horsfieldia iryaghedhi*. Phytochemistry 21(11) (1982): 2719-2723.

[82] 北川勲, 中西勤, 伊藤良久, /吉岡一郎, and Yosioka, I. On the constituents of seeds of *Horsfieldia iryaghedhi* Warb. I. Chemical and Pharmaceutical Bulletin 20(10) (1972): 2278-2281.

[83] Kumar, N.S., Herath, H., and Karunaratne, V. Arylalkanones from *Myristica dactyloides.* Phytochemistry 27(2) (1988): 465-468.

[84] Kostrzewa-Susłow, E. and Janeczko, T. Microbial transformations of 7-hydroxyflavanone. The Scientific World Journal 2012 (2012): 1-8.

[85] Herath, H. and Padmasiri, W. Demethyldactyloidin and other constituents in *Myristica ceylanica.* Natural Product Letters 14(2) (1999): 141-146.

[86] Amic, D., Davidovic-Amic, D., Beslo, D., Rastija, V., Lucic, B., and Trinajstic, N. SAR and QSAR of the antioxidant activity of flavonoids. Current Medicinal Chemistry 14(7) (2007): 827-845.

[87] Clarke, G., Ting, K.N., Wiart, C., and Fry, J. High correlation of 2, 2-diphenyl-1-picrylhydrazyl (DPPH) radical scavenging, ferric reducing activity potential and total phenolics content indicates redundancy in use of all three assays to screen for antioxidant activity of extracts of plants from the malaysian rainforest. Antioxidants 2(1) (2013): 1-10.

[88] Ohtani, I., Kusumi, T., Kashman, Y., and Kakisawa, H. High-field FT NMR application of Mosher's method. The absolute configurations of marine terpenoids. Journal of The American Chemical Society 113(11) (1991): 4092-4096.

[89] Seco, J.M., Quiñoá, E., and Riguera, R. A practical guide for the assignment of the absolute configuration of alcohols, amines and carboxylic acids by NMR. Tetrahedron: Asymmetry 12(21) (2001): 2915-2925.

[90] Seco, J.M., Quiñoá, E., and Riguera, R. The assignment of absolute configurations by NMR of arylmethoxyacetate derivatives: is this methodology being correctly used? Tetrahedron: Asymmetry 11(13) (2000): 2781-2791.

[91]   Slade, D., Ferreira, D., and Marais, J.P. Circular dichroism, a powerful tool for the assessment of absolute configuration of flavonoids. Phytochemistry 66(18) (2005): 2177-2215.

[92]   Li, X.C., Joshi, A.S., Tan, B., Elsohly, H.N., Walker, L.A., Zjawiony, J.K., and Ferreira, D. Absolute configuration, conformation, and chiral properties of flavanone-(3⟶ 8 ″)-flavone biflavonoids from *Rheedia acuminata*. Tetrahedron 58(43) (2002): 8709-8717.

[93]   Silva, D.B., Okano, L.T., Lopes, N.P., and de Oliveira, D.C. Flavanone glycosides from *Bidens gardneri* Bak.(Asteraceae). Phytochemistry 96 (2013): 418-422.

[94]   Li, X.-C., Ferreira, D., and Ding, Y. Determination of absolute configuration of natural products: theoretical calculation of electronic circular dichroism as a tool. Current Organic Chemistry 14(16) (2010): 1678.
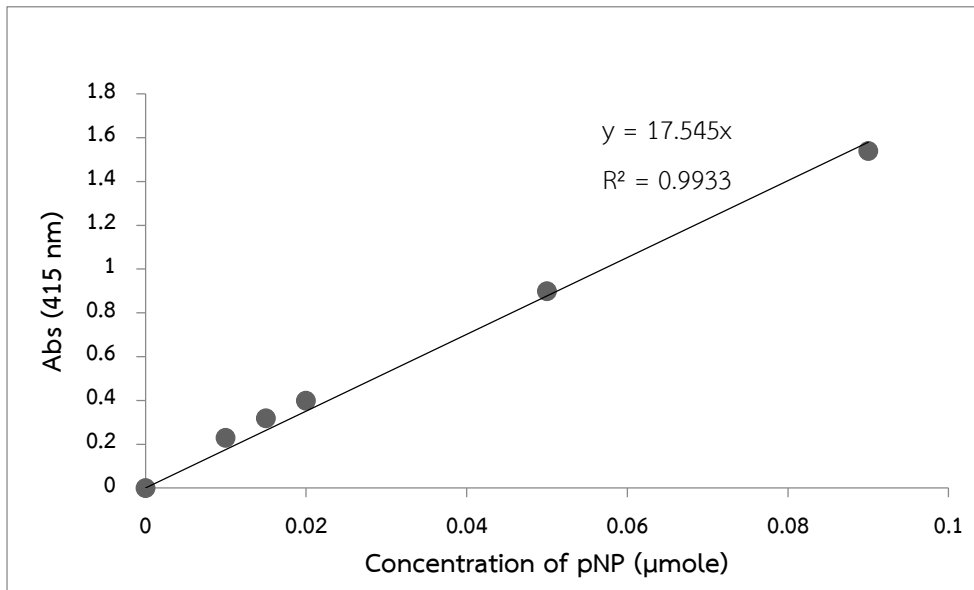
APPENDIX
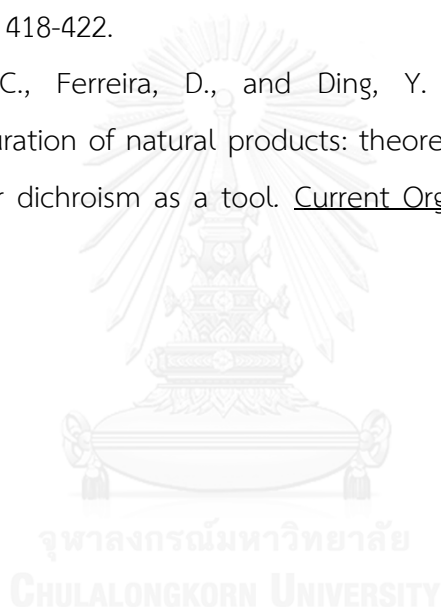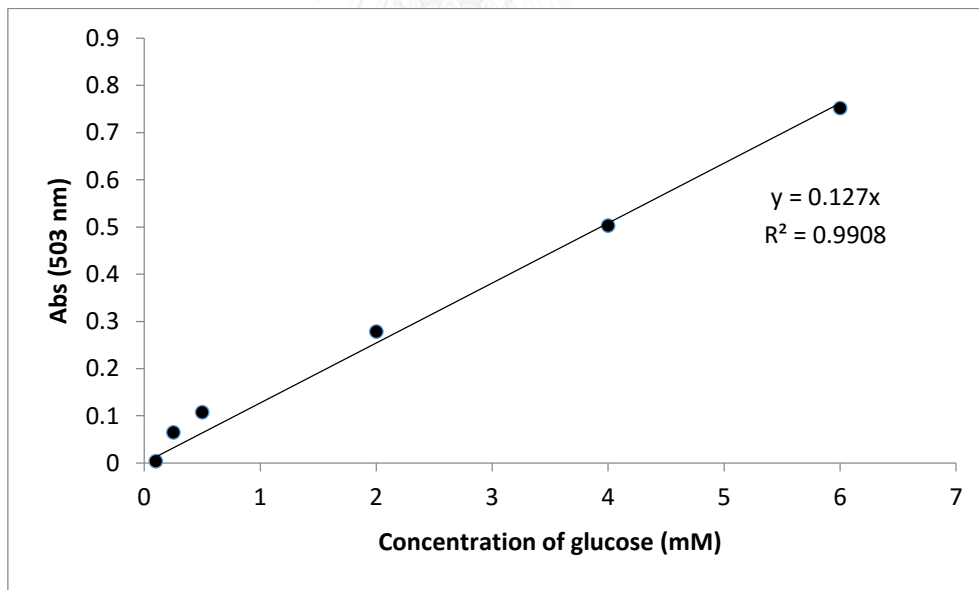
Figure A.1 Standard curve of pNP

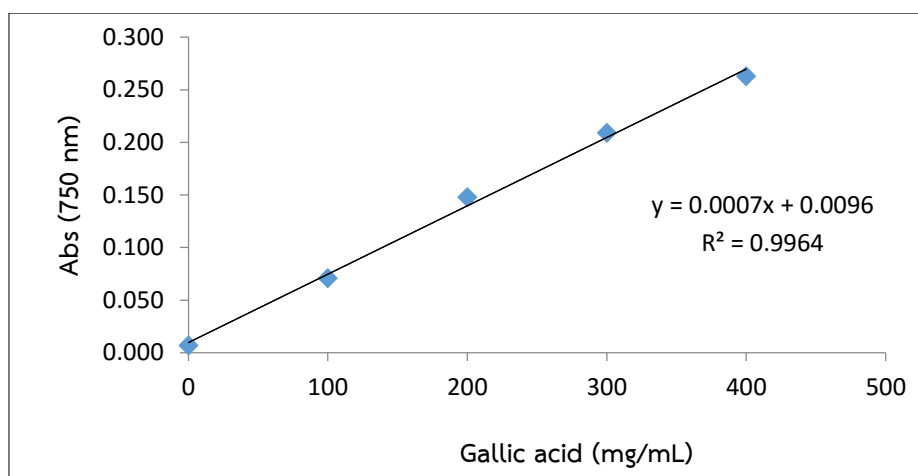**Figure A.2** Standard curve of glucose

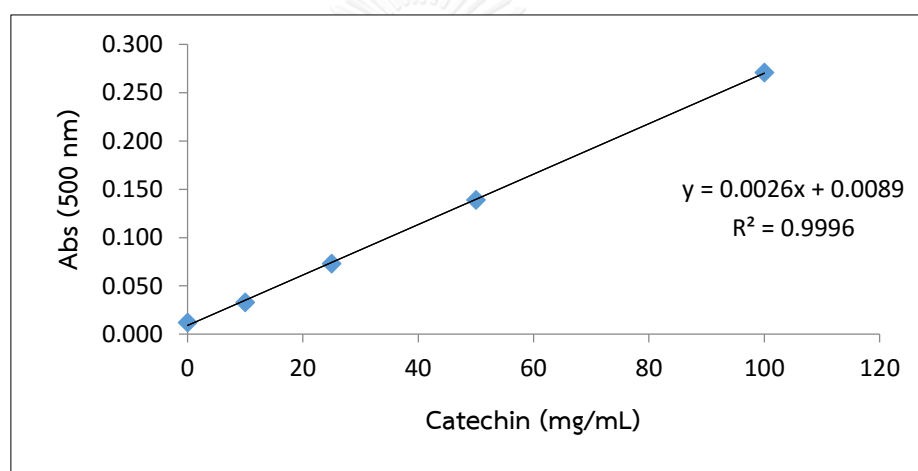**Figure A.3** Standard curve of gallic acid
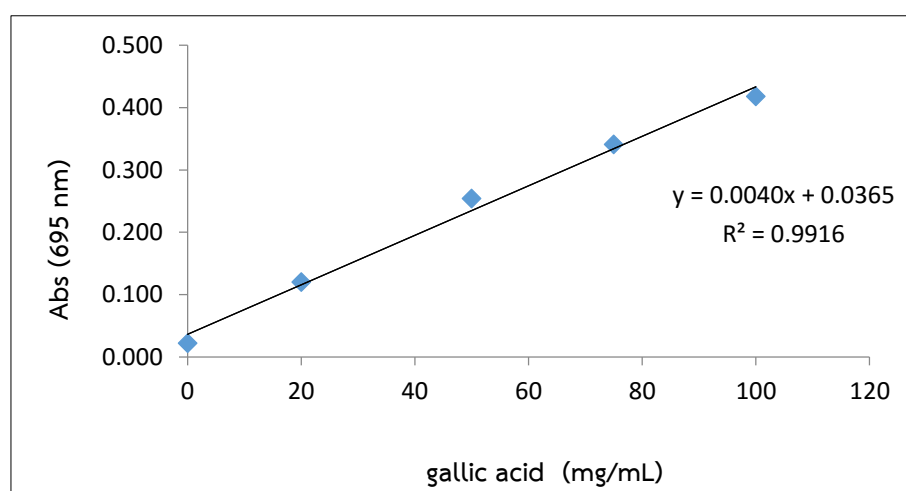

Figure A.4 Standard curve of catechin

Figure A.5 Standard curve of gallic acid (Total antioxidant capacity)

VITA

Mr. Rico Ramadhan was born on June 18, 1985 in East Kalimantan province, Kalimantan Island, Indonesia. He graduated with a Bachelor of Science degree in Chemistry, Faculty of Mathematic and Natural Science, Mulawarman University in 2007 and a Master of Agriculture degree in Forestry, Faculty of Forestry, Mulawarman University in 2012 under scholarship from Directorate General of Higher Education under Ministry of Education, Republic of Indonesia. He has further studied for the Doctor of Philosophy (Ph.D) degree in Biotechnology, Faculty of Science, Chulalongkorn University since 2013.

SCHOLARSHIP

May 2013 – June 2016

Academic scholarship from Goverment of East Kalimantan province under Beasiswa Kaltim Cemerlang Program managed by International Excellent Program, Mulawarman University for Double Degree Ph.D Program Chulalongkorn University and Mulawarman Univeristy.

PUBLICATIONS

Ramadhan, R and Phuwapraisirisan, P. (2015). Arylalkanones from Horsfieldia macrobotrys are effective antidiabetic agents achieved by α-glucosidase inhibition and radical scavenging. Natural Products Communications, 10, 325-328.

Ramadhan, R and Phuwapraisirisan, P. (2015). New arylalkanones from Horsfieldia macrobotrys, effective antidiabetic agents concomitantly inhibiting α-glucosidase and free radicals. Bioorganic & Medicinal Chemistry Letter, 25, 4529-4533.